University of Southampton

Faculty of Environmental and Life Sciences

Ocean and Earth Science

New Insights into Submarine Channel Evolution Revealed by Repeat Seafloor Mapping

by

Maarten Sjaak Heijnen

ORCID ID 0000-0001-5063-2880

Thesis for the degree of Doctor of Philosophy

February 2021

University of Southampton

Abstract

Faculty of Earth and Life Sciences

Ocean and Earth Science

Doctor of Philosophy

New Insights into Submarine Channel Evolution Revealed by Repeat Seafloor Mapping

by

Maarten Sjaak Heijnen

Submarine channel systems are one of the main conduits for the transport of land-derived material, such as sediment, organic carbon, nutrients, and pollutants to the deep sea. The seafloor-hugging flows, called turbidity currents, that transfer this material through these channels can be destructive and can affect the shape and stability of the seafloor. As a result, these flows can damage important seafloor infrastructure such as telecommunication cables that underpin the internet. Despite their importance, these submarine systems are less well understood than rivers. This is because submarine channels are difficult to monitor, since satellite imagery has limited penetration beyond shallow water depths, and because of the destructive nature of turbidity currents. The paucity of direct observations of turbidity currents and how they shape submarine channels means that we lack a complete understanding of how these systems work. This thesis presents two unique sets of repeat seafloor surveys of active submarine channel systems. First, ten repeat surveys of the submarine channel in Bute Inlet, British Columbia, Canada, are presented; each of which covers the system from source to sink. Second, a set of 20-year spanning surveys of the Congo Channel, offshore West Africa, is presented, which show for the first time how a major margin-scale submarine channel system evolves. These high resolution repeat surveys are analysed to document the nature and rate of erosion and deposition that occurs along submarine channel systems from source to sink for the first time. The overarching aim of this thesis is to use these observations to determine which processes control the evolution of submarine channel systems and how they modulate the transport of sediment to the deep sea. This aim is addressed through three sub aims. First, this thesis investigates which processes control the evolution of submarine channels. Previous studies have shown that processes such as meandering, the growth of levees, and the migration of bedforms can control channel evolution. Based on repeat surveys in Bute Inlet, the rapid upstream-migration of steep waterfall-like features, called knickpoints, are instead shown to play the most important role in submarine channel evolution than these other features. Similar knickpoints have been documented from seafloor surveys in many other submarine channels worldwide; hence this mechanism may be globally significant. Second, this thesis investigates how sediment is transported through the submarine channel in Bute Inlet and onto the terminal lobe, that is located at the distal end of the channel. Some sediment transport models suggest that sediment is transported directly from the head of a system to the lobe by a single turbidity current, while others suggest that submarine channel systems undergo cycles of filling and flushing. This thesis demonstrates that sediment is most likely to go through several steps of deposition and re-excavation before reaching the lobe. These steps of reworking are controlled by knickpoints and can generate zones of sediment

bypass on longer timescales. The delivery of sediment to the lobe is discontinuous and does not directly correlate with signals in sediment input into the system; hence, terminal lobes are not necessarily strong recorders of external environmental signals, as was previously often assumed. The third aim is to investigate how different processes control channel evolution along the length of a much longer margin-scale submarine channel system. This thesis shows that the Congo Fan system can be divided in three distinct zones based on the different processes observed: i) a proximal canyon dominated by canyon-flank collapses; ii) a meandering intermediate channel; and iii) a distal knickpoint-dominated channel. The transitions between these zones are controlled by channel maturity and basin structure. Although different zones are present, sediment can be temporarily stored and re-excavated along the entire margin-scale system. This thesis presents new insights into the processes that control submarine channel evolution, recognising that the role played by knickpoints may have been previously underestimated or entirely overlooked in many systems. Furthermore, this thesis shows how the nature of evolution in large submarine channels may act to both temporarily inhibit or promote sediment transfer to the deep sea. Dynamic seascape modification by recurrent flows of variable power ensures that sediment transfer to the system terminus is temporally staggered and discontinous, rather than continuous. In general, the repeat surveys reveal the complexities and importance of different internal processes in sediment transport, storage, re-excavation, and its ultimate fate. Submarine channel systems can be remarkably dynamic, with pronounced reworking along the entire length of active systems. New marine technology has and will continue to provide important new insights in understanding these dynamic systems that play a globally important role in sediment transfer.

Table of Contents

Table of Tables

Table of Figures

Table of Figures

Research Thesis: Declaration of Authorship

Print name: Maarten Sjaak Heijnen

Title of thesis: New Insights into Submarine Channel Evolution Revealed by Repeat Seafloor Mapping

I declare that this thesis and the work presented in it are my own and has been generated by me as the result of my own original research.

I confirm that:

1. This work was done wholly or mainly while in candidature for a research degree at this University;
2. Where any part of this thesis has previously been submitted for a degree or any other qualification at this University or any other institution, this has been clearly stated;
3. Where I have consulted the published work of others, this is always clearly attributed;
4. Where I have quoted from the work of others, the source is always given. With the exception of such quotations, this thesis is entirely my own work;
5. I have acknowledged all main sources of help;
6. Where the thesis is based on work done by myself jointly with others, I have made clear exactly what was done by others and what I have contributed myself;
7. Parts of this work have been published as:

Heijnen, M.S., Clare, M.A., Cartigny, M.J.B. et al. Rapidly-migrating and internally-generated knickpoints can control submarine channel evolution. Nat Commun 11, 3129 (2020). https://doi.org/10.1038/s41467-020-16861-x

Signature: ..... Date:.....

Acknowledgements

When I was writing this thesis, my supervisors told me I had to emphasise all the things that I did. This results in the thesis being presented as a rather individualistic piece of work, while in reality, I couldn't have done it by myself. There are many people who helped and supported me during the past 3.5 years, and I would like the opportunity to thank them here. There are more people than I can mention here, but you know who you are, and I would like to say thank you.

First and foremost, I couldn't have done this PhD project without Mike Clare, who was all and more I could wish for as a primary supervisor. Thank you for giving me the opportunity to start this PhD project, and supervising me through it. Your door was always open for me, and in the last year your webcam. You always had (made) time for me. You have guided me intellectually and professionally, and were good company in more informal occasions. You also stimulated me to take opportunities and make the most of my PhD. Thank you Mike, I am truly grateful for your endless support.

I am also thankful for having great co-supervisors in Pete Talling and Matthieu Cartigny. Thank you for all the scientific discussions. You have taught me many things, and provided much input along the way. Pete thank you for the continuing opportunities in the Congo project and the responsibilities you trusted, and still trust me with. This has stimulated and motivated me tremendously. Matthieu, bedankt voor alle knickpointdiscussies die we hebben gehad, die hebben me meermaals goed aan het denken gezet. Dank je voor hoe je me blijft betrekken bij het werk in Bute Inlet.

I would also like to thank everyone involved in the EU's Horizon 2020 Marie Skłodowska-Curie ITN project SLATE (grant agreement No 721403), for funding my PhD, and for providing training opportunities and a European network. Specifically, I would like to thank Michi Strasser for having me for two and a half months in Innsbruck, and for allowing me to learn new techniques here. Also thanks to the rest of the group in Innsbruck, especially Jasper Moernaut, Christoph Daxer, and Jana Molenaar. Furthermore, I would like to thank Katrin Huhn and Jannis Kuhlmann for the organisation of the SLATE project.

I would like to thank my examiners for taking the time to assess my thesis. Additionally, I would like to thank Hachem Kassem, who, as my panel chair, made sure my PhD was progressing and I was doing well. I would also like to thank Justin Dix for his help and supervision.

I was also fortunate to work with other collaborators and had very enjoyable experiences at various occasions. Firstly, many thanks to Gwyn Lintern and Cooper Stacey for providing the infrastructure to do the research in Bute Inlet, and for many interesting discussions while on the ship. I am also grateful for the time Brent Seymour spent to teach me about multibeam echosounders, and I also would like to thank Kim Conway for the company and scientific discussions. Also I would like to thank Peter Neelands, Brett Pickrill, and Jessica Rutherford for their support. I would further like to thank Steve Hubbard for many fruitful discussion and outside perspectives. I would like to specifically thank Steve for inviting me to the Magallanes Basin in Southern Chile. I would also like to thank Brian Romans, Ben Daniels, Rebecca Englert, Sebastian Kaempfe, Paul Nesbit, and Dan Bell for the great time in Chile. I acknowledge funding from the Society for Sedimentary Geology (SEPM), which allowed me to make the trip. Further collaborations include discussion on seafloor mapping and echosounders with John Hughes Clark, and Arnoud Gaillot, which greatly improved my understanding of the techniques. I am also grateful for the collaboration and discussions I had with Dan Parsons and Steve Simmons. I have also enjoyed working with and learning from Ed Pope at several occasions during my PhD. Lastly, I would like to thank Ricardo Silva Jacinto for both good company as well as interesting scientific discussions.

I was fortunate to be able to travel all around the world during my PhD for conferences, research cruises and fieldwork. I would like to thank Jane Goswell for her support in arranging all the travel. I would also like to thank the captains, crews, and technicians from CCGS *Vector* and RV *James Cook* for the safe and comfortable voyages, and for enabling science at sea.

I've enjoyed the various coffee meetings and pub trips, as well as scientific discussion with the sedimentology group at Southampton. Thanks to Esther Sumner and James Hunt, as well as my peers Maria Azpiroz, Lewis Bailey, Sophie Hage, Age Vellinga, Daniela Vendettuoli, and Zaki Zulkifli. I have also enjoyed the contact I have had with my peers from the extended turbidity current monitoring group including Megan Baker, Ye Chen, Martin Hasenhündl, Kate Heerema, Claire McGhee, and Sean Ruffell.

I also would like to thank the British Sedimentological Research Group, for providing training opportunities and field trips as well as enabling me to meet and spend time with fellow PhD students.

I would also like to thank Joris Eggenhuisen and João Trabucho for supporting me during the application process for this position, and for continuous support, collaboration, and creating opportunities, even after I left Utrecht University. I also would like to thank Ian Harding for all the

demonstrating opportunities, as well as for being pleasant company during several occasions throughout my PhD.

More personally, I would like to thank all the amazing people I met at the National Oceanography Centre Southampton, including my amazing friends Manon Duret, Stacey Felgate, Africa Gomez, Alex Hately, Holly Jenkins, Joe Jones, and Alex Tribolet. Furthermore, I have enjoyed the many tea breaks I've had with all my office mates, including Flo Atherden, Mike Buckingham, Hannah Connabeer, Spencer Long, and Ella McKnight.

Daarnaast wil ik natuurlijk mijn ouders bedanken voor hun steun, advies en liefde. Dank je papa en mama, ik hou van jullie. Verder zijn er nog ontzettend veel vrienden in Nederland die er nog altijd voor me zijn, ook al woon ik niet meer in Nederland. Met een aantal is de band nog net zo sterk, of zelfs sterker geworden, sinds ik weg ben uit Nederland. Ik kan niet iedereen hier noemen, maar ik wil wel graag even Stan, Astrid en Balfred noemen, en ook Jorieke, Nanique, en Suzanna.

Lastly I would like to thank Rhodri for his continuous support, pleasant distractions, joy, and love. You have made my life a lot better over the last two years. I would have a lot of dishes saved up by now, if it wasn't for you. Ooh and I'll let you know when we're having traditional apple strudel and pinot grigio again. Bye.

Chapter 1 Introduction

1.1 Thesis Rationale

Submarine channel systems form some of the largest sediment routing systems on our planet, and are the main conduits for sediment transfer to the deep-sea (Shepard, 1981; Nyberg et al., 2018). These extensive geomorphological features can be found on all of the world's continental margins (De Leo et al., 2010; Harris and Whiteway, 2011). Seafloor-hugging flows of sediment (called turbidity currents) carve and maintain submarine channel systems and can run out for 100s to 1000s of kilometres (e.g. Heezen and Ewing, 1952; Khripounoff et al., 2003; Talling, 2014). The term submarine channel system is used in this thesis to refer to all types of submarine canyon, channel, and fan systems maintained by turbidity currents (or other types of submarine density flows).

This thesis focuses on understanding how: (i) submarine channel systems evolve; and (ii) how sediment is transported through them. All changes to the shape, dimension, or position of any part of a submarine channel system are regarded as channel evolution in this thesis. This evolution is predominantly the result of the interaction of turbidity currents with the substrate in and around the channel. It is important to understand the evolution of submarine channel systems, and the erosional and depositional processes that govern it, because this controls the pathways, timescales and fate of shallow-to-deep-sea transport of sediment, organic carbon, nutrients, and pollutants, (Canals et al., 2006; Galy et al., 2007; Vangriesheim et al., 2009; Azaroff et al., 2020; Hage et al., 2020). Furthermore, understanding the erosional and depositional patterns in and around submarine channel systems helps to assess which areas are prone to geohazards, threatening seafloor infrastructure such as seafloor cables. These cables underpin the internet we use in our daily lives by carrying >95% of global digital data transfer (Carter et al., 2009). Lastly, understanding how submarine channel deposits are formed and the nature of their internal architecture, is important, as they can form important hydrocarbon reservoirs (e.g. Mayall et al., 2006; Baudin et al., 2010).

Sediment transport via submarine channel systems has been suggested to be either direct (i.e. as a result of individual flows that travel from source to deep-sea sink), or as a result of staged transport, whereby flows do not always travel the full length of the submarine channel systems, causing temporary storage (i.e. channel 'filling') and episodic re-exhumation by subsequent longer runout flows (i.e. channel 'flushing') (e.g. Stevenson et al., 2013; Allin et al., 2016). Such steps of temporal burial and re-exhumation can allow previously buried organic carbon to be oxidised. So,

understanding these pathways and the timescales associated with them is important for understanding how efficiently submarine channels 'pump' terrestrial material, including organic carbon into the deep-sea and sequester it during burial (Baudin et al., 2017; Hage et al., 2020). Furthermore, understanding sediment transport through submarine channels is vital in understanding what environmental signals might be preserved in the different deposits left behind (e.g. Prins and Postma, 2000; Moernaut et al., 2014; Burgess et al., 2019).

Due to the powerful and episodic nature of turbidity currents, and the remote locations in which they tend to occur, direct measurements of submarine channels and sediment transport through them have been challenging to obtain (Inman et al., 1976; Prior et al., 1987; Khripounoff et al., 2003; Puig et al., 2014; Sumner and Paull, 2014; Azpiroz-Zabala et al., 2017a; Clare et al., 2020). Therefore, most previous work has necessarily been based on indirect approaches to study submarine channels. Such approaches include scaled-down laboratory experiments, numerical modelling, geophysical (seismic) subsurface analysis, outcrop studies, sediment coring, non-repeat seafloor mapping, and theoretical work including comparisons to rivers (e.g. Heiniö and Davies, 2007; Paull et al., 2011; Sylvester et al., 2011; Armitage et al., 2012; Stevenson et al., 2013; Hubbard et al., 2014; de Leeuw et al., 2016). Many of these studies have advanced our general understanding of submarine channel systems and turbidity currents significantly. However, these methods pose a range of limitations when studying the evolution of individual channels, and how sediment is transported through them. Laboratory experiments suffer from scaling issues, and numerical models lack validation with full-scale field data (Talling et al., 2015; de Leeuw et al., 2016). Field-scale data, such as seismic and outcrop studies, only capture the resulting stratigraphy, making it difficult to understand the role of episodes of erosion and the timescales over which a dynamic seascape changes (e.g. Sylvester et al., 2011; Talling et al., 2015; Covault et al., 2016). Furthermore, subsurface data often lack the resolution to image features within individual channels. Outcrops may allow this level of resolution, but also lack the time constraints on these features, and furthermore usually lack a three dimensional perspective. The lack of a three dimensional perspective also holds for sediment cores. Models derived from comparisons with rivers, or theoretical work also require real-world validation. Furthermore, submarine channels also are suggested to differ in several key aspects from rivers, such as meandering and secondary flow (e.g. Peakall et al., 2000; Corney et al., 2006; Imran et al., 2007; Jobe et al., 2016). Lastly non-repeat seafloor surveys lack information on temporal change measurements, needed to study sediment transport and channel evolution. Hence, due to this lack of data, much less is known about these underwater systems compared to rivers, which have been directly monitored for decades, and can be studied using satellite imagery (e.g. Constantine and Dunne, 2008). Submarine channels and turbidity currents require instruments to be moored

on the seafloor to measure turbidity currents, and repeat seafloor mapping efforts to image their evolution (Talling et al., 2015; Clare et al., 2020).

Recent technological advances in seafloor surveying have catalysed efforts to map submarine channel systems (e.g. Greene et al., 2002; Babonneau et al., 2002; Conway et al., 2012). However, repeat seafloor mapping studies of submarine channels, which show how these systems evolve, remain relatively scarce. Furthermore, repeat seafloor mapping can provide the first steps towards understanding how changes in geomorphic surfaces can result in stratigraphic surfaces (Sylvester et al., 2011; Talling et al., 2015; Hage et al., 2018; Vendettuoli et al., 2019). Repeat seafloor surveys of submarine channels have been performed at around 20 locations worldwide at the time of thesis submission (Table 2.1); however, most of these studies only cover part of a submarine channel system, span only two to four years, or cover very small systems < 10 km long (e.g. (Paull et al., 2010; Hughes Clarke et al., 2014). A longer term (>4 years) time-lapse investigation of a longer (>15 km long) submarine channel system over its full length from source to sink has never been published. This ensures that the evolution of submarine channels on decadal timescales is still unknown.

Besides repeat seafloor mapping, efforts to directly monitor turbidity currents have also rapidly grown over the last decade. Advances from some of these studies include new models of the internal structure of turbidity currents (Azpiroz-Zabala et al., 2017a, b; Paull et al., 2018). Furthermore, these studies showed that these systems were much more active than previously thought, as well as turbidity currents themselves lasting up to 10 days (Azpiroz-Zabala et al., 2017). Other studies have directly observed the migration of bedforms as a result of the interaction between turbidity currents and the substrate (Hughes Clarke, 2016). However, there has never been a dataset showing the occurrence of turbidity currents along a full-length submarine channel, nor has an integrated dataset of turbidity current monitoring and repeat seafloor mapping over a full submarine channel system been published in order to understand sediment transport through submarine channels.

Therefore, there is a compelling need for more extensive and longer timescale repeat seafloor surveys of submarine channels from sediment source to sink to understand how these channels evolve. Furthermore, there is a need for turbidity current monitoring along the full length of a submarine channel as well as the integration between repeat seafloor mapping and their integration with other monitoring techniques. Filling these knowledge gaps is the overarching aim for this thesis.

1.2 Structure and aims of the thesis

This thesis aims to understand the processes that control how submarine channel systems evolve and how these processes affect sediment transported through these systems. High resolution repeat seafloor surveying along the full length of two highly active submarine channel systems over timescales of years to decades are used here to address this aim (Figure 1.1). Repeat seafloor surveys of the active submarine channel system in Bute Inlet, British Columbia, Canada are presented in chapter 2 and integrated with a turbidity current monitoring dataset in chapter 3. The channel in this fjord is around 40 km long and runs from the feeding rivers at the head of the fjord to the floor of the fjord at 660 m water depth. Repeat seafloor surveys from the active submarine channels system on the Congo Fan, offshore west Africa, is presented in chapter 4. The active channalised system starts at the mouth of the river and runs for over 1000 km until reaching a depth of around 5000 m. These datasets are used in these main science chapters to address the following sub-aims:

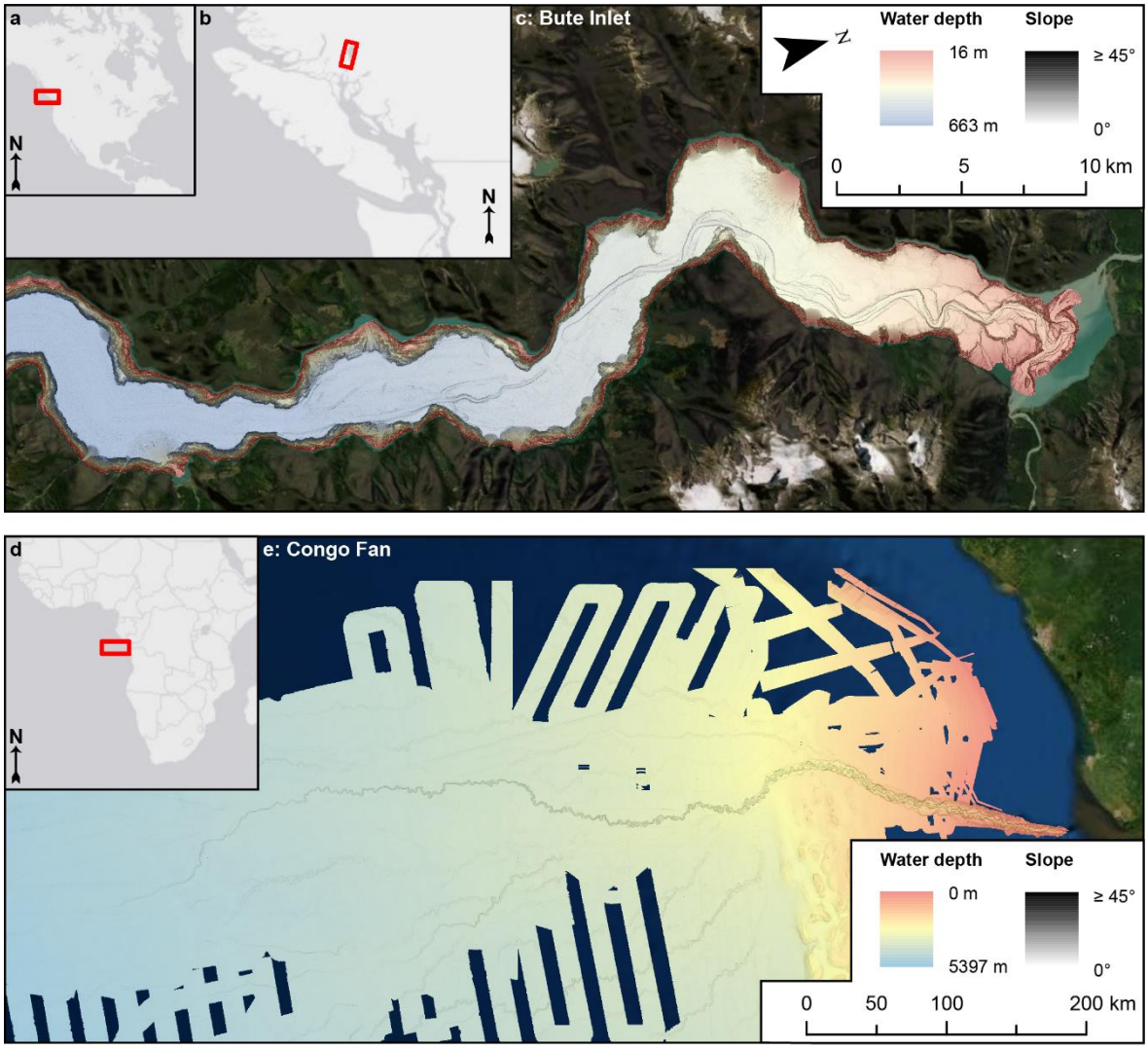

Figure 1.1: Location and overview of Bute Inlet and the Congo Fan. a-b) Location of Bute Inlet. c) Bathymetric overview of the top of Bute Inlet. A 40 km long channel is present on the floor of the fjord that runs from the two feeding rivers until the floor of the base of the fjord at 660 m water depth. d) Location of the Congo Fan. e) Bathymetric overview of the active part of the Congo Fan. The active channel connects to the mouth of the Congo River, is over 1000 km long and reaches a depth of around 5000 m. Background layers a, b and d: Esri, Here, Garmin, © OpenStreetMap contributors, and the GIS user community. Satellite imagery c and e: Esri, DigitalGlobe, GeoEye, Earthstar, Geographics, CNES/Airbus DS, USDA, USGS, AeroGRID, IGN, and the GIS User Community.

Chapter 2: Which processes control the evolution of submarine channels?

The erosional and depositional processes, and resulting channel evolution, has not yet been repeatedly mapped over the full length of a submarine channel. Several studies and comparisons to rivers have suggested meandering is an important control on submarine channel evolution (e.g. Sylvester et al., 2011; Peakall and Sumner, 2015; Covault et al., 2019). However, modern seafloor data suggests that migration of seabed features such as crescentic bedforms and knickpoints can also play a role in controlling how channels evolve (e.g. Covault et al., 2014, 2017; Vendettuoli et al., 2019; Guiastrennec-Faugas et al., 2020a, b). This chapter uses five repeat seafloor surveys, spanning nine years, covering the full length of the submarine channel in the fjord Bute Inlet, British Columbia, Canada. These surveys show how the upstream migration of knickpoints can be the dominant control on how submarine channels evolve. The chapter concludes with a new model for submarine channel evolution based on these new observations.

Chapter 3: How is sediment transported through a submarine channel and onto the lobe?

Several models have been proposed for how sediment is transported by turbidity currents through submarine channels. One of these models suggests that sediment is transferred through submarine channel systems directly without eroding or depositing in the channel (Stevenson et al., 2013). However, other models suggest that submarine channel systems undergo more complex cycles of filling and flushing (Paull et al., 2005; Allin et al., 2016; Mountjoy et al., 2018). An integrated monitoring approach consisting of a decade of repeat seafloor mapping, turbidity current monitoring, and discharge measurements of the main feeding river is used in this chapter to document how sediment is transported through a knickpoint-dominated submarine channel and onto the lobe. Such an approach permits the testing of these existing models of sediment transport through submarine channels, as well as the synthesis of a new model based on the spatial and temporal patterns of erosion and deposition observed. This chapter also explores how this new model impacts the completeness of the resulting stratigraphy, which has implications for

the long-term burial efficiency of organic carbon and the fidelity of submarine channel deposits as recorders of environmental signals.

Chapter 4: How do different processes control channel evolution along the length of a large deep-sea submarine channel system?

Previous studies, and chapters 2 and 3, have shown that different processes can control submarine channel evolution in different systems, or in different parts of individual systems. The third chapter presents a repeat seafloor dataset of one of the largest submarine channel systems in the world (the Congo Fan), to determine how such a large system behaves and evolves. The chapter discusses the nature, rate, and quantity of erosion and deposition that results from spatially and temporally variable processes along the system's length. The chapter continues by discussing how basin structure and channel maturity control the spatial distribution of these different processes. These findings have important implications for the longer-term storage and ultimate fate of sediment in the deep-sea.

Each of the three main science data chapters (i.e. chapters 2 to 4) is presented in the style of a scientific paper, with its own introduction, methods, and geographical setting sections. This introductory chapter gives a broader overview by explaining how these chapters are linked and to give more background on the development of studies focused on the mapping submarine channel systems, and provides some further methodological background. The thesis is concluded in chapter 5, by synthesising future research perspectives from the results of this thesis.

1.3 Historical perspective: Discovery of submarine channel and technologies used to study present-day submarine channel systems

Single-beam echosounders were developed at the end of the 19th century as a naval tool for surveying water depths in the oceans. These instruments determine the water depth by measuring the two-way travel time of an emitted sound wave. Echosounders were soon incorporated in marine geology, where they remain to this day one of the primary tools for imaging the seafloor. An initial spike in efforts, followed by the widespread use of these echosounders in the early 20th century led to the discovery of canyons and channels present on the seafloor in many lacations across the world's oceans (Spencer, 1903; Shepard, 1933 and references therein). Initially these canyons and channels were interpreted either as being formed by rivers during phases of lower sea level, such as during glaciations (e.g. Shepard, 1933), or as a result of faulting (e.g. Gregory, 1931). However, a few years later submarine canyons and channels were interpreted to be created and maintained by seafloor flows of suspended sediment (Daly, 1936). Scaled-down versions of these gravity-driven flows were later successfully generated

in flume tank experiments, leading to a more general acceptance of the hypothesis and naming the flows 'turbidity currents' (Kuenen, 1937).

At around the same time, a turbidity current was triggered as a result of the M_w7.2 Grand Banks Earthquake offshore Newfoundland in 1929. Later analysis of the event showed that the passage of the turbidity current was recorded by a series of breaks in seafloor telecommunication cables (Heezen and Ewing, 1952). The timings of these cable breaks provided the first documented velocity data from a turbidity current, which locally reached 20 m/s, and demonstrated that these submarine mass flows can pose a significant hazard to seafloor infrastructure.

The next major discovery in the field was that large submarine fans are formed downstream of submarine canyons (Menard, 1955). These fans were shown to be traversed by submarine channels, which distribute sediment from the canyon mouth over the fan. Next was the development of depositional models for turbidity currents. The first was described in the early 1960s as a general idealised depositional sequence, referred to as the Bouma sequence (Kuenen and Migliorini, 1950; Bouma, 1962).

The late 1960s until the late 1980s were characterised by an increase in efforts in mapping and studying present-day submarine channel systems. The scientific objectives also moved from just mapping submarine channel systems to understanding their features and patterns, initiation, and evolution (see references in Normark, 1970, 1978; Mutti and Normark, 1987). In terms of technology, sidescan sonar was developed around this time, which images the reflectivity of the seafloor, while being towed behind a vessel. This deep-towing allowed the instrument to be much closer to the seabed, enabling the acquisition of higher-resolution seafloor reflectivity data. Seafloor reflectivity from these sidescan sonars allowed qualitative assessment of the orientation and composition of the seafloor in unprecedented detail (e.g. Damuth, 1983; Farre et al., 1983). Several studies integrated different types of techniques including echosounders, side-scan sonar, and sub-bottom profilers (e.g. Normark, 1970; Scholl et al., 1970; Gnibidenko and Svarichevskaya, 1984).The world's largest submarine channel systems were also mapped for the first time in these years, such as the Congo (Heezen et al., 1964), Amazon (Damuth and Kumar, 1975), Bengal (Curray and Moore, 1971), and Indus (Kolla and Coumes, 1987) fans.

Other technological advances developed around this time included the first successful efforts of monitoring real-world turbidity currents in relatively small-scale systems; channels in fjords in British Columbia, Canada (Hay et al., 1982; Prior et al., 1987; Zeng et al., 1991; Bornhold et al., 1994). Flow monitoring, however, was not pursued much after these efforts until the development of Acoustic Doppler Current Profilers (ADCPs) which started a new spark in turbidity current monitoring in the early 2000s, and has been the dominant technology used in turbidity

current monitoring ever since (e.g. Xu et al., 2004; Hughes Clarke, 2016). These instruments can measure the velocity of flow by emitting a sound pulse and then measuring the Doppler shift in these sound waves as they are reflected from suspended particles in the water.

The next, and maybe the most revolutionary recent technological advance in seafloor imaging has been the multibeam echosounder (or swath echosounder). Multibeam echosounders were developed and first used in the early 1980s and became a common tool in the study of present-day submarine channels by the 1990s (e.g. Taylor and Smoot, 1984; Pratson et al., 1994; Hagen et al., 1996; Kodagali and Jauhari, 1999; Locat and Sanfaçon, 2000). These echosounders use a fan of narrow beams orientated across the ship's track, opposed to the one vertical beam used in single beam echosounders. This fan shape allows multibeam echosounders to map the seafloor over an area, rather than along a line, as with singlebeam echosounders (e.g. Hughes Clarke, 2018a). Multibeam echosunders, especially combined with the improvements to the global positioning systems, allowed the construction of detailed elevation models. It is this data quality that allows quantitative comparisons between repeat surveys, which is the fundamental technique applied in this thesis.

1.4 Submarine channel systems: the basics

This section introduces some terminology and concepts associated with submarine channel systems that are used throughout this thesis.

1.4.1 Morphology of submarine channel systems

In this thesis I use the term 'submarine channel system' as a general term for any type of confined conduit created and maintained by turbidity currents (or any other sediment density current). Many ocean scale submarine channel systems consist of an upstream canyon incised into the shelf, and a fan at the mouth of the canyon (Menard, 1955; Figure 1.2). Submarine channels cross this fan and depositional lobes form at their termini (Normark, 1970). Usually only one of these channels is active at a time. Aggradation and avulsion of these channels and lobes forms the higher hierarchical level referred to as fans (e.g. Normark, 1978; Flood et al., 1991). Some older studies refer to these channels as 'fan valleys' (e.g. Normark, 1970). In some systems, certain parts of a submarine channel system might not be as well developed. For example, systems can lack a distinguishable canyon and channel when they are smaller or younger, or when they are in locations without clear shelf, such as lakes and fjords (e.g. Vendettuoli et al., 2019). In cases where there is no clearly distinguishable canyon or channel, the entire conduit is referred to

as a channel in this thesis. Furthermore, younger systems or laterally confined systems, such as in fjords, might not have a radial fan, but are more linear in shape (e.g. Zeng et al., 1991).

The aims of this thesis concern individual channels and lobes and these aims are addressed through the analysis of datasets spanning years to decades. Implications of the results discussed in this thesis will span from a few years up to the 'life cycle' of a single channel (Fildani et al., 2013; Maier et al., 2013; Hodgson et al., 2016). Channel life cycles have been established mainly through subsurface and outcrop data, and consist of: (i) an inception phase, during which the channel forms and deepens, but is relatively straight; (ii) a maintenance phase, during which the channel reaches is maximum depth, and sinuosity, and can aggrade; and (iii) abandonment, during which the moves away from the current channel the channel is filled. All analyses and implications described in this thesis are well below the timescales on which fans develop, or even individual channels avulse over fans.

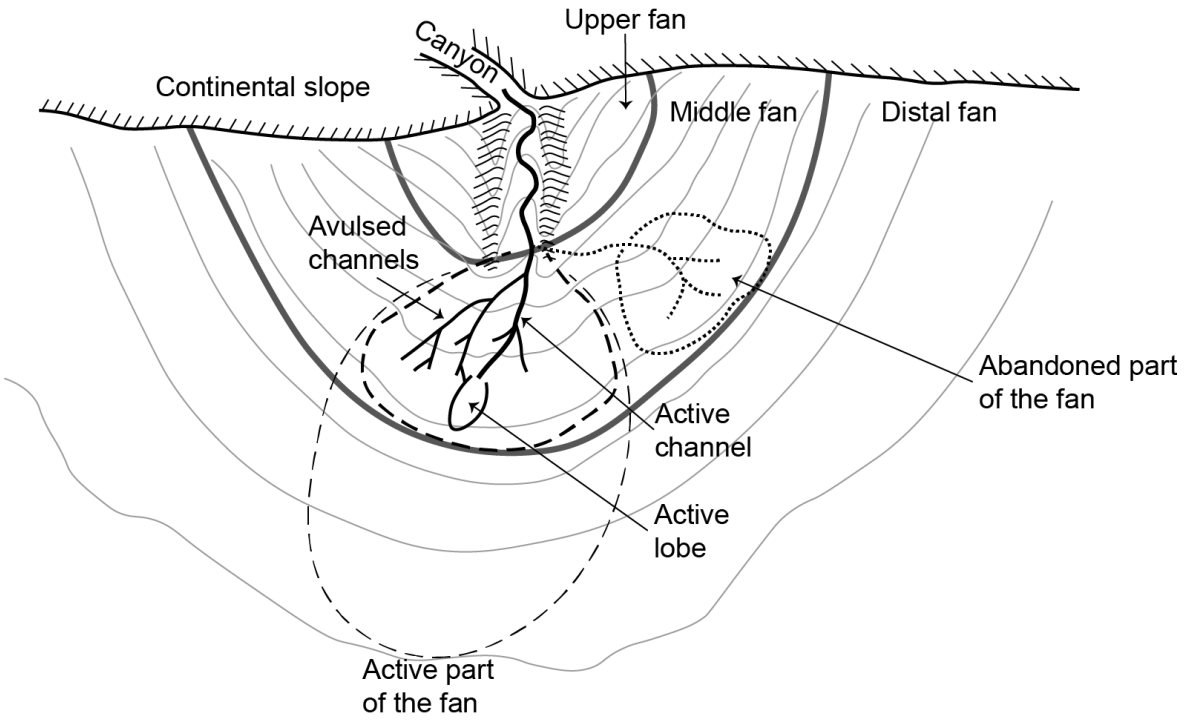

Figure 1.2: Schematic model of a submarine fan (redrawn from Normark, 1978). The fan is the depositional part of a submarine channel system that is often fed by a canyon. The transition from canyon to the channel on the fan typically coincides with a break of slope such as at the base of the continental slope. The fan is formed by avulsion of channels and their depositional terminal lobes. Activity on the fan tends to be focussed in one part of the fan with relatively local avulsions, until a major avulsion occurs and the activity shifts to a different part of the fan (e.g. Picot et al., 2016).

1.4.2 Features within canyons, channels and lobes

This section summarises some of the features and terminology associated with submarine channel systems, and how they might be formed. Channels are typically elongated concave-up geomorphic features, and come in a range of shapes and sizes (e.g. Deptuck and Sylvester, 2018). The path along the deepest point of the channel is referred to as the thalweg (Figure 1.3). This thalweg is not necessarily in the middle of the channel, but can be located towards one side of the channel resulting in an asymmetric channel shape, which is common, for example, in meandering channels where the thalweg is located towards the outer bend (Figure 1.3d; e.g. Babonneau et al., 2002; Reimchen et al., 2016). The flanks of the channel can be characterised by sub-horizontal steps, commonly referred to as terraces (Figure 1.3; e.g. Babonneau et al., 2004; Paull et al., 2013). Terraces can be formed through incision and lateral migration, or through deposition in and around channels (e.g. Hansen et al., 2017). The term terrace is most commonly used, however depositional steps can be referred to as bars, benches, or inner levees (e.g. Hübscher et al., 1997; Nakajima et al., 2009; Maier et al., 2013). As the difference between depositional and erosional steps is not always obvious, the term terrace is used in this thesis for all sub-horizontal steps along channel flanks.

Channels are often bound by features elevated above the surrounding seafloor that taper-out away from the channel (Figure 1.3). These features are referred to as levees (e.g. Flood et al., 1991; Babonneau et al., 2002; Curray et al., 2002). Areas outside of the channel that are influenced by the channel system are called the overbanks. These areas are affected by turbidity currents that are higher than the depth of their confinement. When this happens, the top of such flows can flow over the edge of the channel and onto the overbank. This is referred to as overspill, and is especially common around channel bends (Kane and Hodgson, 2011). This overspill can generate bedforms commonly referred to as sediment waves (Figure 1.3b; e.g. Carter et al., 1990; Migeon et al., 2000)

Lastly, a whole range of different bedforms are occur within the channels, which are increasingly recognised based on increasing resolution of seafloor surveys (e.g. Symons et al., 2016). One of the more commonly identified bedform type is crescentic bedforms which are smaller than sediment waves on the overbanks and are often linked to cyclic step instabilities in turbidity currents (e.g. Paull et al., 2010b; Hughes Clarke, 2016).

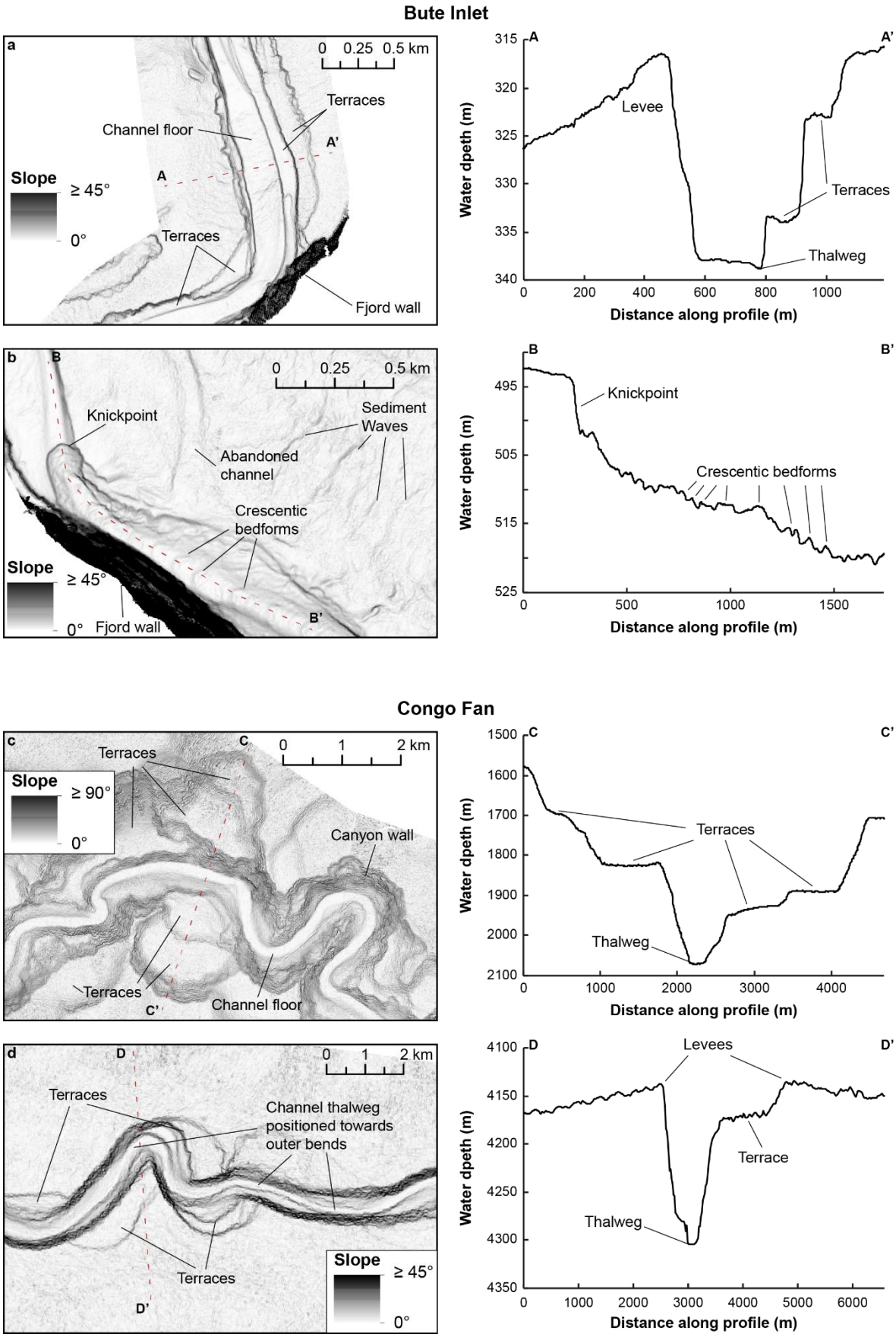

Figure 1.3: Examples of sections along the channels from Bute Inlet and the Congo Fan containing features commonly observed in submarine channels. a) A section along the channel in Bute Inlet,

showing several steps of terraces and a levee. The terraces are elongated and not clearly linked to channel bends. b) A section along the channel in Bute Inlet showing a knickpoint, crescentic bedforms, and sediment waves. c) A section along the Congo Canyon showing several steps of rounded terraces. d) A section along the channel on the Congo Fan showing a sinuous with curved terraces that appear to be related to the bends. Also note the presence of levees.

1.5 Multibeam echosounders and survey design in this thesis

1.5.1 How do multibeam echosounders work?

A multibeam echosounder consists of a tranducer array and a receiver array. The transducer applies beamforming and beam steering to generate a sound wave that is made up of many different beams. These beams are directed to form a swath perpendicular to the orientation of the ship's track (Figure 1.4a). This sound is then reflected off the seafloor and recorded by the receiver array, which consists of a series of individual receivers that listen for sounds from a specific direction. The measured two-way travel time of the beams allows determination of the water depth. The design of multibeam echosounders thus enable depth measurements over an area as the vessel is moving.

Several variables have to be taken into account when designing a multibeam survey. First, the frequency (or frequency range) of the multibeam echosunder. Higher frequency echosounders can resolve the seafloor elevation with a higher vertical accuracy. However, higher frequency sounds are attenuated more easily by water, so do not work in deeper waters. The water depth, therefore, controls what frequency multibeam echosounders should be used. Typical multibeams operate at 500 kHz in coastal waters, up to 12 kHz in the deepest oceans. Second, the number of beams, often referred to as amount of sounding, the system produces per swath has to be considered. The more beams per swath, the better the quality of the data. The number of beams is set for a certain system and newer systems of the same type will tend to have more beams per swath. Another way to increase the number of soundings, is through dual swath systems. These multibeam echosounders produce two parallel swaths of beams, to increase the amount of soundings. Another set property of multibeam echosounders is the angle of the beams generated by the transducer (Figure 1.4a). The angle of the individual beams determines the footprint of each sounding on the seafloor. If this footprint is smaller, smaller scale features can be resolved. Lastly, the maximum width of the swath has to be set (Figure 1.4), which in current models can be as big as six times the water depth (swath angle of 140°). However, the swath width can be decreased, if desired. High swath widths are preferable when coverage is the main aim of the

survey. However, if the highest resolution is desired, smaller swath widths are preferred, as this focuses the same number of beams in a smaller area, resulting in a higher sounding density.

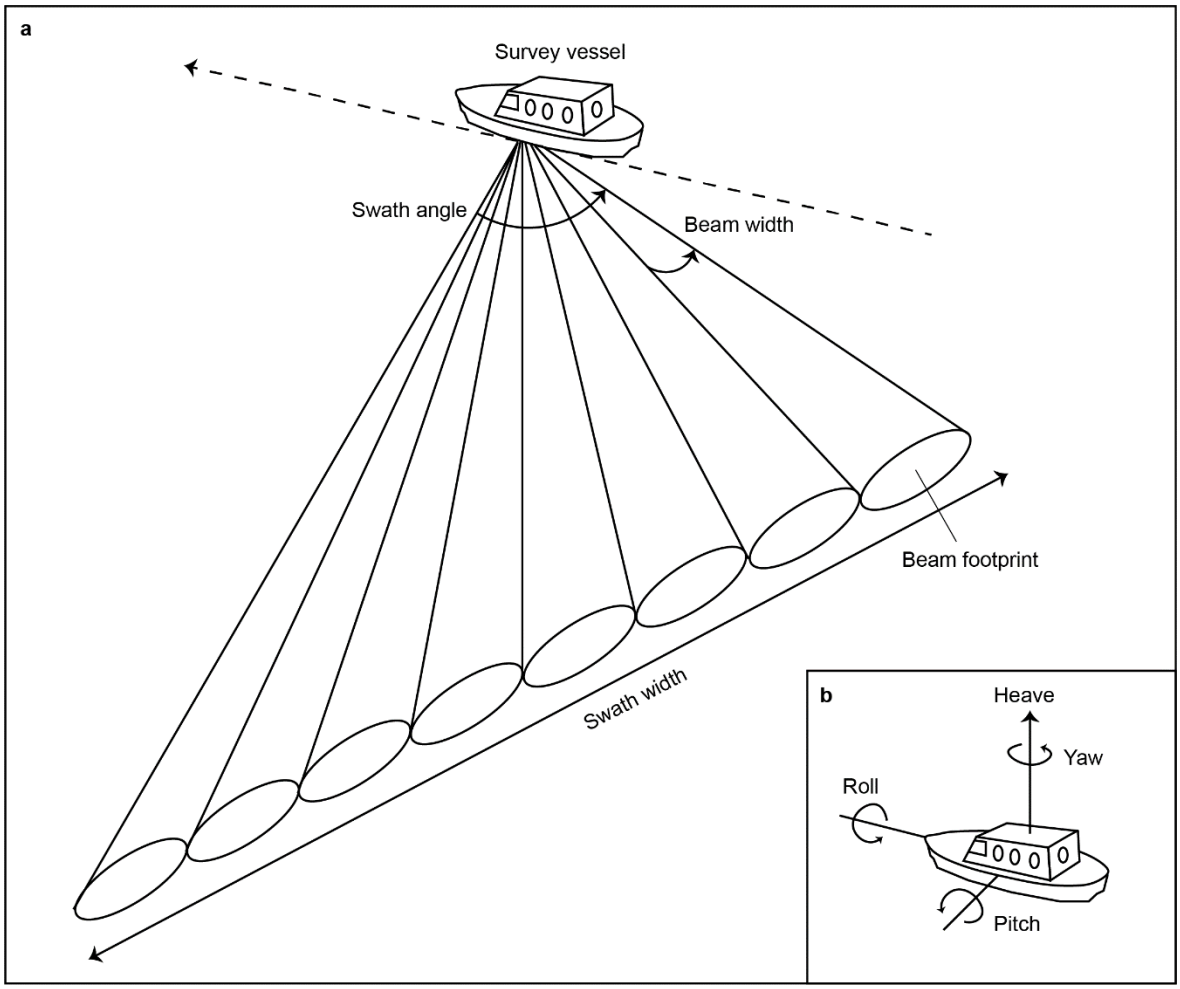

Figure 1.4: Principles of multibeam echosounders and surface vessel motions. a) schematic overview of some of the parametres of a multibeam survey. Not how swath width and beam footprint will increase with water depth (after Seabeam, 2000). b) common types of motions that cause errors in seafloor surveying when not corrected for properly.

1.5.2 High resolution mapping in this thesis

The term 'high resolution' is often attributed to newly acquired bathymetry surveys, since resolution typically increases as technology develops. Furthermore, the term high resolution is often used subjectively, and cannot be straightforwardly linked to a certain grid size of the resulting digital elevation model. This thesis uses high resolution bathymetry data to indicate the results of a survey that is designed to achieve high resolution data given a certain water depth and using the available technology at that time. This is in contrast to surveys that aim to cover a large area. This section first discusses what influences the vertical accuracy and horizontal resolution of multibeam bathymetry. This is followed by a description of how the multibeam

surveys, of which the results are presented in this thesis, have been designed and how this design results in bathymetry data with a high resolution.

The horizontal resolution of multibeam bathymetry is the result of sounding density and the footprints of individual beam width. Sounding density refers to the amount of soundings per area. The higher the sounding density, the higher the resolution. However, if sounding density is high enough, the resolution of multibeam bathymetry is limited by the footprint of individual beams. This footprint ensures that features smaller than this cannot be resolved. However, a grid size finer than the beam footprint can be helpful, if the sounding density is high enough, as it can show the overall shape of larger features in more detail. The footprint of individual beams increases with water depth, while sounding density decreases with water depth, so horizontal accuracy rapidly decreases with water depth.

The vertical accuracy of multibeam bathymetry is also affected by several factors. First, multibeam echosounders themselves have an accuracy that varies with water depth and typically is between 0.2% – 0.5% of the water depth, depending on the device. Vertical accuracy can be further compromised as a result of changes in the water column structure. Typically, the vertical structure of the water column is accounted for upon commencing a survey, either through a sound velocity profile taken at the start of the survey, or historical sound velocity databases. However, the vertical velocity structure can be subject to spatial and temporal variation. Such variations are especially common in coastal environments, and fjords, where different water bodies collide. Stratification of the water column can refract beams, therefore outer beams (higher angle of incidence) are especially affected by variations in the structure of the water column. Lastly, the vertical accuracy can be affected by errors related the ship's motion. Although the ship's motion is corrected for, when acquiring multibeam data, motion sensors have errors of their own. Errors in heave, pitch, roll, and yaw corrections can all lead to reduced vertical accuracy (Figure 1.4b).

Therefore, both horizontal resolution and vertical accuracy of multibeam bathymetry obtained using a surface vessel progressively decrease with increasing water depth. So, a certain grid size might be regarded as high resolution in deep water, but as low resolution in shallow water. Therefore, regarding high resolution as a survey design property that opposes high coverage, rather than a certain grid size, makes it a usable term in all water depths. However, the development of unmanned underwater vehicles such as Remotely Operated Vehicles (ROVs) and Autonomous Underwater Vehicles (AUVs), which maintain a fixed height above the seabed, can result in seafloor surveys in deep water with the resolution of surveys in shallow water (Huvenne

et al., 2018). However, ROV or AUV surveys of submarine channels remain uncommon and often only cover small areas (Paull et al., 2011; Dennielou et al., 2017).

The high resolution surveys presented in this thesis have all been obtained with a reduced swath width (90°), which decreases coverage, but increases the sounding density. Furthermore, they consist of highly overlapping survey lines, that ensure that the features of interest (the submarine channel) are surveyed multiple times, from different angles, by the inner part of the swath (Hughes Clarke, 2018b). This inner part of the swath uses a different type of pulse (CW pulse, instead of FM pulse), which results in more accurate data (Hughes Clarke, 2018b). Lastly, the surveys have all been obtained using low speeds of around 5 to 6 knots, which increases sounding density.

1.5.3 Distinguishing real patterns of change from noise and error, on scales close to the vertical accuracy

Scientific objectives when analysing seafloor data, especially seafloor change, often reach as far as (or further than) what can be visualised with multibeam echosounders mounted on surface vessels. It is therefore important how to distinguish what patterns in the seafloor data are generated by noise or other errors, and which might be actual seabed change. As data resolution is often the main limitation in analysing seabed change, it is important to be able to use the surveys to their full potential, and understand how to distinguish between errors and real change (e.g. Hughes Clarke, 2018b). This section first shows error patterns in multibeam difference mapping, encountered in this thesis, and other potential errors. This section then continues by showing a few examples of seabed change close to the scale of the background noise or magnitude of other errors, that still can be interpreted as real change. The section ends by setting up a few criteria for making this distinction.

Random noise is generated as a result of the overall accuracy of the multibeam echosounder and survey set-up (Hughes Clarke, 2018a). The overall pattern of this error is typically random and tends to be equal to the general vertical accuracy associated with regular multibeam surveying of up to 0.2% – 0.5% of the water depth (Figure 1.5). However, in theory this error can be twice the size of this vertical uncertainty.

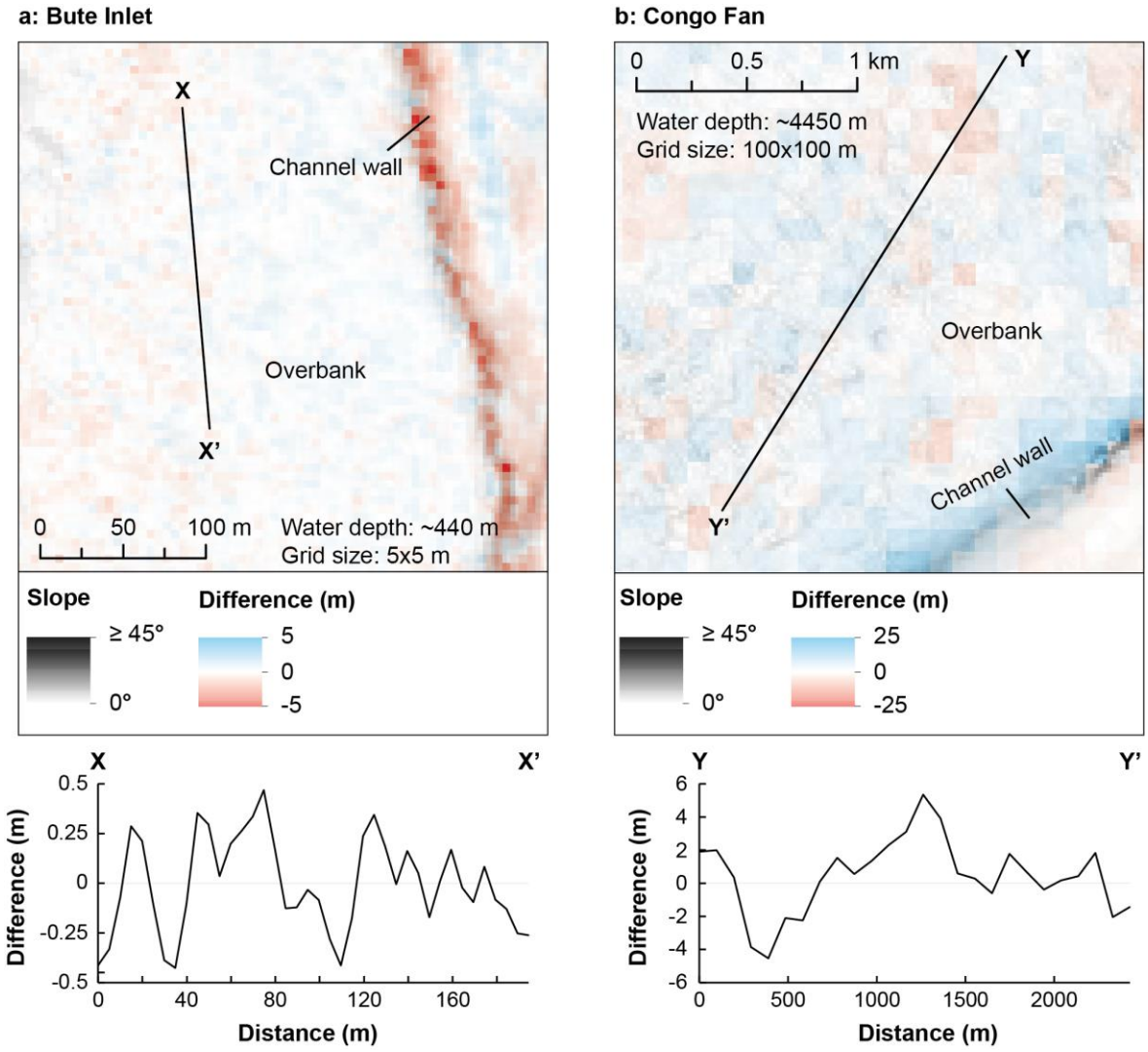

Figure 1.5: Examples of noise in difference maps. a) noise on the overbanks of the submarine channel in Bute Inlet. b) noise on the overbanks of the Congo submarine channel. Note how the noise is much smaller in the shallower waters of Bute Inlet.

Another common error pattern in difference mapping is differences aligned with the survey track lines. These errors express themselves as errors along the edges of a survey, if the track lines were orientated along the edge of one of the surveys (Figure 1.6). However, when the track lines are oriented in the direction across the edges this error will express itself as regular waves of errors (Figure 1.7). These errors can have a range of causes, such as a systematic error in the correction of the roll of the ship, or uncaptured variations in sound velocity structure of the water column. All these causes especially affect the more outer beams of swatches, and therefore, these errors are partly subdued in high resolution surveys that limit the swath width.

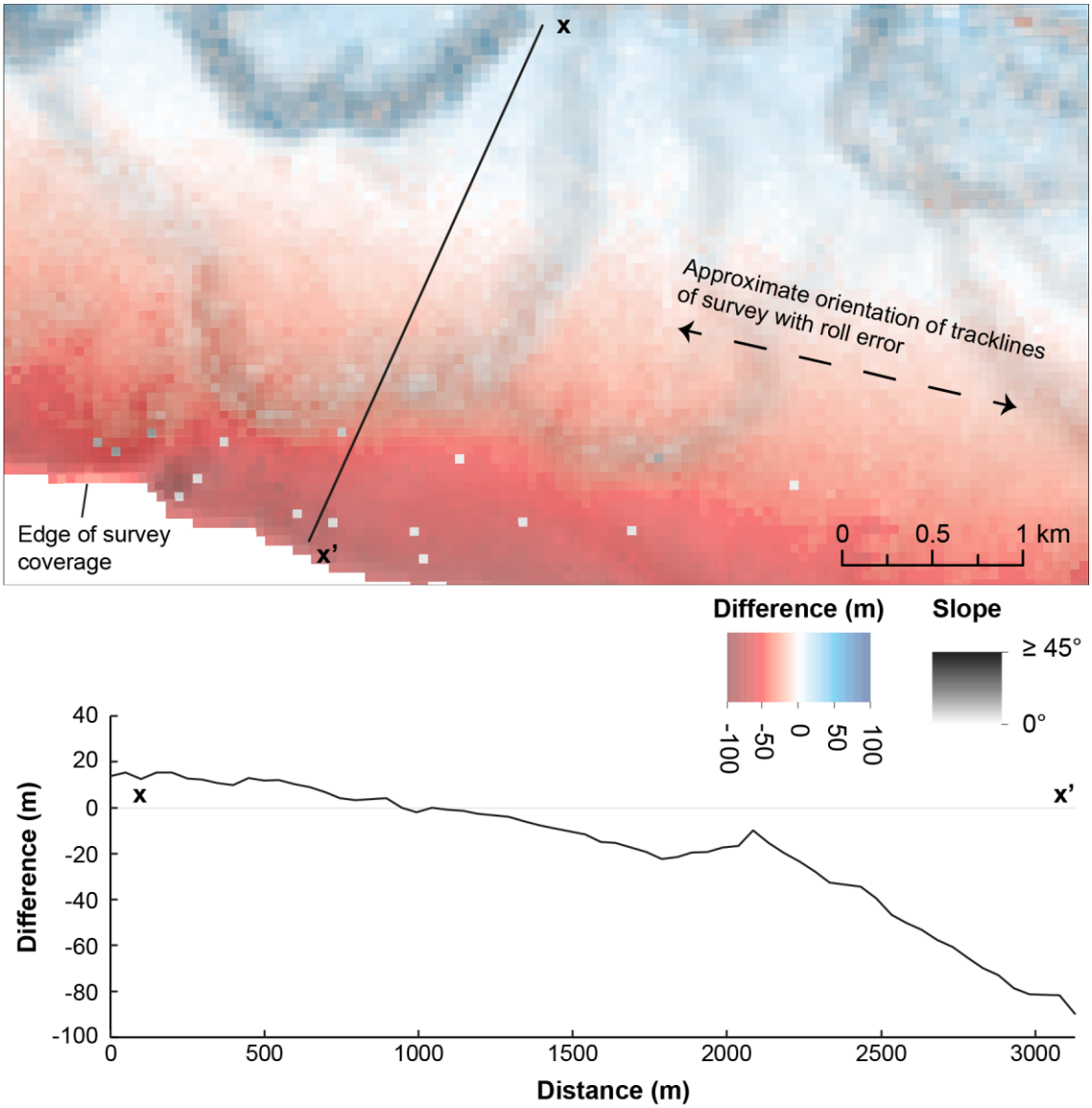

Figure 1.6: Large error found in difference mapping in the Congo Canyon that aligns with the track line of one of the two surveys. The error aligns with the edge of the survey, so that strong erosion is found along the edge of the survey, and progressively turns into deposition further away from the edge. The area is outside the main canyon, and is not expected to have experienced such change. This error appears to be caused by not properly corrected roll of the ship. The colour bar in this figure has been chosen to accentuate the error in this specific location.

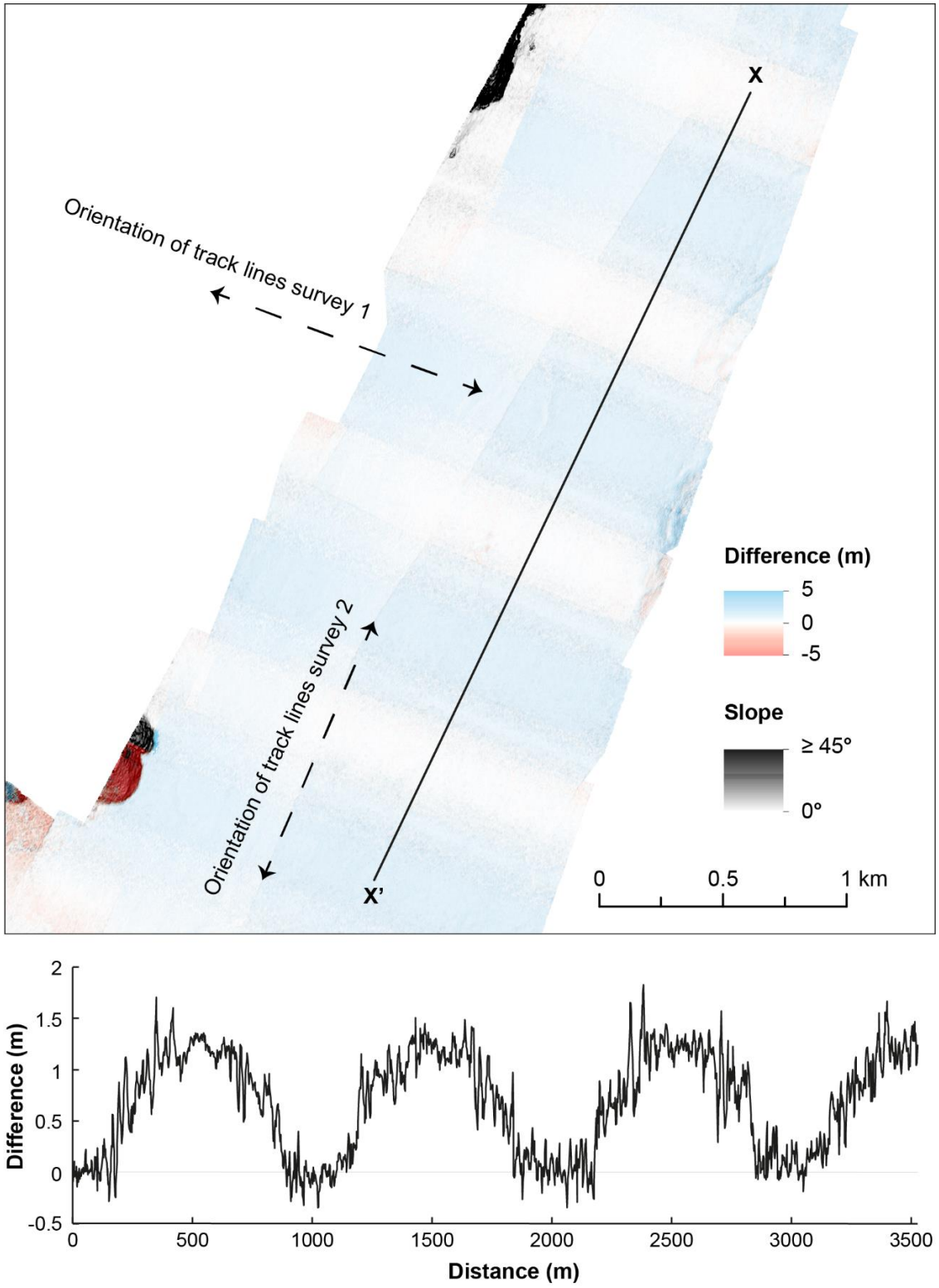

Figure 1.7: Regular occurring waves of positive change that align with the orientation of the ship's tracklines in the distal parts of Bute Inlet. Both the regular spacing and perfect alignment with the ship's tracklines indicates this pattern is the result of an error. Note how another, much smaller, error occurs that aligns with the tracklines of the other survey. Furthermore, note how the random noise can be clearly seen superimposed on the larger magnitude waves of errors. The colour bar in this figure has been chosen to accentuate the error in this specific location.

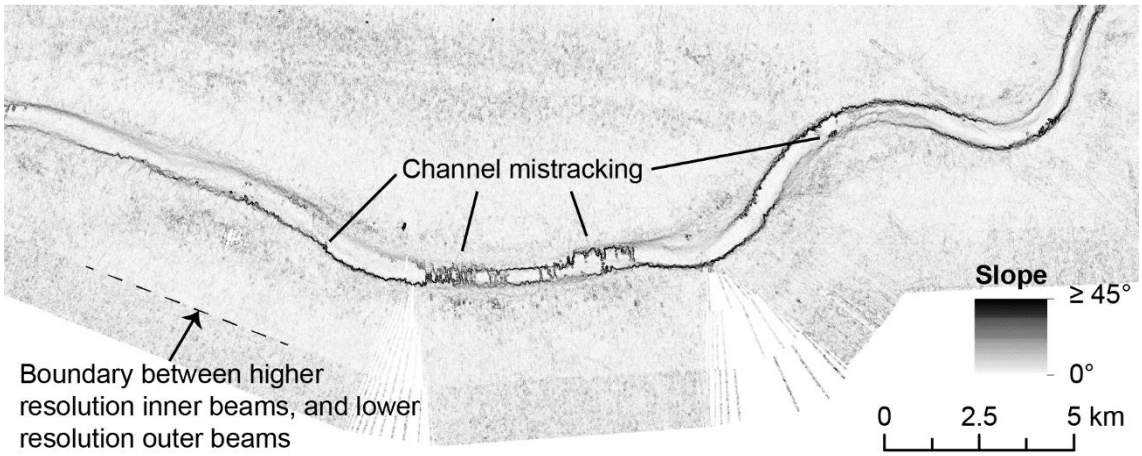

Figure 1.8: Errors resulted from mistracking of the channel walls in the Congo submarine channel system. The errors result in discontinuous and erratic channel edges.

The last error encountered in this study is the mistracking of steep features close to the ship's trackline (Figure 1.8). Software used to setup and log a multibeam survey uses a set of algorithms to determine which set of echo returns should be considered the seabed. This algorithm tends to not always work perfectly when the seabed goes down in a steep step, and can mistakenly track side lobe echo soundings as the real seafloor. Such mistrackings can be removed during post-processing if reliable soundings from overlapping passings are available. However, mistrackings cannot always be easily removed in areas with lower data coverage.

Other potential errors can occur in repeat mapping of submarine channels, but are not encountered in the data presented in this thesis. First, a horizontal offset can occur due to a positioning error. These errors have been less common over the last 10 – 20 years due to increases in accuracy of positioning systems. They tend to be an issue when mapping in very shallow water at resolutions less than 1 m. However, with the rapid development of unmanned underwater vehicles (such as AUVs and ROVs), which map at much higher resolution than surface vessels, but suffer from positioning errors, positioning errors are becoming more relevant again. Another potential error can result from not correctly accounting for tidal variations. This can result in absolute vertical errors which magnitude depends on the tidal amplitude at the survey location

Second, an error referred to as shadowing occurs when parts of an area are not covered as a result of steep features, both positive and negative steep features can cause shadowing. Steep positive features can block areas behind them from being surveyed. Steep negative features themselves can suffer from being not properly surveyed, which occurs when their slope has a similar orientation as the beams from the multibeam echosounder. It is therefore important to survey steep topographical features, like canyons and channels, from at least two different directions, as performed in the high resolution surveys presented in this thesis.

Based on the patterns of common errors, it is possible to now construct some guidelines on how to determine whether certain patterns are real change, or errors. First, it is import to avoid interpreting patterns that are close to both horizontal resolution and vertical accuracy. If patterns are below the vertical accuracy, it is necessary they are widespread enough to be able to distinguish between real change and errors. Second, the main way to distinguish between error or real change is to evaluate whether the pattern resembles one or a combination of error patterns, or whether the patterns make morphological sense. It is therefore important to understand the patterns of errors as well as the sedimentological processes and features present in the system mapped. Patterns that make morphological sense often align with features already present on the seafloor, e.g. in case of this thesis, bedforms, channel bends, etc. Error patterns often do not align with seafloor features. Two examples are shown in Figure 1.9.

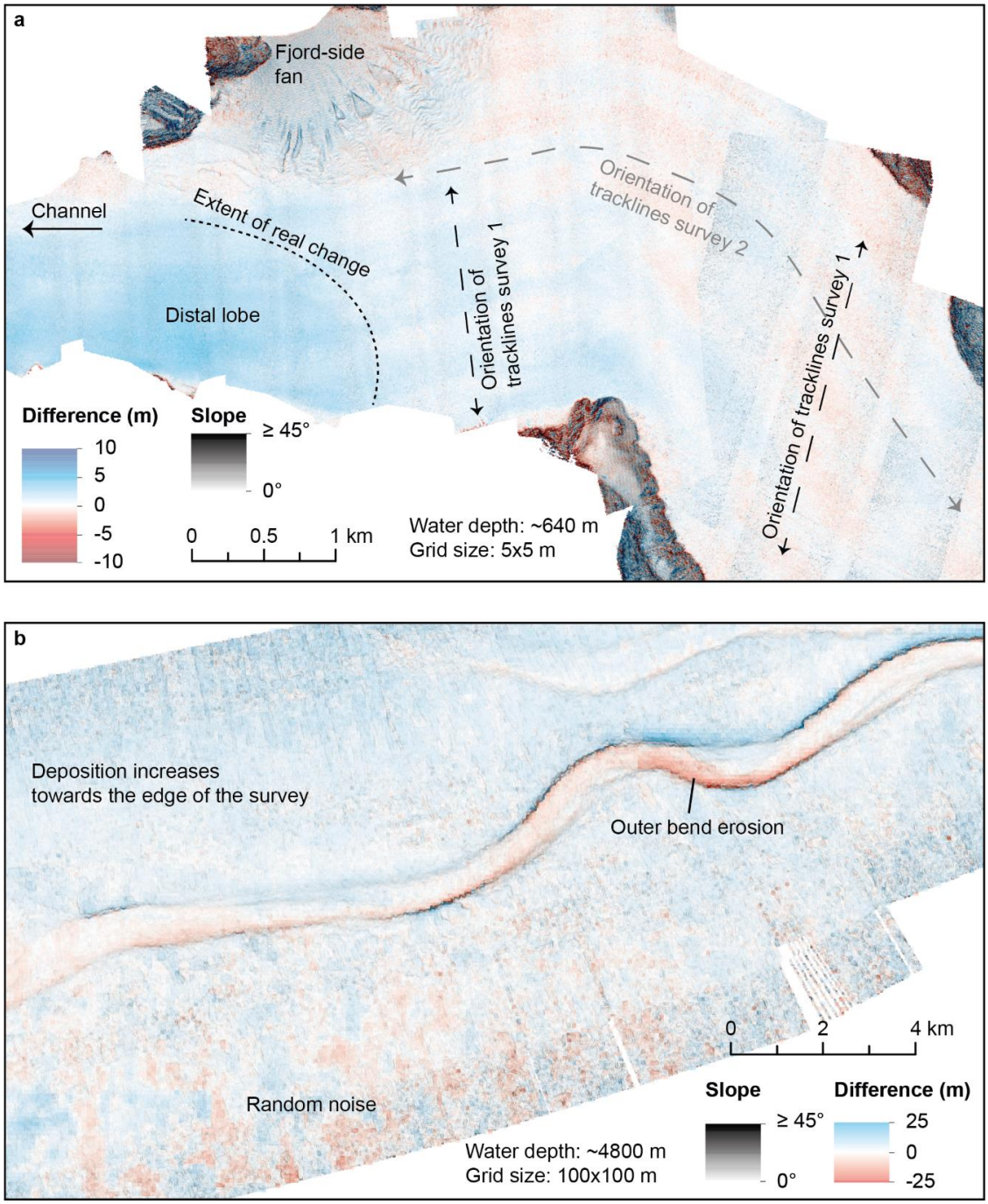

Figure 1.9: Examples of patterns of change interpreted to be real that are close to the resolution of the bathymetric surveys. a) The distal lobe in Bute Inlet ends in an area characterised by regular errors that align with the track lines of the surveys. Two sets of orientations of errors can be observed, which correspond to the track line orientations of the two surveys that form the basis for the shown difference map. The extent of the real change is interpreted as where the change is fully regular orientated along the track lines of the surveys. b) A section of the Congo submarine channel showing random noise on one overbank and deposition that increases towards the survey edge on the other overbank, and erosion in an outer bend interpreted to be real. This outer bend erosion is interpreted to be real, as it location and pattern makes sedimentological sense and is different than the error patterns.

Chapter 2 Rapidly-migrating and internally-generated knickpoints can control submarine channel evolution

This chapter has been published as a peer reviewed article in the journal Nature Communications as: Heijnen, M.S., Clare, M.A., Cartigny, M.J.B., Talling, P.J., Hage, S., Lintern, D.G., Stacey, C., Parsons, D.R., Simmons, S.M., Chen, Y., Sumner E.J., Dix, J.K., Hughes Clarke, J.E., Rapidly-migrating and internally-generated knickpoints can control submarine channel evolution. Nat Commun 11, 3129 (2020). https://doi.org/10.1038/s41467-020-16861-x

M.S.H. is the main author of the manuscript and performed the majority of the data analysis. M.A.C., M.J.B.C., P.J.T., E.J.S., and J.K.D. contributed to writing the manuscript. S.H., S.M.S., and Y.C. helped in data analysis. M.A.C., M.J.B.C., P.J.T., D.G.L., C.S., D.R.P., and J.E.H.C. designed the overall project, secured the funding, and were involved in data collection. D.G.L. and C.S. planned the majority of expeditions. S.H. was also involved in data collection.

2.1 Abstract

Submarine channels are the primary conduits for terrestrial sediment, organic carbon, and pollutant transport to the deep sea. Submarine channels are far more difficult to monitor than rivers, and thus less well understood. Here we present 9 years of time-lapse mapping of an active submarine channel along its full length in Bute Inlet, Canada. Past studies suggested that meander-bend migration, levee-deposition, or migration of (supercritical-flow) bedforms controls the evolution of submarine channels. We show for the first time how rapid (100 – 450 m/year) upstream migration of 5-to-30 m high knickpoints can control submarine channel evolution. Knickpoint migration-related changes include deep (>25 m) erosion, and lateral migration of the channel. Knickpoints can be caused by external factors, such as tectonics, or base-level change. However, the knickpoints in Bute Inlet appear internally generated. Similar knickpoints are found in several submarine channels worldwide, and are thus globally important for how channels operate.

2.2 Introduction

Seafloor sediment flows called turbidity currents transport globally important volumes of sediment, and form some of the deepest canyons, longest channels, and largest sediment accumulations on Earth (Curray et al., 2002; Khripounoff et al., 2003; Talling, 2014). These widespread underwater channel systems can extend for tens to thousands of kilometres offshore, and their dimensions may rival or even exceed those of terrestrial river systems (Wynn et al., 2007; Peakall and Sumner, 2015). Turbidity currents that flush submarine channels can be very powerful (reaching velocities of 20 m/s), and they pose a serious hazard to seafloor infrastructure, which includes telecommunication cables that carry >95% of global data traffic (Heezen and Ewing, 1952; Carter et al., 2009; Pope et al, 2017a, b). Furthermore, sediment, organic carbon, nutrients, and pollutants that are transported via submarine channels, influence deep marine ecosystems and climate on long time scales (Canals et al., 2006; Vangriesheim et al., 2009; Kane and Clare, 2019), while ancient channel deposits can form reservoirs and source rocks for hydrocarbon production (Mayall et al., 2006; Baudin et al., 2010), and act as an archive for the Earth's history (Prins and Postma, 2000; Clift and Gaedicke, 2002).

Despite the global occurrence and importance of submarine channel systems, there are very few detailed time-lapse seabed surveys showing directly how channels evolve and change through time. Channels can evolve over different timescales, ranging up to "channel life cycles", encompassing channel inception, maintenance and abandonment, which can span over geological times (Fildani et al., 2013). Here we describe channel evolution during its active (maintenance) stage.

We are aware of 17 locations where multiple bathymetric surveys of the modern seafloor have provided time-lapse information on how active channels evolve (Table 2.1). These studies typically involve two surveys, cover periods of less than 5 years, do not cover the full extent of a system from source to sink, or capture relatively small delta-front systems. The highest resolution time-lapse study of a full-length system is from the 1 – 2 km long delta-front channels on the Squamish Delta, but this system is re-establishing itself after a man-made river diversion (Hughes Clarke, 2016; Vendettuoli et al., 2019). This lack of time-lapse studies is in stark contrast to the very large number of time-lapse studies of how river channels evolve, which benefit from abundant airborne lidar, aerial photographs, and satellite images (Constantine and Dunne, 2008). There is a compelling need for detailed time-lapse studies to understand how submarine channels evolve.

This lack of time-lapse data from full-length systems ensures that previous studies of submarine channel evolution were mainly based on physical laboratory-scale modelling, numerical models, geophysical (seismic) data, outcrop studies, comparisons to rivers, and non-time-lapse seafloor

mapping (Heiniö and Davies, 2007; de Leeuw et al., 2016; Paull et al., 2011; Sylvester et al., 2011; Hubbard et al., 2014). These studies have advanced considerably our understanding of how submarine channels work. However, laboratory models suffer from scaling issues (de Leeuw et al., 2016), and numerical models have to make assumptions that are often poorly validated against full-scale field data. Seismic data and rock outcrops only capture the end result of channel evolution, rather than a time series of how the channel evolved in response to certain environmental conditions. Intervals dominated by erosion are especially difficult to reconstruct using seismic data or rock outcrops. The resolution of seismic data is often insufficient to resolve small features within channels. Rock outcrops also lack detailed chronological data for quantifying rates of short-term processes, and may not give a full three-dimensional perspective (Peakall et al., 2007).

Despite these limitations, previous work has proposed three main processes that might control the evolution of submarine channels. First, it has been proposed that submarine channels evolve in a broadly comparable way to meandering rivers, via gradual outer-bend erosion and inner-bend deposition, and meander bend cut-off (Sylvester et al., 2011; Peakall and Sumner, 2015; Sylvester et al., 2019). Bend migration and cut-off is primarily driven by cross-channel (secondary) flow and has long been known to be a dominant control on how rivers evolve (Dietrich et al., 1979; Parker and Andrews, 1986; Lewis and Lewin, 2009; Sylvester et al., 2019), and also occurs in submarine channels (Azpiroz-Zabala et al., 2017b). However, submarine channels have been suggested to differ in key regards from rivers (Peakall et al., 2000). Second, deposition of flanking levees may control channel evolution through confinement of turbidity currents; hence fixing the system in place (Imran et al., 1998). Third, it has been suggested that turbidity currents have a greater tendency than rivers to be Froude-supercritical (i.e. exist in a thin and fast state) (Komar, 1971). Flow instabilities called cyclic-steps can characterise these supercritical turbidity currents, causing repeated hydraulic jumps. Crescent-shaped bedforms and repeated seabed scours are common expressions of these cyclic steps, which previous authors propose play a key role in submarine channel initiation, evolution, and deposit geometries (Fildani et al., 2006; Paull et al., 2010, 2011; Fildani et al., 2013; Covault et al., 2014; Hughes Clarke, 2016; Covault et al., 2017; Hage et al., 2018).

Another possible major control on submarine channel evolution could be the rapid migration of internally generated knickpoints. Knickpoints are steep steps in channel gradient that migrate upstream via erosion (Gardner, 1983; Howard et al., 1994), and they are common in rivers (van Heijst and Postma, 2001; Hayakawa and Matsukura, 2003; Crosby and Whipple, 2006). The knickpoint's steep face enhances the erosive potential of flow, causing the knickpoint to migrate upstream. Sediment flux downstream of the knickpoint increases as a result of this enhanced

erosion, causing more deposition on the next lower gradient section downstream45. Previous studies have shown that knickpoints are common in submarine (and sublacustrine) channels in various settings worldwide (Table 2.2). A recent study of the head of a submarine canyon has shown that knickpoints can migrate up to 600 m/year, and leave a distinct pattern of erosion and deposition in the channel (Guiastrennec-Faugas et al., 2020a).

2.3 Aims

Here we present the most detailed time-lapse mapping yet for an active submarine channel, over its full length of ~40 km, to understand the role of migrating knickpoints in submarine channel evolution. These data comprise five bathymetric surveys over 9 years (2008–2016) in Bute Inlet, British Columbia, Canada (Figure 2.1). These data allow us to document how a submarine channel evolves along its full length, for almost a decade. Our initial aim is to understand what factors can control the evolution of submarine channels. These time-lapse surveys show that the evolution of this submarine channel is dominated by rapidly-migrating knickpoints. Our second aim is therefore to understand what causes these very fast-moving knickpoints. Our third aim is to understand the implications of these rapidly-migrating knickpoints for submarine channel-bend evolution, and deposits preserved within channels. We provide new generalised models for both bend evolution and channel deposits. We conclude by showing that similar submarine knickpoints occur in many locations, and may thus have widespread importance for how submarine channels work, and how their deposits form.

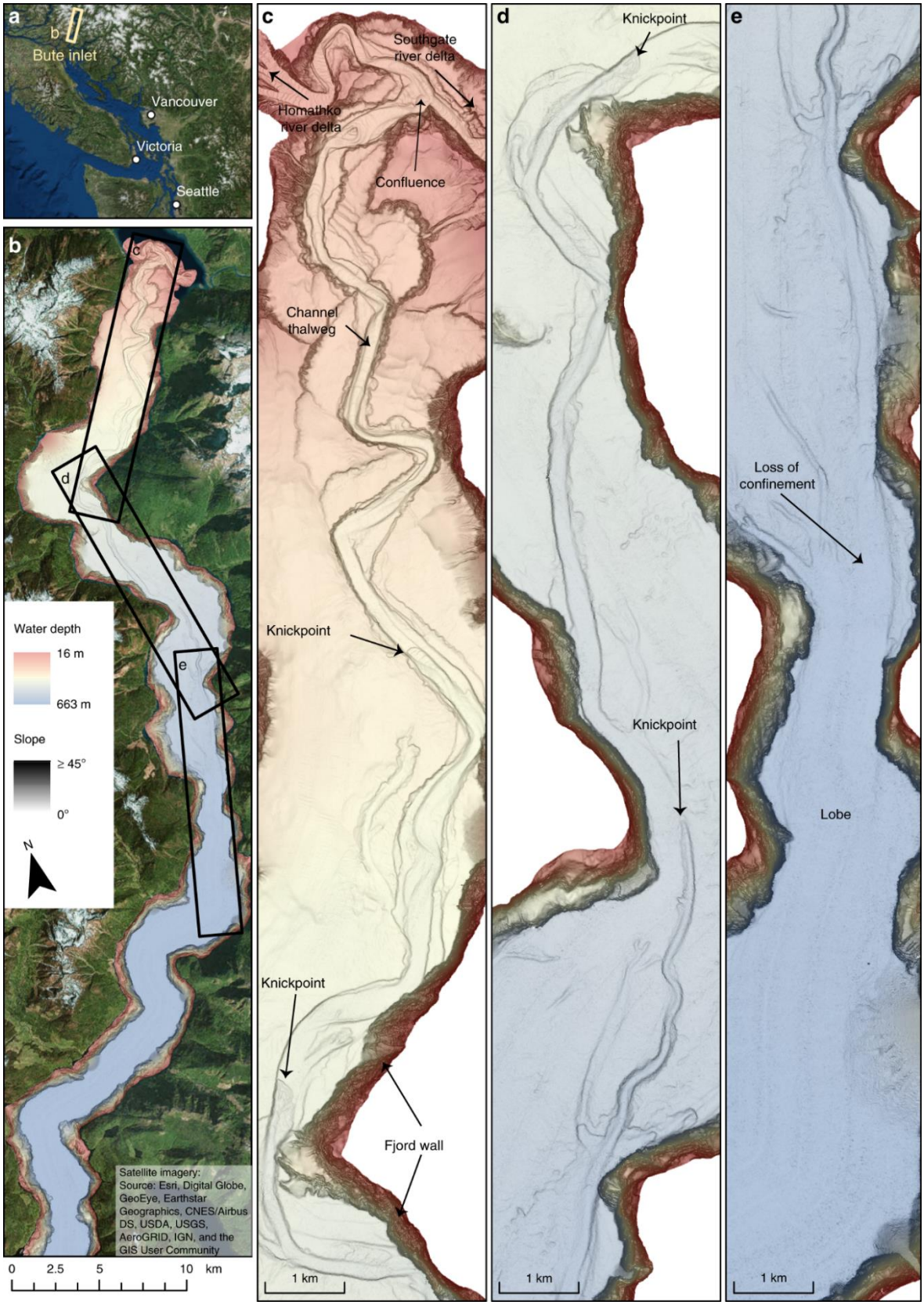

Figure 2.1: Overview of the submarine channel system in Bute Inlet. a) Location of Bute Inlet in British Columbia, Canada. b) Map of Bute Inlet showing the location of more detailed images shown in panels c–e). Bathymetric surveys are presented here as maps of seabed gradient, which optimally visualize small and steep topographical features, such as knickpoints. Seabed gradient maps are then overlain by a transparent bathymetry map. c-e Detailed maps of the 40 km long

submarine channel within Bute Inlet, showing the location of river deltas, knickpoints and lobe beyond the channel mouth.

2.4 Geographical setting

Bute Inlet is located in British Columbia, West Canada (Figure 2.1a). The head of this fjord is fed by the Homathko River and Southgate River, which are responsible for, respectively, 80% and 15% of the freshwater input in the system, with the remaining 5% from smaller rivers on the side of the fjord (Syvitski and Farrow, 1983). The rivers are mainly fed by glacial meltwater, with much higher discharges in summer. The Homathko River has an average summer discharge of 600 m^3/s, with maxima above 1000 m^3/s, while winter discharges are typically below 100 m^3/s. It has been estimated that these rivers supply 1.6×10^6 m^3 of sediment to the fjord each year (Syvitski and Farrow, 1983). A ~40 km long submarine channel is present on the floor of Bute Inlet, and it originates at the prodeltas of the two main rivers (Prior et al., 1986, 1987). The channel is 35 m deep in the most upstream part of the system, and its depth decreases gradually downstream towards the depositional area (terminal lobe), beyond the channel termination at 620 m water depth (Figure 2.2; Zeng et al., 1991).

The floor of the channel comprises sand, whilst the surrounding fjord is dominated by mud (Prior et al., 1986; Zeng et al., 1991). Turbidity currents occur frequently along the upper channel, with over 10 flows a year, which occur coincident with periods of higher river discharge in the spring and summer (Prior et al., 1987; Zeng et al., 1991; Bornhold et al., 1994). More recent and higher resolution bathymetric surveys demonstrated that the submarine channel in the Bute Inlet system is strongly altered by these turbidity currents, with 25% of the channel having changed elevation by 5 m or more within 3 years (Conway et al., 2012) and showed active upstream-migrating knickpoints (Gales et al., 2019). Here we analyse a longer time series over a more extensive area of the submarine channel.

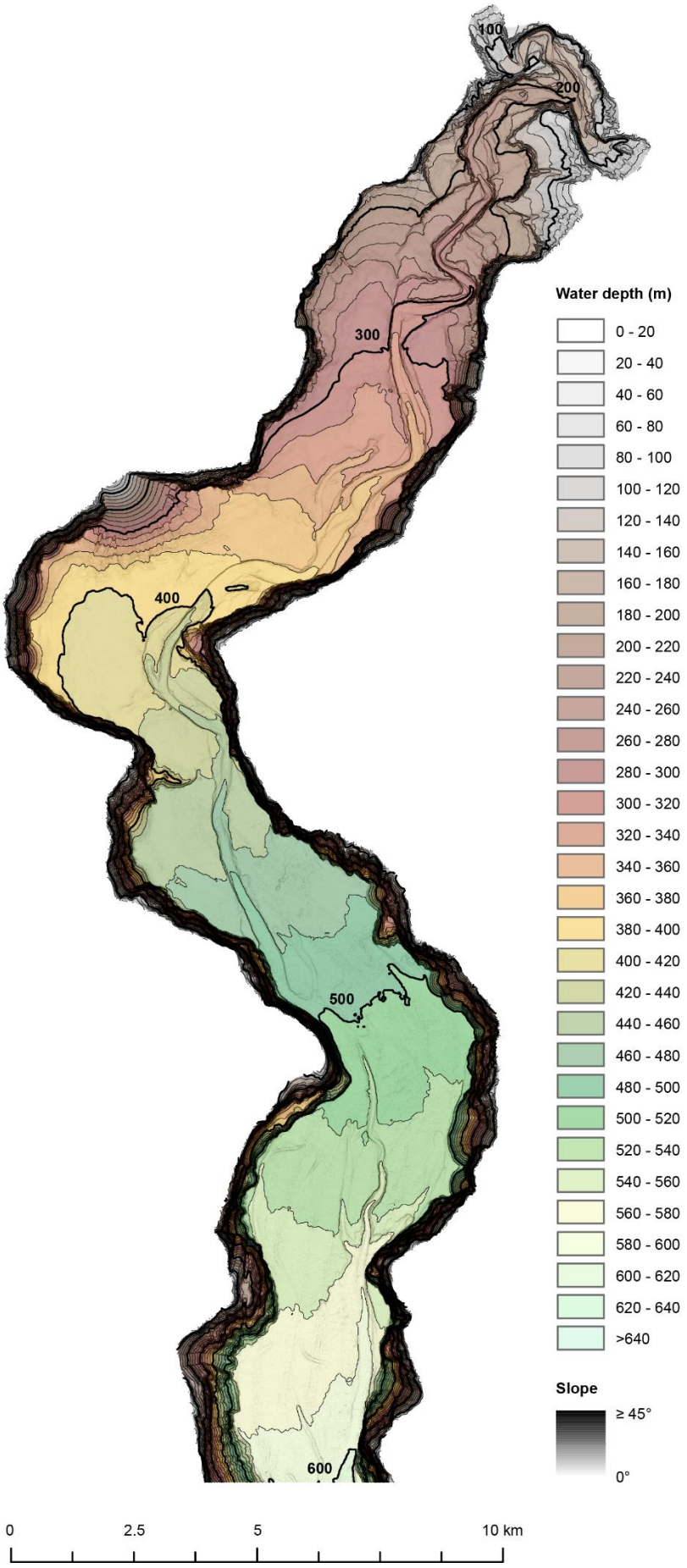

Figure 2.2: Bathymetric map of Bute Inlet classified in 20 m intervals.

2.5 Methods

2.5.1 Multibeam bathymetry acquisition

This study uses five bathymetric surveys spanning a total of 9 years, collected in March 2008, November 2010, February 2015, June 2016, and October 2016. Past work has considered only the first two surveys in 2008 and 201052,53. The survey in March 2008 survey was obtained using a Kongsberg-Simrad EM 1002 (100 kHz) multibeam echosounder. The later surveys used a Kongsberg Maritime EM710 (70–100 kHz) multibeam echosounder, controlled using Kongsberg Maritime SIS software. Data were processed to correct for differences in sound velocity of the water (using data from a sound velocity profiler), together with tides, waves, and ship's motion. The vertical resolution of bathymetric data is ~0.5% of the water depth, and is thus a maximum of ~3 m at the channel termination at water depths of ~600 m (Figure 2.3b – d). Bathymetry was then processed to calculate the local gradient, in order to optimally display small steep topographic features such as knickpoints.

2.5.2 Difference maps

Patterns of erosion and deposition are visualised using bathymetric difference maps, calculated by subtracting two surveys from each other. These difference maps were then used to estimate volumes of different erosional processes. First, the total eroded volume within the active channel is calculated (Figure 2.4). Then, parts of that eroded volume are attributed to either outer-bend erosion or knickpoint migration, based on the geometry and location of erosional areas (Figure 2.4). Steep areas such as fjord sidewalls and the overbanks have not been taken into account, because volumetric calculations including these areas will reflect uncertainties rather than real change. Reliable volumetric calculations and mass balances of the deposition cannot be made, as the thin and widespread geometry of depositional bodies often falls below resolution of the surveys, especially on the overbanks.

2.5.3 Channel profiles

The bathymetric surveys were used to construct along-channel profiles. The position of the channel shifts as the channel evolves, so profiles were constructed along the position of the thalweg in that survey. The different along-channel profiles were all normalised to facilitate comparison.

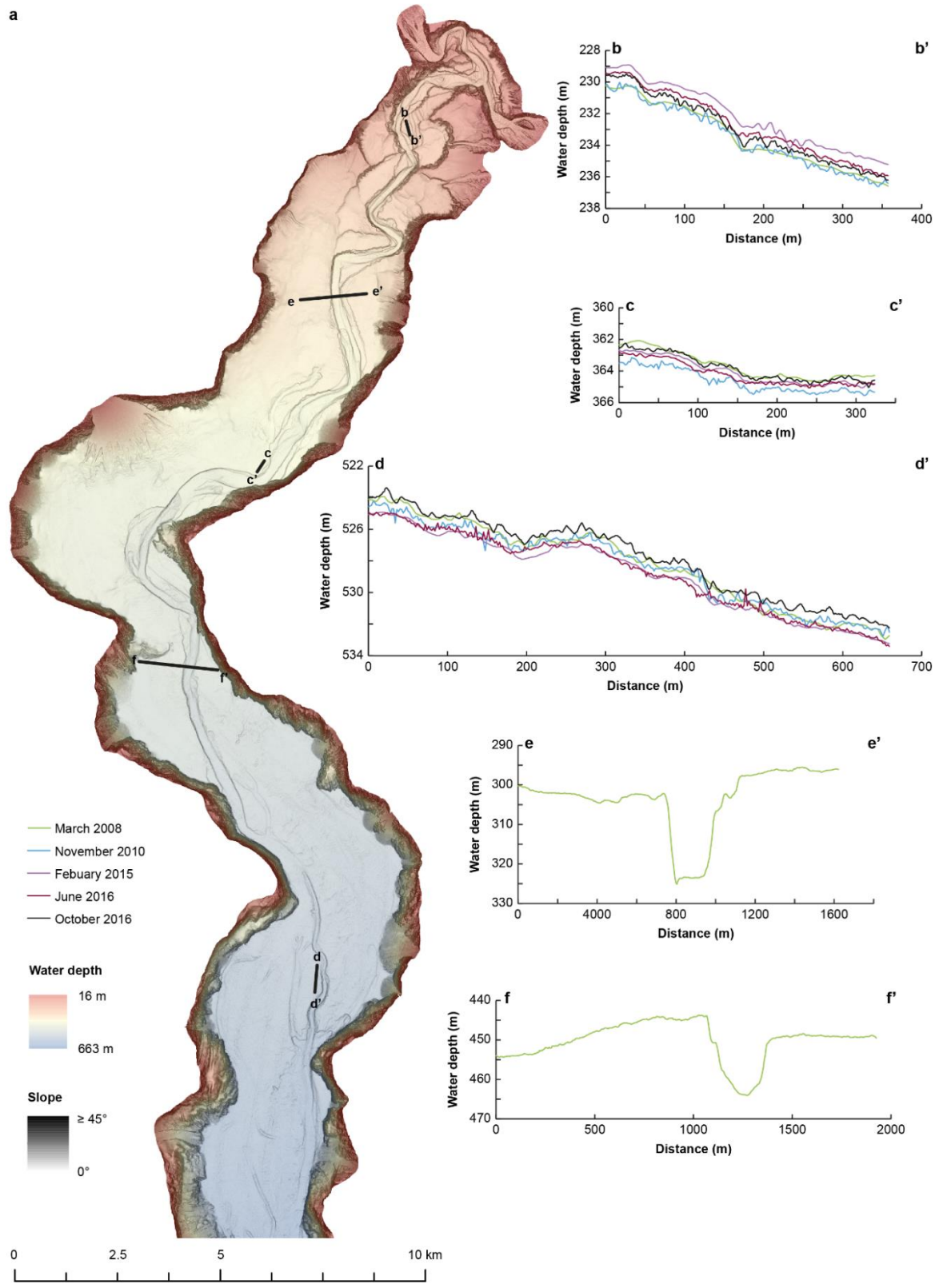

Figure 2.3: Profiles along the seafloor of Bute Inlet in 2008 demonstrating vertical resolution and the system's levees. a) location of cross sections. b-d) profiles of areas that are assumed to not be subject to seafloor change. The variability within the different surveys is up to ~0.5% of the water depth. e) profile through the channel, showing that levees can be completely absent and the system is incised in the surrounding seafloor. f) profile through channel, showing a particular well developed levee of about 10 m high.

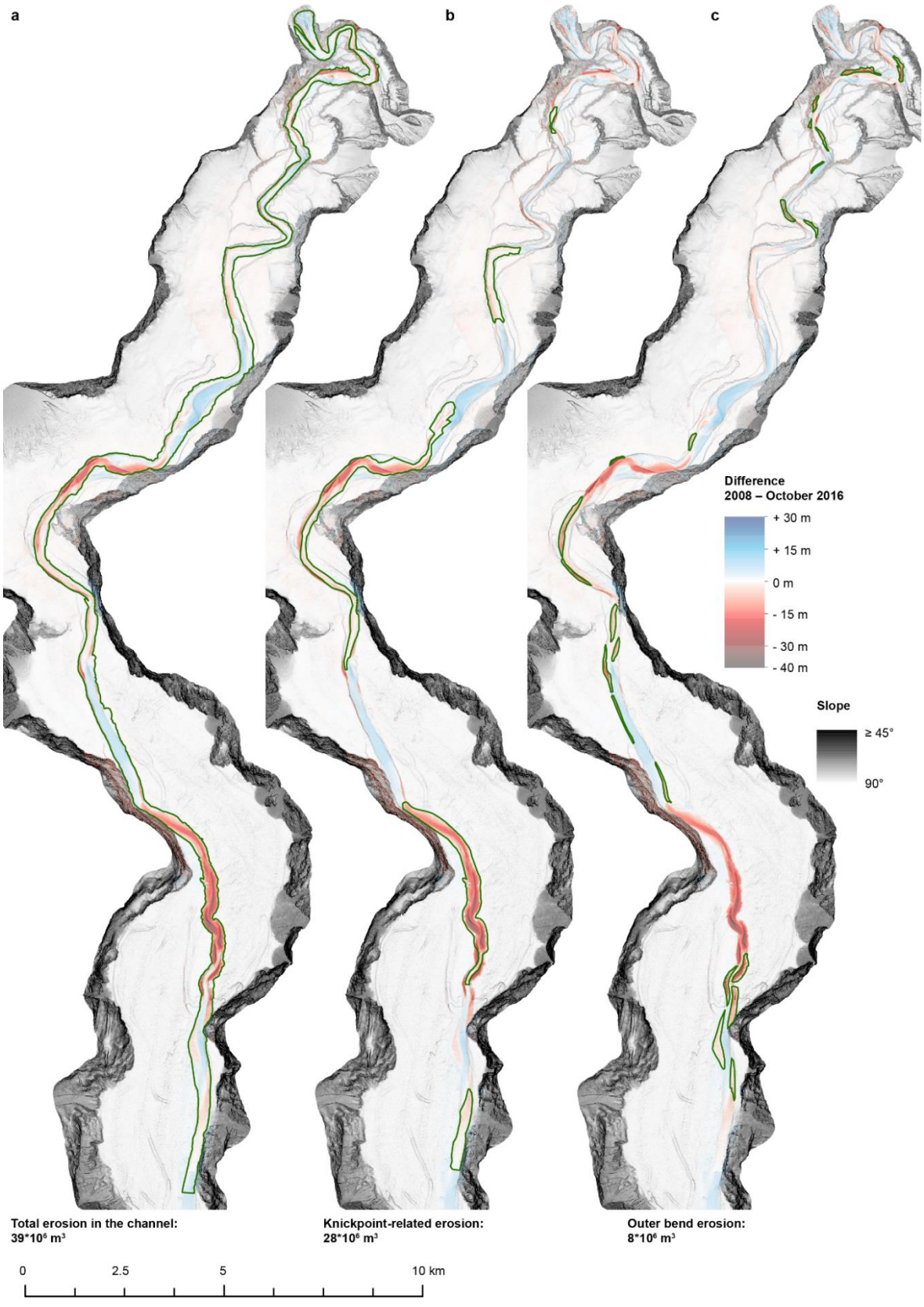

Figure 2.4: Overview of areas selected for volumetric estimates (outlined in green). a) the total erosion in the channel, b) Knickpoint-related erosion, and c) Outer-bend erosion.

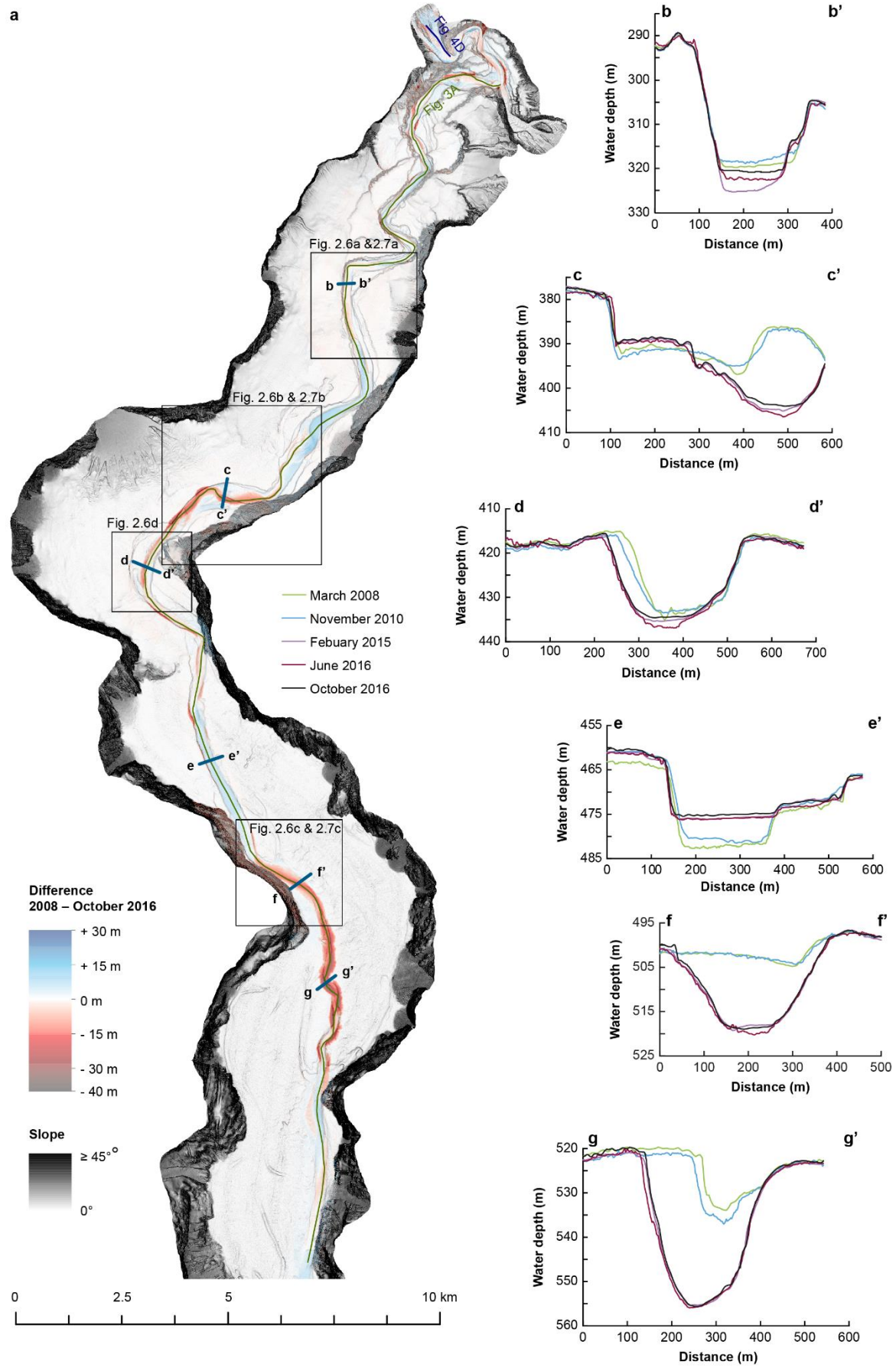

Figure 2.5: Changes in the submarine channel in Bute Inlet. a) Map of changes in seabed elevation between March 2008 and October 2016, overlaying a seabed gradient map. Note the alternations

of deposition and erosion along the channel. b–g) Changes in seabed elevation at a series of cross-sections. Locations are shown in panel a. 10x vertical exaggeration. b) The channel gradually fills except during knickpoint migration between 2010 and 2015, when previous deposits are eroded. c) Lateral migration of channel thalweg as a result of knickpoint migration. Note how the channel floor in 2008-2010 becomes a terrace from 2015 onwards. d) Section showing largest observed amount of outer-bend erosion away from migrating knickpoints. e) Progressive filling of a channel in a depositional area. f) Knickpoint migration creates a channel, where the channel was previously shallow and poorly-defined. g) Cross section at a location affected by both outer-bend erosion and knickpoint migration.

2.6 Results

2.6.1 Bathymetric changes and knickpoints

A difference map captures bathymetric changes in the channel for the entire study period between March 2008 and October 2016 (Figure 2.5a). It covers the full length of the channel, and the area immediately beyond the channel termination (start of the terminal lobe). The channel floor is characterised by alternating areas of erosion and deposition (Figure 2.5a), a pattern that is repeated three times along the channel (Figure 2.5a; Figure 2.6a). The three main erosional areas are bounded at their upstream sides by a steep (up to ~30°) face that is 5–30 m high. Similar steep steps are found within each erosional area. These steep steps are called knickpoints, and here we refer to erosional areas that consist of several knickpoints as knickpoint-zones. Knickpoints bounding the knickpoint-zone at its upstream side are termed frontal-knickpoints. Repeat surveys show that frontal-knickpoints and associated knickpoint-zones migrate upstream between each pair of surveys (Figure 2.6a; Figure 2.7a – c; Figure 2.8a – c; Figure 2.9a – c). Since the system is active only during summers (Bornhold et al., 1994), we determine migration rates based on the amount of summers between surveys, rather than exact time.

We also observe crescent shaped bedforms in the channel. We differentiate between these bedforms and knickpoints based on scale and shape. The crescent shaped bedforms are smaller (1–5 m high), and have a more consistent wavelength (50–100 m) than the knickpoints. The bedforms have a rounded crest, and an upstream-dipping stoss side. Crescent shaped bedforms can be superimposed on knickpoints. The knickpoints themselves are 5–30 m high, are spaced 1–3 km apart in knickpoint-zones, and have a sharp crest.

The pattern of alternating zones of erosion and deposition is lost in the most upstream part of the channel, above 300 m water depth (Figure 2.5a; Figure 2.6). The knickpoints and the erosion in

the knickpoint-zones progressively decrease in size upstream. Very small knickpoints might occur in this upstream part of the system, but it becomes difficult to distinguish them from crescent shaped bedforms. To understand the role of knickpoints in channel evolution, we therefore focus on the well-defined knickpoints in the main three knickpoint-zones.

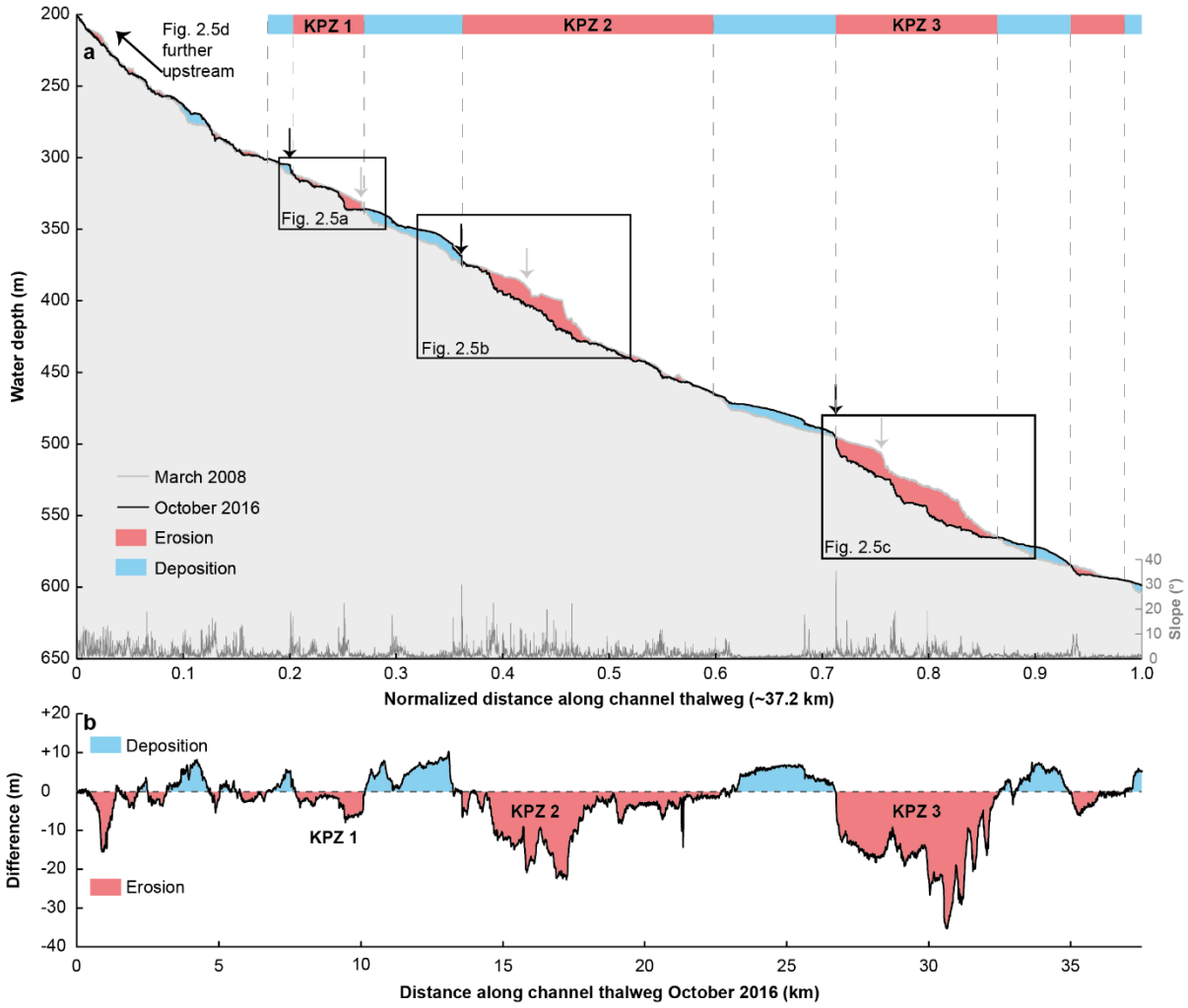

Figure 2.6: Changes along the channel profile in Bute Inlet. Location is shown in Figure 2.5a. KPZ = knickpoint-zone. a) Bathymetric profiles along the channel thalweg in 2008 and October 2016. 50x vertical exaggeration. The position of the channel shifts as the channel evolves, so profiles were constructed along the position of the thalweg in that survey. Profiles were then normalised to allow comparison. Slope was generated using the survey from October 2016. Note the downstream alternation of deposition (blue) and erosion (red). Three main erosional areas (knickpoint-zones) are bounded at their upstream end by steep steps (frontal-knickpoint) in the channel profile. Additional smaller knickpoints are often present within wider knickpoint-zones. Proximal erosion upstream of knickpoint-zone 1 is due to lateral migration of the channel, unrelated to knickpoint migration. b) Difference in channel elevations between March 2008 and October 2016 along the channel thalweg. Migration of three knickpoint-zones (KPZ 1 to 3) produces erosional areas.

2.6.2 Knickpoint-zone 1

We now describe each of the three main knickpoint-zones, which are numbered from 1 to 3 in a down-channel direction (Figure 2.6). Knickpoint-zone 1 migrates through a pre-existing channel bend during the time covered by the surveys (Figure 2.8a; Figure 2.9a). The knickpoints are focussed towards the outside of the bend (Figure 2.9a). The knickpoint-zone consisted of a single frontal-knickpoint that was around 20 m high in March 2008 (Figure 2.7a; Figure 2.8a). A second knickpoint developed in the knickpoint-zone by February 2015 (Figure 2.7a; Figure 2.8a; Figure 2.9a). Both knickpoints are about 10 m high from February 2015 onwards. The frontal-knickpoint migrated ~2.5 km upstream between March 2008 and October 2016, averaging at 280 m/year. The knickpoint migration has caused up to 20 m erosion of the channel floor.

2.6.3 Knickpoint-zone 2

Knickpoint-zone 2 migrated through a relatively wide segment of the channel (Figure 2.8b; Figure 2.9b). The frontal knickpoint is 5 m high and migrated with an average rate of around 300 m/year over the entire survey, with the fastest rates of 440 m/year occurring between 2010 and 2015. The main knickpoint is 25 m high and migrated through the outside of a pre-existing channel bend. After 2010, migration of this main knickpoint completely reshaped the channel morphology, creating a new narrower and more sinuous channel. The thalweg in one of the new bends migrated partly outside the original channel (Figure 2.5b; Figure 2.8b; Figure 2.9b). Part of the original channel became a terrace after knickpoint migration. The main knickpoint is smaller (around 15 m) and less active after February 2015.

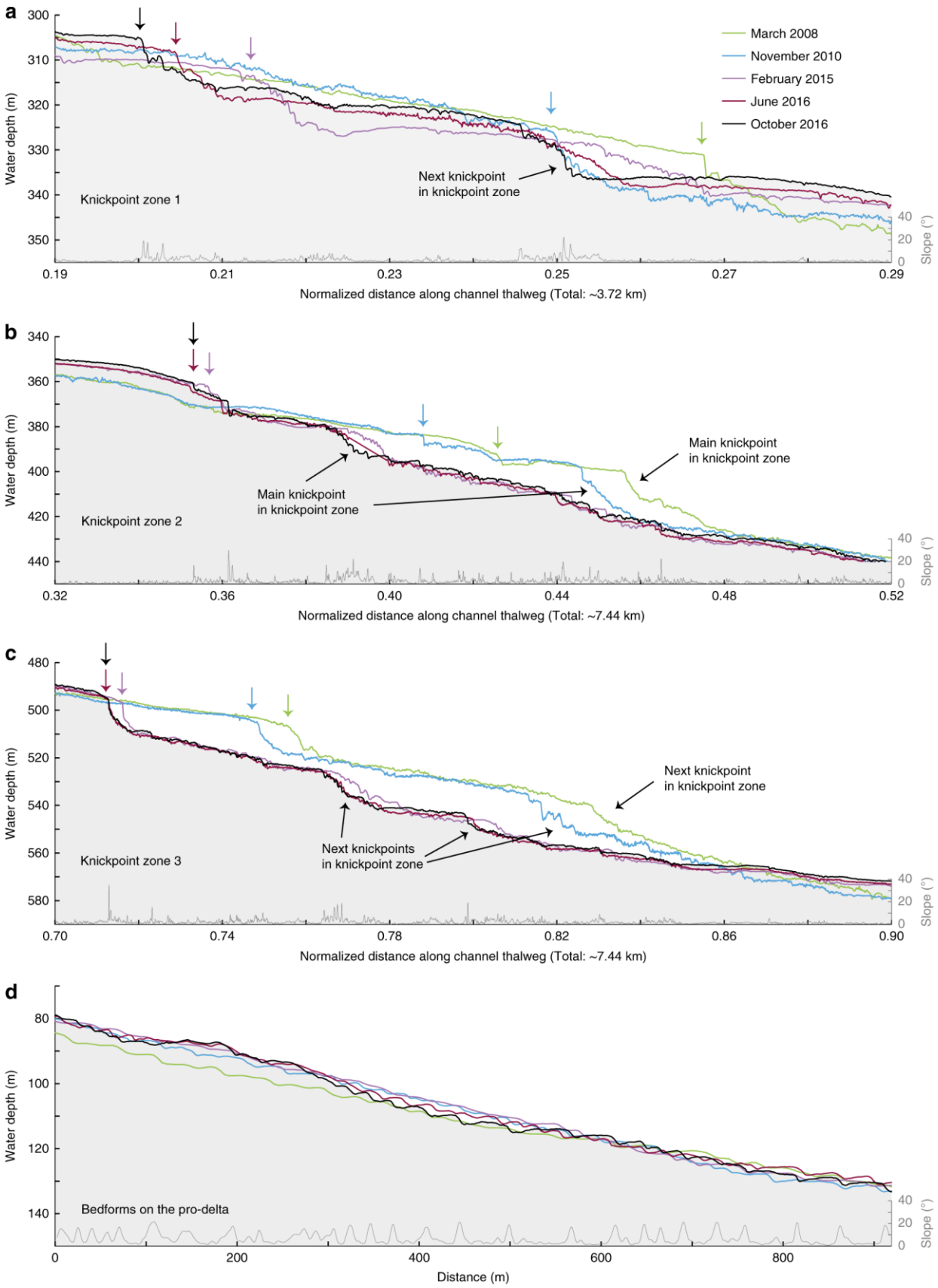

Figure 2.7: Time-lapse evolution of sections of the submarine channel profile. a–c) Detailed time-lapse changes in profiles across knickpoint-zones 1, 2 and 3, whose locations are indicated in Figure 2.6a. 20x vertical exaggeration. Slope was generated using the survey from October 2016.Arrows indicate the position of the frontal frontal-knickpoint in each survey. d) Profile along

the shallow-water prodelta channel, as indicated in Figure 2.5a, where crescentic shape bedforms dominate and no knickpoints are present. 5x vertical exaggeration. Note the relatively small amount of bathymetric change, when compared to the three knickpoint-zones.

2.6.4 Knickpoint-zone 3

Knickpoint-zone 3 migrated through an area where the channel was not well developed (Figure 2.5e; Figure 2.8c; Figure 2.9c). The height (around 15 m) of the frontal-knickpoint remains near-constant through the study period. Migration of the frontal-knickpoint involved erosion into previously deposited (before 2008) sediments, creating a 20 m deep and well-defined channel in locations where the channel was previously much shallower (10 m). The frontal-knickpoint migrated 1.8 km upstream during the 2008–2016 period, at a rate of around 200 m/year. A second large (around 30 m), but less-steep knickpoint can be recognised in 2008 and 2010, whilst two smaller (around 15 m high) knickpoints follow the frontal-knickpoint from 2015 onwards.

2.6.5 Outer-bend erosion

Outer-bend erosion resulting in lateral migration of the channel is common in Bute Inlet, causing channels to migrate laterally up to 120 m over the entire length of the survey (Figure 2.5a, c, d, g and 5d). While some progressive outer-bend erosion is observed in locations unaffected by knickpoint migration (Figure 2.5d), outer-bend erosion is enhanced strongly where it is coincident with knickpoint migration (Figure 2.5f).

2.6.6 Crescent shaped bedforms

Crescent shaped bedforms are not easily resolvable in the deeper part of the system, due to the vertical resolution of the multibeam surveys. However, the prodeltas are dominanted by crescent shaped bedforms, and do not experience knickpoint migration. Changes in seabed elevation (<10 m) associated with crescent shaped bedform migration here are less than changes (of up to 25 m) associated with knickpoint migration (Figure 2.6d).

2.6.7 Levee development

Levees are a distinct feature in many submarine channels, where levee crests may rise over 100 m above the surrounding seafloor (Curray et al., 2002; Damuth et al., 1988). The levees in Bute Inlet are up to 10 m high, but typically <5 m high (Figure 2.3e, f). Channels here have a negative relief compared to the surrounding floor of the fjord, rather than bound by levees. No significant levee aggradation is recorded during the time of the survey.

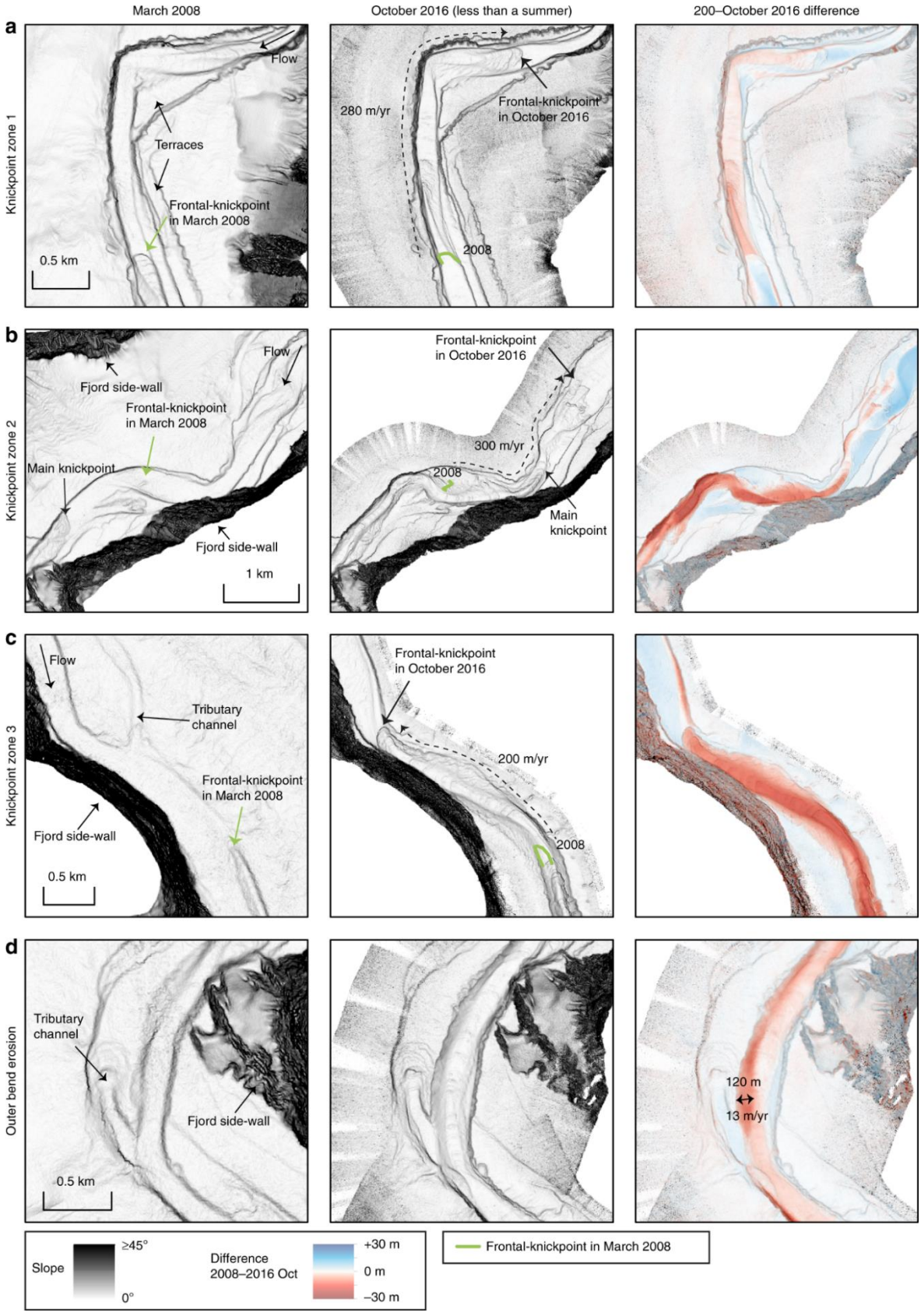

Figure 2.8: Detailed maps showing overall change in the three knickpoint-zones and in a meander bend. Locations shown in Figure 2.5a. Average migration rate of the frontal-knickpoint is indicated. a) Bathyemtric change in knickpoint-zone 1. b) Bathymetric change in knickpoint-zone 2. c) Bathymetric change in knickpoint-zone 3. Knickpoint migration creates a channel, where

previously no well-developed channel existed. d) Largest erosion in an outer-bed not affected by knickpoint migration.

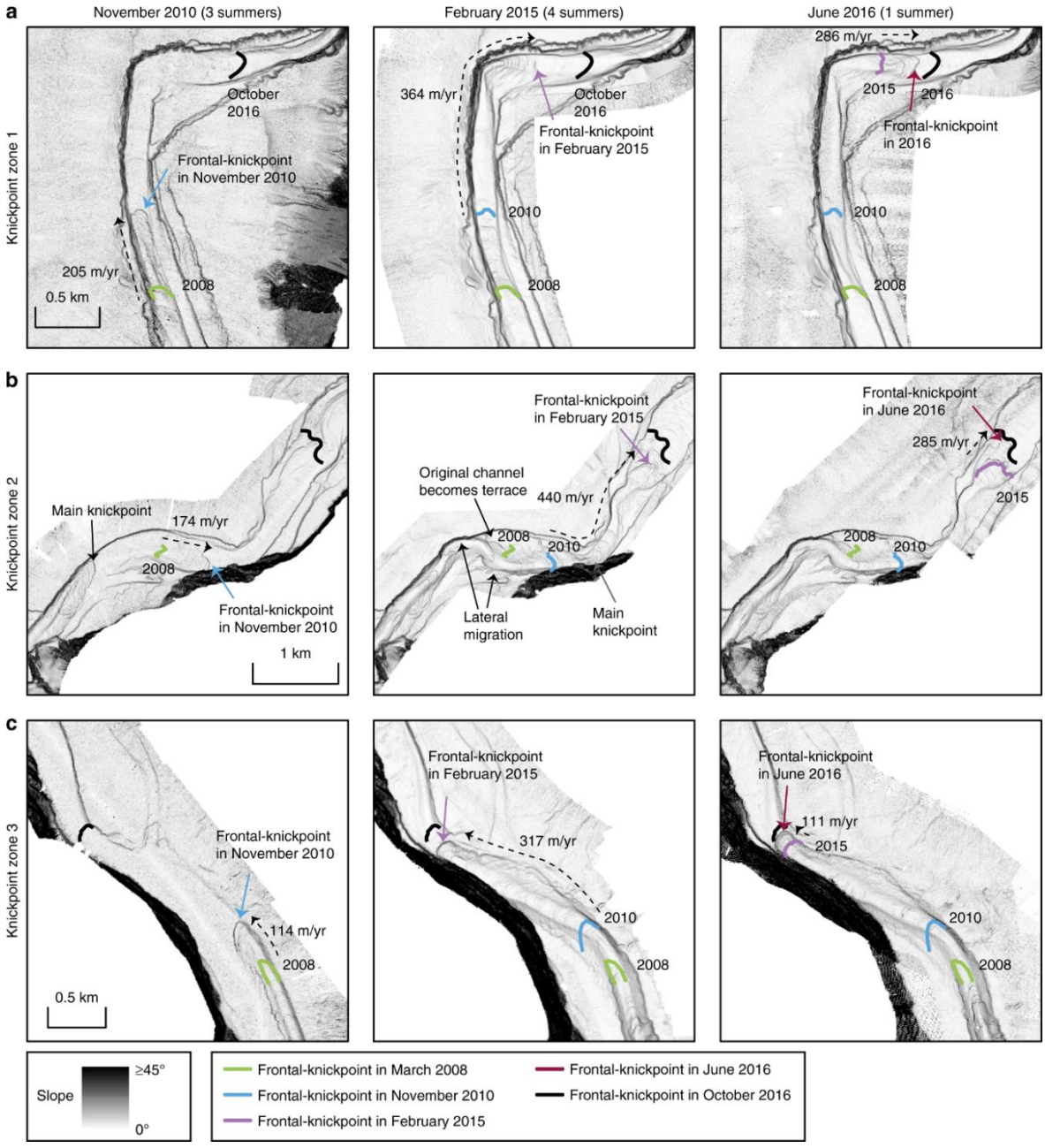

Figure 2.9: Detailed time-lapse maps in the three knickpoint-zones. Locations shown in Figure 2.5a. Time steps from March 2008 and October 2016 are shown in Figure 2.8. a) Time-lapse evolution of knickpoint-zone 1. b) Time-lapse evolution of knickpoint-zone 2. Knickpoints migrate outside of the original channel, causing lateral migration of the channel in some parts. The original channel floor locally becomes a terrace. The resulting channel is narrower and more sinuous. c) Time lapse evolution of knickpoint-zone 3. Knickpoint migration creates a channel where previously no well-developed channel existed.

2.6.8 Eroded volumes

Difference maps were used to calculate volumes of erosion. We compared the total erosion in the channel, erosion caused by knickpoint migration, and outer-bend eroded sediment independent from knickpoint migration. The total amount of erosion in 9 years over the entire length of the active channel is 39×10^6 m^3. Of that total eroded volume, 28×10^6 m^3 can be attributed to knickpoint migration, which is 72% of the total eroded volume, and similar to the amount of sediment delivered into the system (Syvitski and Farrow, 1983). Outer-bend erosion accounts for 8×10^6 m^3 (21%) of the total eroded volume, and about 30% of the amount of sediment delivered to the system (Figure 2.4).

2.7 Discussion

2.7.1 Testing previous models for channel evolution

Our first aim is to understand what controls submarine channel evolution. It has previously been suggested that secondary (across-channel) helical flow causing gradual bend migration, is the main control on submarine channel evolution, as is the case for many rivers. There has been considerable debate over whether the sense of submarine secondary circulation is river-like or reversed (Corney et al., 2006; Imran et al., 2007; Peakall et al., 2007; Azpiroz-Zabala et al., 2017b). Outer-bend erosion causing lateral migration is common in Bute Inlet and can locally reach rates of over 10 m/year. This is fast, even compared to rapidly migrating meandering rivers (Sylvester et al., 2019), and almost an order of magnitude higher than the incision rate. However, our study shows that outer-bend migration can often be linked to knickpoint migration (Figure 2.5g), rather than occurring gradually, as observed in rivers. This knickpoint-related lateral migration may explain the punctuated migration inferred from submarine channel deposits (Maier et al., 2012). However, we do not observe substantial sediment deposition at inner-bends. Furthermore, long stretches of the channel in Bute Inlet are straight (around Figure 2.5e), and not characterised by expanding meander bends and resulting cut-offs, as seen as in some other submarine channels (Kolla et al., 2012; Covault et al., 2019). It appears that meander bend cut-offs are not a major control on channel evolution in Bute Inlet, as none are observed in our surveys, nor are any signs of previous cut-offs observed. Secondary flow therefore does not always play the key role in submarine channel evolution, irrespective of the sense of that secondary flow compared to rivers.

Secondly, previous work has suggested that deposition of levees plays a key role in fixing channels in place, and creating flow-confinement, and thus channel evolution (Imran et al., 1998). However, the exact role of levees in channel initiation and evolution remains a topic of debate

(Imran et al., 1998; Rowland et al., 2010; Fildani et al., 2013; de Leeuw et al., 2016). Levee development may be especially important in highly depositional channels, such as channels on the Amazon Fan and Bengal Fan (Damuth et al., 1988; Curray et al., 2002). If this process is important in Bute Inlet, it acts on longer timescales, since we do not see significant deposition on the levees. However, we do see new confinement being formed independent of levees through the migration of knickpoints. These knickpoints can create a well-developed channel, where no clear channel existed previously (Figure 2.8c; Figure 2.9c). Similar processes have been shown in flume tank experiments where new channels were initiated by upstream-migrating erosional features (Yu et al., 2006; Toniolo and Cantelli, 2007). However, such fast-moving knickpoints were only monitored once in this detail previously at field scale (Guiastrennec-Faugas et al., 2020a). Furthermore, the channel in Bute Inlet confines flows by being incised in the seafloor rather than through deposition of levees rising above the seafloor.

Finally, pervasive crescent shaped bedforms on the delta-front are most likely a record of cyclic steps in supercritical turbidity currents, as similar-scale bedfoms have been linked to cyclic steps in supercritical flows at nearby Squamish Delta (Hughes Clarke, 2016; Hage et al., 2018). These bedforms can be an important control on submarine channel evolution in other systems (Covault et al., 2017; Vendettuoli et al., 2019). However, we show that knickpoints play a more dominant role in Bute Inlet channel. We later discuss whether the knickpoints themselves are a supercritical flow bedform, albeit at a larger scale.

2.7.2 Rapid knickpoint migration can dominate channel evolution

Here we show for the first time that fast-moving knickpoints can dominate the evolution of a submarine channel. Upstream-migrating knickpoints in Bute Inlet are fast-moving (100–450 m/year). This is 2–6 orders of magnitude faster than commonly reported knickpoint migration rates in rivers, which is 0.001–1 m/year, depending on substrate strength and discharge (van Heijst and Postma, 2001). However, knickpoints in rivers can occasionally migrate up to 1000 m/year due to flash-floods or weak substrate (van Heijst and Postma, 2001; Hayakawa and Matsukura, 2003; Crosby and Whipple, 2006). Migration rate of knickpoints has only been documented in three other subaqueous channels (Hill, 2013; Corella et al., 2016; Guiastrennec-Faugas et al., 2020a), but in all cases they migrate upstream at fast rates of 50–600 m/year, comparable to those seen in Bute Inlet. Flume tank experiments of knickpoints previously suggested fast migration rates of knickpoints (Toniolo and Cantelli, 2007), however direct comparison of erosion rates between experiments and natural systems remains difficult, due to scaling issues inherent in experiments. The migration rate of these knickpoints is also very high compared to other large-scale bedforms, such as tidal bars and aeolian dunes, that migrate up to

10 s of m/year (Marín et al., 2005; Levoy et al., 2013). Submarine knickpoints can also cause lateral migration of a channel thalweg, or incise new channel sections in places where no well-defined channel was previously present (Figure 2.8b, c; Figure 2.9b, c).

Rapid sediment deposition occurs in channel reaches between knickpoint-zones. These deposits most likely represent downstream accumulation of sediment eroded by the upstream knickpoint, as can occur in rivers (Burbank and Anderson, 2012). However, the volume of sediment deposited downstream of the knickpoints appears to be smaller than the eroded volume upstream (Figure 2.5a; Figure 2.6). This difference could be due to part of the initially eroded knickpoint sediment being transported further downstream, and deposited on the distal lobe.

Volumetric estimates of surface change also demonstrate the dominance of knickpoints. Within the channel, the volume of sediment eroded by upstream-migrating knickpoints accounts for ~72% of the total observed erosion, equalling the volume of sediment supplied by the main river at the top of the channel during the same period. Even though erosion related to knickpoint migration appears to exceed the deposition during the survey period, knickpoints migrated during erosion into recently deposited channel-filling sediments (Figure 2.5b; Figure 2.7a). This re-incision into recent deposits can explain why migration of many individual 5–30 m deep knickpoints, over periods of centuries to millennia, has not carved a deeper channel along this fjord. Phases of erosion caused by upstream-migrating knickpoints, followed by phases of deposition, appear to create a balance such that the channel depth is approximately that of a single knickpoint (5–30 m).

Reworking of recently deposited, and thus poorly consolidated sediment could partly explain why knickpoint migration is so rapid. Fresh channel deposits are mostly sand-dominated (Prior et al., 1986; Zeng et al., 1991), and they may be prone to erosion and failure, especially when loaded or scoured by fast moving turbidity currents. This kind of substrate may be much weaker than older, and consolidated or cemented sediments, or bedrock, which underlies many river systems.

2.7.3 How do knickpoints migrate?

Knickpoints migrate upstream along the channel, so we infer that their migration is caused by turbidity currents which are common in Bute Inlet (Prior et al., 1987; Zeng et al., 1991; Bornhold et al., 1994). We propose three internal flow-substrate processes that could trigger knickpoint migration, either in isolation or in combination (Figure 2.10). The first model is that submarine knickpoints, and intervening areas of deposition, are a large-scale bedform produced and maintained by instabilities within supercritical flow (Fildani et al., 2006; Lamb et al., 2008; Postma and Cartigny, 2014; Zhong et al., 2015), but with far longer wavelengths (>1–5 km) than those of

the crescent shaped bedforms (typically 50–100 m in Bute Inlet; Figure 2.7d). The second model is that migrating knickpoints are formed by seabed failures triggered by rapid undrained loading of the substrate, as a turbidity current passes. Unusually rapid rates of sediment accumulation (up to 1 m/year) in the depositional areas of the channel floor may favour such failure (Paull et al., 2010; Iverson et al., 2011). Past work suggested this model to explain the migration of sub-lacustrine knickpoints in tailing deposits (Turmel et al., 2012). These studies show that failure and subsequent knickpoint migration can even occur unrelated to an overpassing turbidity current. Third, the base of knickpoints may be gradually eroded and undercut by turbidity currents, leading to oversteepening and failure (Heiniö and Davies, 2007). This process is similar to headwall undercutting described in waterfalls and is known to cause migration of knickpoints in rivers, albeit at much slower rates (Holland and Pickup, 1976; Hayakawa and Matsukura, 2003). We conclude that all three models are potentially consistent with our field data. It is thus uncertain which model is correct, and more detailed monitoring will be needed to discriminate between competing hypotheses with confidence.

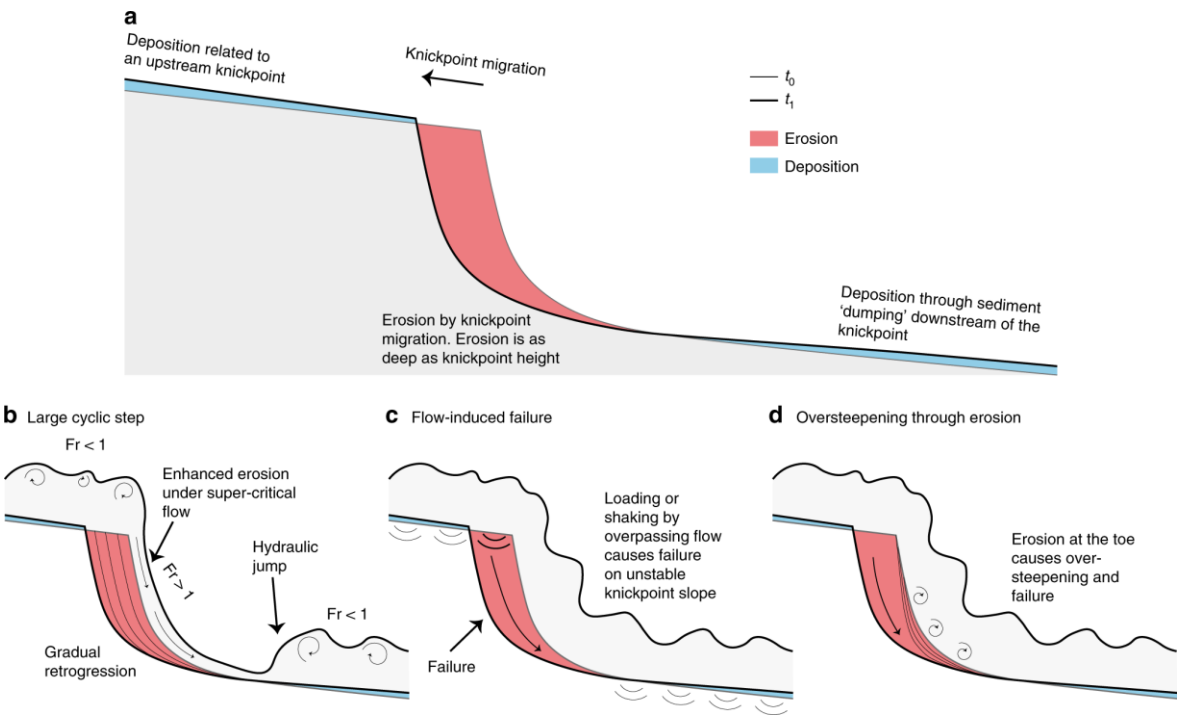

Figure 2.10: Models for knickpoint migration. a) Generalised pattern of erosion and deposition associated with upstream-migration of knickpoints. b) Cyclic step model. Knickpoint is formed by repeated instabilities (termed cyclic steps) that are self-generated by supercritical turbidity currents going through a hydraulic jump. c) Flow-induced slope-failure model. Knickpoint results from sudden failure of the channel floor, when loaded during passage of a turbidity current. d) Oversteepening through undercutting in which erosion at the toe of the steep face causes oversteepening, and eventual failure.

2.7.4 How are submarine knickpoints created or destroyed?

These three models (Figure 2.10) explain the movement of existing knickpoints, rather than their origin or final disappearance. We consistently observe three knickpoint-zones in our time-lapse surveys (Figure 2.6; Figure 2.7a – c). Some additional knickpoints appear within these zones, but they may be due to break-up of a larger knickpoint (Figure 2.7a – c). Thus, we do not record a clear example of a new knickpoint-zone forming, though we can speculate on their creation. Knickpoints are common in river systems, where they are often related to external factors, including local tectonic movement, variability in substrate or bedrock strength, or base-level change (Howard et al., 1994). Similar external controls have been suggested for submarine knickpoints (Mitchell, 2006; Heiniö and Davies, 2007).

However, none of the knickpoints in Bute Inlet can be related to any of these external factors. There is no evidence of local active tectonics, based on seismographs that locate earthquakes. The submarine knickpoints are carved mainly into recently deposited channel-fill sediment Figure 2.5b; Figure 2.7a; Prior et al., 1986; Zeng et al., 1991), making a strong bedrock or substrate control unlikely. As the channel is underwater, changes in sea-level (base-level) will not produce knickpoints. Furthermore, these submarine knickpoints are not created by meander-bend cut-offs, as observed in rivers, and modelled for submarine channels (Covault et al., 2016). There are no meander bend cut-offs or remnants of meander bend cut-offs along the Bute Inlet submarine channel (Figure 2.1; Figure 2.5a).

The lowermost knickpoint in knickpoint-zone 3 was in 2008 only 5–10 km away from the channel to lobe transition zone (where channel confinement ends and sediment deposits in a lobe; Mutti and Normark, 1987). A migration rate of 200 m/year in knickpoint-zone 3 would suggest this knickpoint was at the channel-to-lobe transition zone around 1958–1983. We would expect to see signs of some such external controls, if those created knickpoints in the recent past. Therefore, it appears that knickpoints can be created internally in submarine channels. If we rule out that knickpoints are created far beyond the downstream end of the system, we suggest that knickpoints are created by internal dynamics around the channel-to-lobe transition zone. A small steep step in channel gradient can be observed around this area, which may eventually form the next knickpoint-zone (Figure 2.6a).

The exact origin of these knickpoint-zones thus remains unclear at present. Similarly, we do not see the disappearance of knickpoint-zones as they migrate up-channel over the 9 years of our surveys. Further observations are thus also needed to establish how knickpoints are born and disappear, potentially through even longer sequences of repeat surveys.

2.7.5 Implications for evolution of submarine channel-bends

We now seek to understand how knickpoint migration affects the evolution of submarine channel bends. The planform evolution of meandering river bends is dominated by secondary (across-channel) helical flow, which causes point-bar deposition on the inner-bend, and erosion of the outer-bend (Figure 2.11a; Dietrich et al., 1979). This in turn causes river meander bends to progressively increase in amplitude (swing) and translate downstream (sweep) (Figure 2.11a; Hickin, 1974; Parker et al., 1983; Sylvester et al., 2019). A recent review found that submarine channel bends evolve in different ways, depending on what kind of bend-related (often bank attached) bars form (Peakall and Sumner, 2015). These bars are controlled by patterns of near-bed secondary flow, or direct suspended load fallout. This would result in submarine channel evolution being driven by deposition in bend-related (often bank-attached) bar deposits.

However, here we observe that submarine channel-bend evolution is dominated by rapid knickpoint migration, causing sudden channel-wide erosion (Figure 2.5). Rapid sediment deposition then occurs in channel-reaches downstream from knickpoint-zones (Figure 2.5a, e), rather than formation of distinct bend-related bars. Our surveys also show that migration of knickpoints can extend outside the original channel, and thus create terraces (Figure 2.8b; Figure 2.9b). This, combined with the lack of meander bend cut-offs or gradually migrating bends, produces a rather different view of evolution of channel-bends than previously described (Figure 2.11b; Sylvester et al., 2011; Peakall and Sumner, 2015).

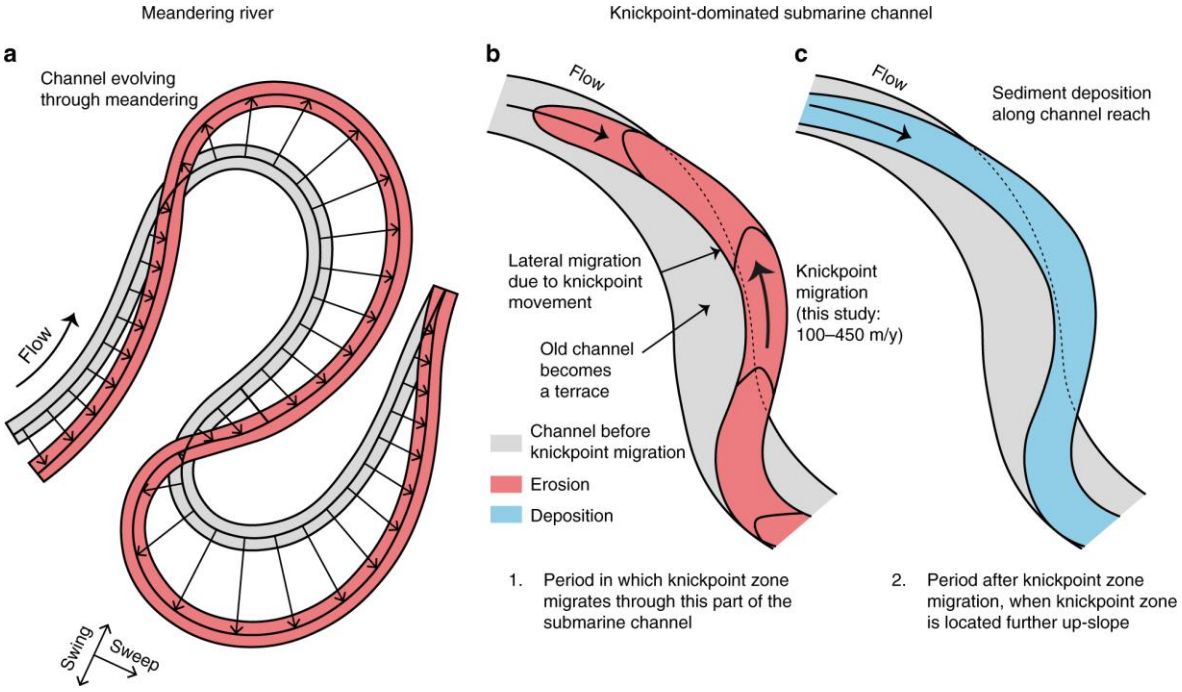

Figure 2.11: Comparison between migration of channel bends in meandering rivers and submarine channels dominated by fast-moving knickpoint-zones. a) Outer-bank erosion leads to swing and

sweep of bends in a meandering river (after Sylvester et al., 2019). b) Rapid knickpoint-zone migration in a submarine channel leads to incision, lateral migration, and terrace formation. c) Knickpoint-zone migrates further up-slope, and this part of the submarine channel is then infilled by deposition. Deposited sediment is partly sourced from knickpoint erosion occuring further up-slope.

2.7.6 Implications for submarine channel deposits

Knickpoint migration can also have a profound impact on the detailed architecture of channel-fill deposits (Figure 2.12). Knickpoint migration is mainly associated with erosion into and reworking of previous sandy deposits within the channel-fill (Figure 2.5b). Sediment is deposited gradually (~1 m/year) downstream of knickpoints in channel-wide sheets extending several kilometres along the channel (Figure 2.5a, b; Figure 2.12b). These patterns of deposition and erosion due to knickpoints are fundamentally different to the bend-related bars predicted previously, based on more gradual bend-migration driven by secondary across-channel flow (Figure 2.12a; Sylvester et al., 2011; Peakall and Sumner, 2015). Indeed, channel-wide deposits of similar dimensions as the deposits in Bute Inlet can be found in the geological record (*Figure 2.13: Comparison between deposits in the channel in Bute Inlet, and examples of channel deposits from the geological record. Note how sub-horizontal channel-wide deposits are present in both Bute Inlet as well as in the examples from the geological record. Vertical exaggeration: 5x.*Figure 2.13)

Submarine channels can be subdivided according to whether they are net-erosional, net-depositional, or there is a balance between erosion and deposition over longer (100 s to 1000 years) periods (Covault, 2011). Channels formed by long-term net-erosion, often termed submarine canyons, may contain only thin deposits with limited preservation potential. In contrast, areas of net-deposition will tend to produce systems confined by levees raised high above the surrounding seafloor (Curray et al., 2002), and they will have better potential for preservation in the rock record. Bute Inlet appears to represent an intermediate situation, in which erosion and deposition along the submarine channel are nearly balanced. Thus, over longer time scales, the knickpoint deposits in such settings will not be fully preserved as they are formed here; they will be mostly reworked by successive knickpoint erosion and deposition. Only if the channel reaches a net-depositional stage or moves laterally, parts of these deposits might be preserved.

2.7.7 Similar knickpoints occur in other locations worldwide

Various types and dimensions of seabed knickpoints have been documented in numerous locations worldwide (Table 2.2; Mitchell, 2006; Heiniö and Davies, 2007). These locations include knickpoints with broadly similar dimensions that occur in active submarine and sub-lacustrine channel systems. Knickpoints in other systems are often linked to tectonics, bedrock outcrop or meander-bend cut-off (Heiniö and Davies, 2007; Sylvester and Covault, 2016). However, similar knickpoints are found in Monterey Canyon, South China Sea, Capbreton Canyon, and others, where a clear external trigger is also lacking (Paull et al., 2011; Zhong et al., 2015; Guiastrennec-Faugas et al., 2020a). The type of knickpoints seen in Bute Inlet and other locations, can occur in a wide range of systems, including locations with low (<1°) gradients. Furthermore, erosional features that share similarities with knickpoints have been reported to migrate up the channels in Squamish Delta (Vendettuoli et al., 2019). This suggests that the processes that form fast-moving channel-knickpoints, and their impacts on submarine channel evolution and deposits, might be of widespread importance.

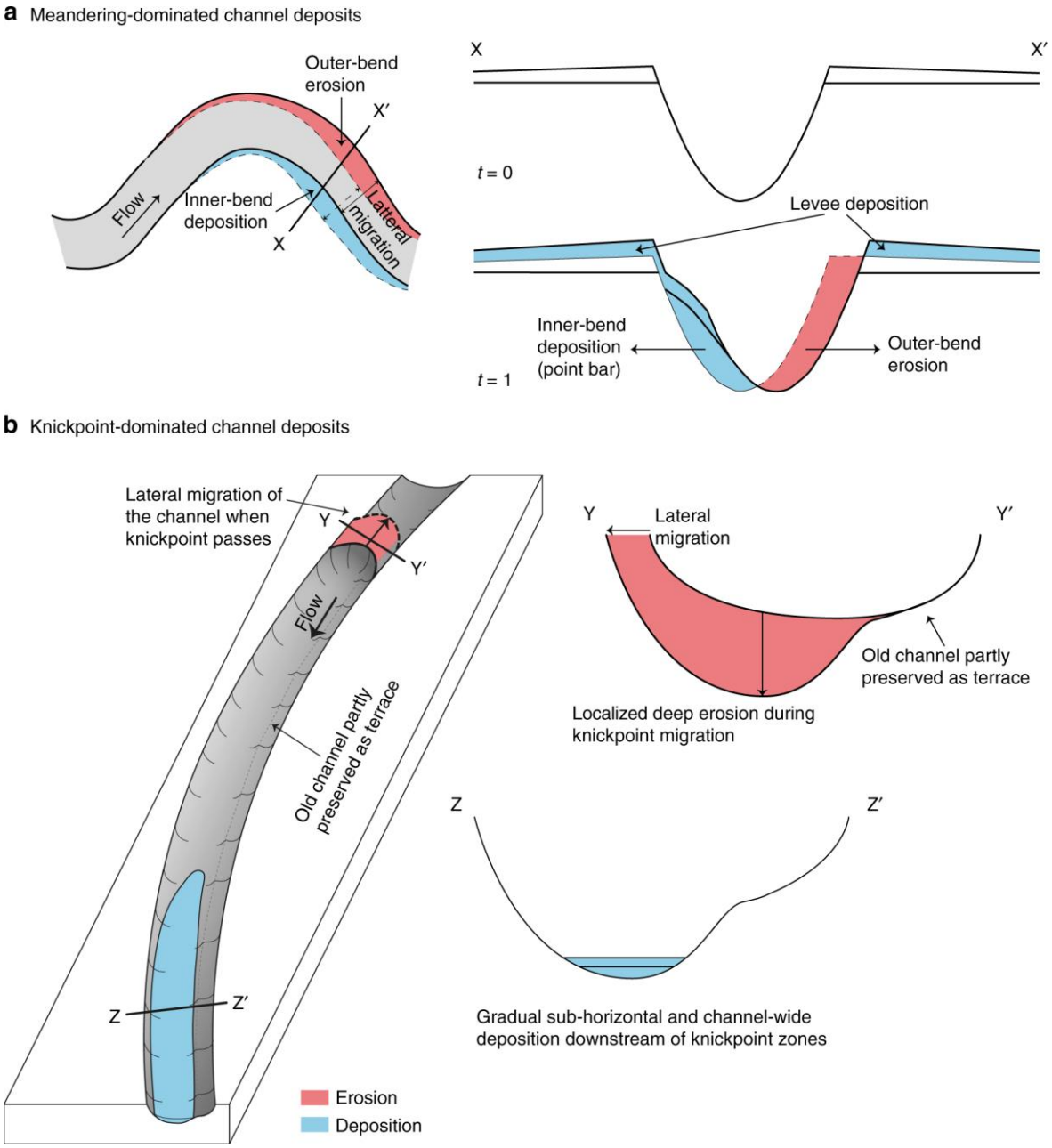

Figure 2.12: Generalized models for submarine channel evolution and deposits. a) Deposition and erosion in meandering dominated channels (after23). This results in bars (shown in light blue) deposited in the inner bends, and erosion in the outer bends. The erosion causes outward and downstream propagation of bends. b) New model for submarine channel deposits in locations dominated by fast-moving knickpoints, such as Bute Inlet. Knickpoint migration causes deep erosion, and potential channel migration. This is then followed by channel-wide deposition, once the knickpoint has migrated further upslope.

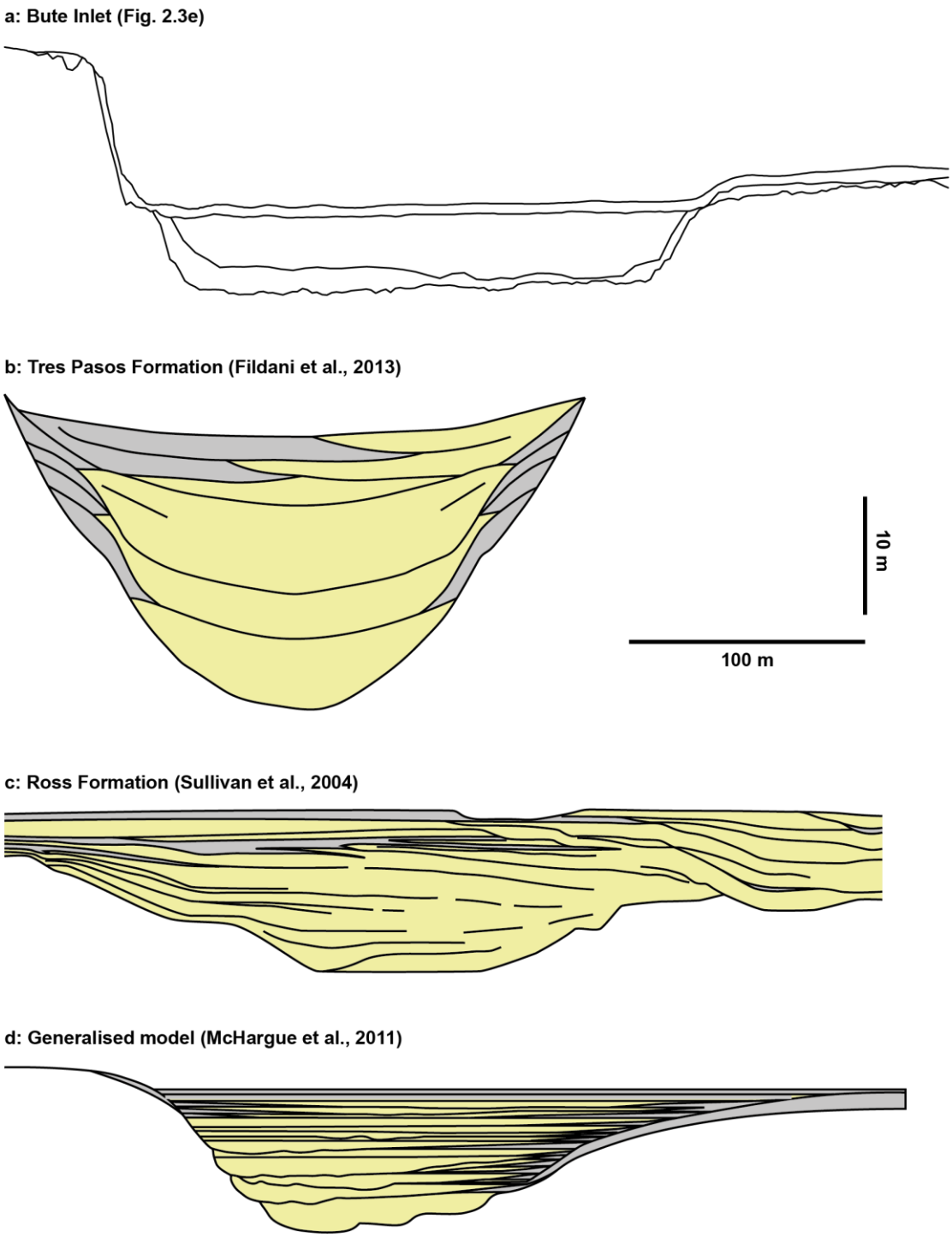

Figure 2.13: Comparison between deposits in the channel in Bute Inlet, and examples of channel deposits from the geological record. Note how sub-horizontal channel-wide deposits are present in both Bute Inlet as well as in the examples from the geological record. Vertical exaggeration: 5x.

2.8 Conclusions: A new generalised model for submarine channels

We use 9 years of time-lapse bathymetry from an active submarine channel in Bute Inlet, British Columbia, to study how submarine channels evolve. Rapid (100–450 m/year) upstream-migration of knickpoints was the dominant process driving channel evolution. Previously described

processes such as meander-bend migration, levee aggradation, and migration of smaller bedforms all play a minor role in channel evolution on this time scale in Bute Inlet. Knickpoints are steep (up to angle of repose) steps in channel gradient, with heights of up to 30 m. Sediment upstream of a knickpoint is eroded during migration and deposition occurs further downstream of the knickpoint. Deposits form long and thin channel-wide deposits, rather than previously proposed bend-related bars. Knickpoints can migrate outside the banks of the original channel, causing lateral migration of the channel and development of channel bends. Previous models proposed outer-bend erosion and inner-bend deposition due to across-channel (secondary) flow, as the main control on evolution of channel bends and their resulting deposition. However, here we propose an alternative model for submarine channel evolution and deposits, controlled by upstream-migrating knickpoints. Finally, as similar knickpoints occur in sedimentary channels in a variety of subaqueous settings worldwide, we suggest the processes described here are common globally.

Table 2.1: Time lapse bathymetric surveys of subaqueous channel systems worldwide.

Location	**Key Reference(s)**	**Notes**
Fraser Delta, BC, Canada	(Hill, 2013)	Channels on a delta slope. Up to 300 m water depth. 8 surveys between 1994 and 2006. Channel is occasionally dredged. Kickpoints (referred to as erosional scarps or scallop shaped depression) are seen. Several other different bedforms are observed.
Bute Inlet, Knight Inlet and Toba Inlet, BC, Canada	(Conway et al., 2012)	Fjords. Submarine channels fed by fjord head deltas. Up to 660 m waterdepth. 2 surveys per fjord between 2005 and 2010 years. Includes this study area. Knickpoint and associated erosion in Bute Inlet is visible in the figures.
Squamish Delta, BC, Canada	(Hughes Clarke et al., 2009, 2012, 2016; Hughes Clarke, 2016; Hizzett et al., 2018; Hage et al., 2018; Vendettuoli et al., 2019)	Fjord. Recently reset system fed by a fjord head delta. Up to 200 m water depth. Single beam and sidescan surveys from 1974 onwards. 9 multibeam surveys between 2004 and 2009; 93 surveys in 2011, including daily during the summer of 2011. Sub-daily surveys in the summer of 2013. 6 daily surveys in the summer of 2015.

Location	Key Reference(s)	Notes
Monterey Canyon, California, west coast USA	(Smith et al., 2005, 2007; Paull et al., 2010)	Marine. Canyon on continental slope fed by littoral cells. 7 surveys of the upper 4 km of the canyon between 2002 and 2005. 3 more surveys in 2007 using an AUV. 2 surveys cover the system up to 2100m water depth, one in 2002 and a large AUV effort obtained in 2008-2009. 6 more AUV surveys in specific locations between 2015 and 2017. Crescentic shaped bedforms and knickpoints are observed.
Capbreton Canyon, Bay of Biscay, France	(Mazières et al., 2014; Guiastrennec-Faugas et al., 2020a, b)	Marine. Canyon on continental slope. Up to 3500 m water depth. Focus on the canyon head (up to 400 m water depth). 10 surveys between 1998 and 2018. Crescentic shaped bedforms and knickpoints are abundant.
Lake Geneva, Switzerland/France	(Corella et al., 2016)	Lacustrine. Up to 300 m waterdepth. Surveys in 2000 and 2012. Contains knickpoint and crescentic shaped bedforms.
Malalay Canyon, Mindoro Island, the Philippines	(Sequeiros et al., 2019)	Marine. Canyon in continental shelf. Up to 350 m water depth. 26 surveys between 1997 and 2018, but variable coverage. Canyon-wide surveys at least in 2007, 2008, 2011, and 2018. Crescentic shaped bedforms are common.
Pearl River Mouth Basin, South China Sea	(Yin et al., 2019)	Marine, canyons in upper continental slope. 500-1700 m water depth. One survey in 2004/2005 and one in 2018

Location	Key Reference(s)	Notes
Wabush Lake, NL, Canada	(Turmel et al., 2015)	Lacustrine, system created by tailings. Up to 100 m water depth. Surveys in 1999, 2004, 2006, and 2008. Knickpoints are common.
Pointe Odden, Gabon	(Biscara et al., 2012)	Marine, several smaller channels in a bay fed by a littoral cell. Up to 75 m water depth 6 surveys between 2004 and 2009. Channel incision and a landslide.
Ligurian Margin (incl. Var canyon), Mediterranean, France	(Kelner et al., 2016)	Marine. Several channels/canyons on an active margin. Fed by rivers. Single beam surveys from 1960s and 1970s. Multibeam surveys from 1991, 1999, 2006, and 2011. Focus on landslide history. Erosional areas in several channels can be distinguished.
Kaikoura Canyon, New Zealand	(Mountjoy et al., 2018)	Marine. Canyon on a continental slope. Over 2000 m water depth. 2 surveys, one before and one after the 2016 earthquake. Focus on earthquake triggered mass movement.
Stromboli, Southern Messina Strait and Punta Alice, Italy	(Casalbore et al., 2011)	Marine, canyon on active margin. Up to 400 m water depth. Two surveys between 2005 and 2007. Focus on terrestrial debris flows triggering hyperpycnal flows.
Begwan Solo Delta, Java, Indonesia	(Syahnur, 2018)	Prodelta channels on continental shelf. Up to 30 m water depth. Surveys in 2008 and 2012.
Westerschelde, Netherlands	(Mastbergen et al., 2016)	Estuary. Up to 25 m water depth. Dredging induced failure of the side of the main estuary channel.

Location	**Key Reference(s)**	**Notes**
Lower St. Lawrence Estuary, Eastern Canada	(Normandeau et al., 2014, 2019)	Inner continental shelf. Sediment starved canyons. Up to 325 m water depth. seven surveys between 2007 and 2017. Upstream-migrating crescentic shaped bedforms.
Eastern Baffin Island, north-eastern Canada	(Hughes-Clarke et al., 2015; Normandeau et al., 2020)	Mapped 31 fjord-head deltas between 2006 and 2014. Repeat bathymetry is available for several of these fjords.

Table 2.2: Subaqueous knickpoints in literature.

Location	**Setting**	**Comments**	**Key Reference(s)**
Wabush Lake, NL, Canada	Lacustrine. Iron tailings dumping; 10 km long, up to 100 water depth.	Around 10 main knickpoints. Typically 1–2 m high and 10–30 m wide (up to 4 m high and 70 m wide)	(Turmel et al., 2010, 2015)
Offshore New Jersey, east coast USA.	Continental slope, up to 2200 m water depth.	8 knickpoints, typically a few tens of meters high. One major knickpoint of 200 m high. Knickpoints probably formed due to differences in lithology	(Mitchell, 2006)
Gulf of Alaska, USA	Accretionary prism, up to 4500 m water depth.	13 knickpoints, typically 50–150 m high, but up to 350 m high. Knickpoints have a tectonic origin (localised vertical movement; anticlines), however fault related knickpoints cannot be ruled out in some cases.	(Mitchell, 2006)
Astoria Canyon, offshore Oregon, west coast USA	Canyon on accretionary wedge. Up to 2300 m water depth.	Six tectonically controlled knickpoints, tens of meters high.	(Mitchell, 2006)
San Antonio Canyon, offshore Chile	Canyon in forearc basin. Up to 5500 m water depth.	A single 500-1000 m high knickpoint. The shape may suggest a landslide origin, rather than usual erosion by turbidity currents. Also a 50 m high knickpoint.	(Mitchell, 2006)

Location	Setting	Comments	Key Reference(s)
Southern Barbedos Accretionary Prism, Caribbean.	Canyons through fold ridges on an accretionary prism. Up to 3500 m water depth.	Knickpoints related to tectonic structures, several hundreds of meters high.	(Huyghe et al., 2004; Mitchell, 2006)
Niger Delta, offshore Niger	Continental slope. Up to 3400 m water depth. Reconstructed using seismic surfaces.	Five knickpoints, or knickpoint zones of tens of meters high per zone. Related to a fault and thrust belt and diapirsim.	(Adeogba et al., 2005; Heiniö and Davies, 2007)
Espirito Santo Basin, offshore Brasil	Continental slope influenced by salt tectonics. Reconstructed using seismic surfaces.	Five 18-30 m high knickpoints recognized below present-day seabed depressions.	(Heiniö and Davies, 2009)
North Sardinia Slope, Mediterranean	Passive margin with three main channels reaching up to 1000 m water depth.	Several smaller (around 10 m) knickpoints and two large (around 50 m) knickpoints.	(Dalla Valle and Gamberi, 2011)
Monterey Canyon, offshore California, west coast USA	Continental slope, up to 3600 m water depth.	5-10 m high knickpoints are common in the upper (up to 1300 m water depth) canyon. Five up to 200 m high steep steps outside main channel, referred to as discontinuous scours. Interpreted to be cyclic steps associated with channel inception.	(Fildani et al., 2006; Paull et al., 2011)
La Jolla Canyon, offshore California, west coast USA.	Continental slope. Up to 700 m water depth.	Seven up to 30 m high knickpoints referred to as ‘distinctive canyon floor scarps’ in the axial channel.	(Paull et al., 2013)

Location	Setting	Comments	Key Reference(s)
Lake Geneva, Switzerland.	Lacustrine. Up to 300 m water depth.	Upstream-migrating incision, and steep steps in channel profile. Additionally, knickpoint-bound headless channels are present.	(Corella et al., 2016)
South China sea	Continental slope. Several canyons/channels. Up to 3500 m water depth.	Around 40 10-81 m high steps and several smaller steps in two canyons. Steps are interpreted as cyclic step bedforms.	(Zhong et al., 2015)
Knight, Toba, and Bute Inlets, BC, Canada	Fjords. Up to 650 m water depth	16 up to 40 m high knickpoints in channels in three different fjords.	(Gales et al., 2019)
Santa Monica and Redondo Canyon, California, west coast USA	Continental slope. Up to 800 m water depth.	Six up to 70 m high knickpoints and three 'distinctive canyon floor scarps'. Large scours (up to 70 m high) are found outside the channel too.	(Tubau et al., 2015)
Amazon fan, offshore Brazil	Continental slope. Up to 3700 m water depth. Reconstructed using seismic surfaces.	Single large knickpoint related to channel avulsion.	(Pirmez et al., 2000)
East Breaks, Gulf of Mexico	Salt-withdrawal mini-basins.	Fault related knickpoints.	(Pirmez et al., 2000)
Rhone Fan, offshore France, Mediterranean	Active margin. Up to 2500 m water depth.	Several knickpoints related to channel avulsion.	(Pirmez et al., 2000)
Congo Canyon, offshore West Africa	Continental slope. Up to 5000 m water depth.	Several knickpoints recognised in the channel-levee part of the system and are linked to avulsions.	(Babonneau et al., 2002)

Location	Setting	Comments	Key Reference(s)
Magdalena Channel, offshore Columbia	Active margin. Up to 3500 m waterdepth.	Knickpoints are common and associated with avulsions.	(Estrada et al., 2005)
Madeira channel system, Southwest of Madeira, Atlantic Ocean	Intra basins channel system on passive margin. 4400–5400 m water depth.	Knickpoints bound upstream sides of headless channels. Suggested that knicpoints are the channel initiators.	(Stevenson et al., 2013)
Tenryu Canyon, offshore Japan	Active margin canyon, up to 4000 m water depth.	One steep fault related knickpoint.	(Soh and Tokuyama, 2002)
Offshore Angola	Channel surface of an ancient channel system on a passive margin. Reconstructed using seismic surfaces.	Avulsion related knickpoints in order of tens of meters high.	(Gee and Gawthorpe, 2006)
Danube Canyon, Black Sea	Canyon-channel system up to 1000 m water depth.	One knickpoint, marking the shift between the canyon and channel regime.	(Popescu et al., 2004)
Central Atlantic USA margin	Canyons on passive continental margin. Up to ~1800 m water depth.	Knickpoints are observed and attributed to variability in substrate erodability.	(Mitchell, 2004)
Capbreton Canyon, Bay of Biscay, France	Canyon in continental slope. Up to 3500 m water depth. Focus on the canyon head up to 375 m water depth.	Up to 80 potential knickpoints present. Up to 7 m high. Migrate upstream at 90-600 m/yr.	(Guiastrennec-Faugas et al., 2020)

Chapter 3 How do submarine channel systems fill and flush, and build lobes?

This chapter is being prepared for submission to a peer-reviewed journal, and is co-authored by Maarten S. Heijnen, Michael A. Clare, Matthieu J.B. Cartigny, Peter J. Talling, Sophie Hage, Ed L. Pope, Lewis Bailey, Esther Sumner, D. Gwyn Lintern, Cooper Stacey, Brent Seymour, Daniel R. Parsons, Stephen M. Simmons, Ye Chen, Stephen M. Hubbard, Joris T. Eggenhuisen, Ian Kane, and John E. Hughes Clarke.

M.S.H. is the main author of the manuscript and performed the majority of the data analysis. M.A.C., M.J.B.C., P.J.T., S.M.H., and I.K., assisted with writing the manuscript. M.S.H., E.L.P, L.B, S.M.S., and Y.C. were involved in analysis of the ADCP data. B.S. and J.E.H.C. and planned, performed, and processed the seafloor surveys. M.S.H., M.A.C. M.J.B.C., P.J.T., S.H., L.B., D.G.L., C.S., D.R.P. S.M.S., Y.C., S.M.H., J.T.E., and J.E.H.C. were involved in data collection. D.G.L., C.S. J.E.H.C., planned and were in charge of the different expeditions. Figure 3.5 was produced by E.P. Only M.A.C., M.J.B.C., and P.J.T. reviewed this chapter.

3.1 Abstract

Submarine channels are the main conduits for the transport of sediment, organic carbon, and pollutants into the deep ocean. However, due to their inaccessibility, we have a poorly developed understanding of how this material is transported through submarine channels and onto their terminal lobes. Here, we present the first combination of repeat seafloor surveying, flow monitoring, and source-river discharge for an active submarine channel system along its full length. This allows a source to sink analysis of how these systems operate. We show that most flows deposit their sediment in the proximal part of the system. This sediment is then reworked and transported stepwise further downstream by progressively bigger flows. The upstream-migration of crescentic bedforms and knickpoints is the most important processes for this reworking on the prodelta and in the channel respectively. Upstream-migration of knickpoints creates alternating zones of erosion and deposition that migrate up the channel. These zones can balance over longer timescales and result in net sediment bypass. We record an exponential decrease in the number of turbidity currents recorded downstream, with tens of flows per year in the proximal channel, but only around one per year reaching the lobe. Sediment delivery to the lobe is discontinuous and cannot be directly linked to sediment input at the head of the system, and provides a highly incomplete and buffered record of the flow activity in the channel further

upstream. Within the survey period, around 20 – 30% of the sediment input from the main feeding river was captured and buried by the submarine channel-lobe system. However, the step-wise sediment transport and amount of reworking observed indicates that terrestrial material may be buried and re-excavated numerous times, before final burial. This re-excavation might allow further oxidation of previously buried organic matter. This suggests that the burial efficiency of terrestrial material such as organic carbon and pollutants, over decadal or longer timescales, within submarine channels may be very low.

3.2 Introduction

Submarine channel systems are the main conduits for the transfer of land-derived material to the deep ocean. These systems form some of the world's largest sediment accumulations, such as the Bengal (Curray et al., 2002), Indus (Kolla and Coumes, 1987; Clift and Gaedicke, 2002), and Amazon fans (Damuth and Kumar, 1975). Previous studies have suggested these channels can experience complex cycles of sediment storage and release, while others have suggested a more direct sediment transport mechanism (e.g. Paull et al. 2005; Stevenson et al., 2013). Understanding the spatial and temporal patterns of sediment transport through submarine channels and onto fans is important for a number of reasons. Submarine channel-lobe systems play a vital role in sustaining deep-sea ecosystems, as they deliver organic carbon and nutrients to the deep sea; however, the same channels are also increasingly recognised as pathways for pollutants that are detrimental to marine biological communities (Heezen et al., 1955; Quadfasel et al., 1990; Canals et al., 2006; Galy et al., 2007; Baudin et al., 2010; De Leo et al., 2010; Masson et al., 2010; Pierdomenico et al., 2019, 2020; Kane et al., 2020). The often-powerful sediment-laden flows that traverse these systems (known as 'turbidity currents'), sculpt the seafloor and pose a hazard to critical seafloor infrastructure such as pipelines and cables, which carry >95% of global data traffic (Heezen and Ewing, 1952; Carter et al., 2009; Pope et al., 2017a, b). Furthermore, submarine channel and lobe deposits form important archives of Earth history, providing information on past climate and geohazards, such as earthquakes, floods, and storms (e.g. France-Lanord et al., 1993; Prins and Postma, 2000; St.-Onge et al., 2004; Moernaut et al., 2014).

Sediment transport through submarine channel-lobe systems is difficult to directly observe, because of the often-remote locations, and the destructive and episodic nature of turbidity currents (Clare et al., 2020). Most of our understanding of submarine channel-lobe systems, has therefore necessarily been inferred from the deposits left behind by turbidity currents, scaled-down laboratory models, uncalibrated numerical models, or low resolution static seabed surveys (e.g. Babonneau et al., 2002; Sylvester et al., 2011; Armitage et al., 2012; Hubbard et al., 2014; de

Leeuw et al., 2016). Previous studies using such data have shown that over geological timescales, the most upstream and deeply confined part of channel-lobe systems (often referred to as canyons) are generally characterised by erosion (Figure 3.1a; e.g. Shepard, 1981; Carlson and Karl, 1988). Submarine channels are typically described either as zones characterised by bypass, or by gradual aggradation (Normark, 1970; Deptuck et al., 2003; Stevenson et al., 2015). Bypass is used as a spatial term in submarine channels, referring to an area within the channel where erosion and deposition are in balance. However, it is also used as a property of a turbidity current, indicating that a flow is neither erosive nor depositional at a certain location within the channel (Stevenson et al., 2015). The downstream termini of submarine channels are referred to as lobes and these are dominantly depositional areas (Normark, 1970). It remains unclear, however, how this spatially-segregated signature of an erosion-dominated canyon, bypass-dominated channel and deposition-dominated lobe is generated (Figure 3.1a).

First, individual flows may generate this overall erosional and depositional pattern in submarine channel systems ('ignition and autosuspension model', Figure 3.1b). In this first model, an initial catastrophic triggering event such as an earthquake-generated landslide or flood, generates a high energy and erosive turbidity current in the steep upper part of a canyon. As a turbidity current entrains sediment, it can reach a state of autosuspension, in which a flow is in equilibrium with the channel and the substrate (Bagnold, 1962; Pantin, 1979; Parker et al., 1986; Sequeiros et al., 2009; Stevenson et al., 2013, 2015). In this scenario, flows are erosive in the canyon, where they ignite. Flows then carry their sediment load through the channel without any discernible erosion or deposition ('bypassing' flow), before depositing the transported sediment on the lobe (Figure 3.1b).

A second model comprises a bimodal distribution of flows of differing energy and runout distance ('fill and flush model', Figure 3.1c). Successive small and short-runout flows may deposit sediment in the proximal part of the system, which is subsequently flushed downstream by much less frequent (100 – 1000s of years recurrence), but larger magnitude flows. It has been proposed that such powerful, long-runout flows require a similar catastrophic external trigger as proposed for the 'ignition autosuspension model' (Parker, 1982; Piper and Normark, 2009; Allin et al., 2016; Mountjoy et al., 2018). Indeed, it has been recently demonstrated that turbidity currents can reach a state of autosuspension after igniting by picking up unconsolidated sediment deposited by previous flows (Heerema et al. 2020). In this second scenario, the episodic down-channel flushing of sediment can generate deep erosion in the canyon by exhuming canyon-fill deposits. However, the longer term balance between canyon flushing and filling will result in much lower incision rates than those observed over a flushing event.

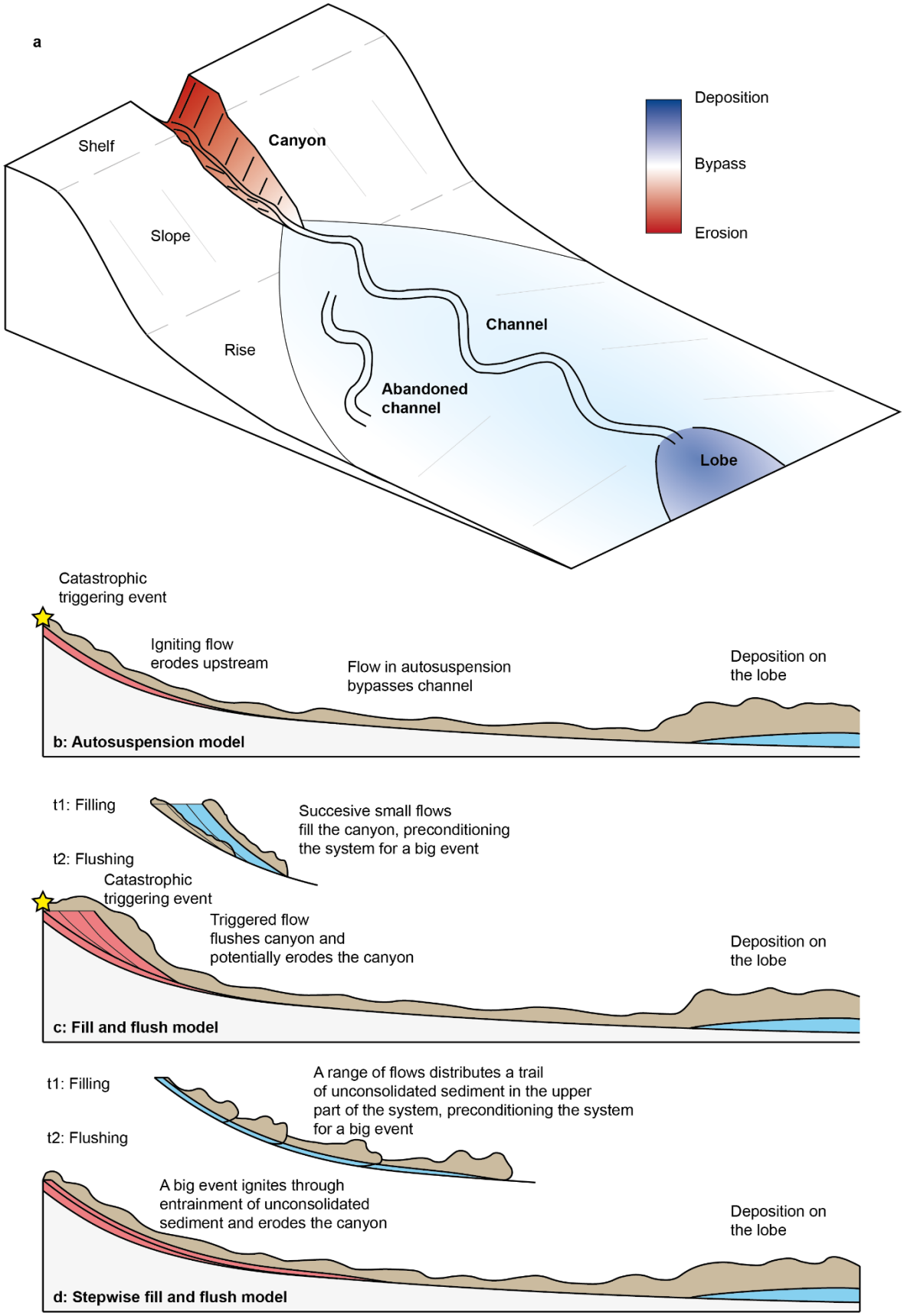

Figure 3.1: Generalised models of how submarine channel systems evolve over longer timescales and different models of sediment transport through submarine channel systems. a) generalised model showing how erosion and deposition is distributed over longer timescales in a submarine

channel system. The upstream canyon is characterised by erosion, the channel by bypass or slight deposition and the lobe is depositional (redrawn from Wells and Cossu, 2013)*. b) autosuspension model: a single big flow triggered by a catastrophic event erodes in the canyon, then reaches a state of autosuspension and bypasses the channel, and deposits its sediment on the lobe. c) fill and flush model: frequent successive small flows fill the upper canyon, preconditioning a large flow triggered by a catastrophic event. This large flow then flushes this preconditioned sediment and ignites, then bypasses the channel and deposits on the lobe. d) stepwise fill and flush model: successive flow decreasing in frequency with distance, distribute a trail of unconsolidated sediment in the upper part of the system. A larger turbidity current is generated as it picks up this sediment, balancing out the original deposition in the channel before depositing on the lobe.*

A modified version of the fill and flush model has also been suggested, wherein sediment is stored over a much longer part of the system than the upper canyon alone (Paull et al., 2005). In this stepwise fill and flush model, a range of flow runout exists within the canyon and upper channel, which decreases in frequency with runout length (Figure 3.1d). Longer runout flows pick up sediment deposited in the upper canyon and deposit it further downstream in the canyon or channel; creating a stepwise transport of sediment down-channel. This causes a trail of unconsolidated sediment to accumulate much further down the system than suggested in the traditional 'fill and flush model'. This unconsolidated sediment preconditions larger flows to ignite and flush sediment onto the lobe. The smaller flows deposit their sediment in the canyon and upper part of the channel, while the big flushing flows erode sediment and flush this to the lobe. Deposition by the successive smaller flows and the erosion by the big flushing flow can balance to generate net sediment bypass. In this modified fill and flush model, each flow does not necessarily bypass the channel, but the long-term effect is one of a sediment bypass zone in the channel.

Each of these three models have markedly different implications for how and when sediment, is transferred via submarine canyons and channels onto terminal lobes, how organic carbon is buried and re-excavated and potentially oxidised, and what might be recorded in the deposits formed by these systems. The 'ignition and autosuspension model' suggests that turbidity currents hardly rework previously deposited channel deposits and all flows reach the lobe. This implies that each flow leaves a depositional signature on the lobe. Therefore, in this first model, lobe deposits would preserve a complete record of past catastrophic environmental events, and the activity of the system. In contrast, most sediment in any 'fill and flush model' is initially deposited in the upstream part of the system. This sediment is then reworked before being transported to the lobe. This implies that in the 'fill and flush model' the lobe deposits hold an incomplete record of the activity of the upstream system. Depending on how flushing flows are triggered, the lobe might reliably preserve past environmental signals.

However, the lack of direct source to sink monitoring data means that these three models remain untested in active submarine channel-lobe systems. Unlike in subaerial settings, detailed time-lapse imagery of these systems is difficult to obtain, since satellites cannot image seaward of the shallow coastal zone (e.g. Vendettuoli et al., 2019). Monitoring flows themselves is logistically challenging, and instruments need to withstand destructive flows (Inman et al., 1976; Puig et al., 2014; Clare et al., 2020 and references therein). Recent developments in technology and instrument design now permit detailed studies of modern seafloor systems, including the first field scale measurements of turbidity current structure (Azpiroz-Zabala et al., 2017a, b; Paull et al. 2018), and repeated multibeam echosounder surveys that reveal how repeated flows shape the seafloor and build stratigraphy (e.g. Paull et al., 2010; Hage et al. 2018; Vendettuoli et al., 2019; Guiastrennec-Faugas et al., 2020a; Englert et al., 2020; Heijnen et al., 2020). Despite these technological and scientific advances, such surveys remain relatively rare due to the time and costs involved, and hence cover limited parts of systems and only involve relatively short timescales. This shortage of observations has caused a knowledge gap of how sediment is transported along an entire submarine channel from source to sink.

Here we present the first direct monitoring dataset for an active submarine channel-lobe system along its full length; focused on the 50km-long submarine channel in Bute Inlet, British Columbia. The dataset comprises: i) repeat seafloor surveys that record erosional and depositional changes across the entire system during a period of ten years; ii) detailed monitoring using acoustic Doppler current profilers (ADCPs) to record the runout and velocity of flows at six locations along the channel and lobe; iii) and monitoring of the discharge of the main river that feeds the head of the system to understand temporal variations in sediment supply.

3.3 Aims

Our overarching objective is to understand the patterns of sediment filling (deposition) and flushing (erosion) within submarine channels, and their implications for deposition on lobes. To address this, we ask the following specific questions. First, how do patterns of erosion and deposition vary spatially and how do these patterns change over time? Such patterns can reveal to what extent sediment is reworked along submarine channel systems, and how sediment bypass zones are generated in submarine channels. Second, when and how efficiently is sediment delivered to the terminal lobe? We investigate whether all flows contribute to lobe-building, or whether the sediment delivery is episodic and discontinuous in nature. Third, what controls the timing of sediment delivery to the lobe? Previous studies have suggested that catastrophic triggers such as floods and earthquakes are required, but here we also explore whether sediment delivery to the lobe can occur independently from such triggers. We then go on to test previous

models for sediment transport through submarine channels and onto lobes before presenting a modified model based on the development of the channel-lobe system over a decade at Bute Inlet. Finally, we discuss the implications of this study for interpreting the stratigraphic record of channel-lobe systems in terms of reconstructing flow occurrence and past environmental signals, such as floods and earthquakes, as well as the implications for the burial efficiency of organic carbon and anthropogenic pollutants.

3.4 Geographical and oceanographical setting

Bute Inlet is a fjord in British Columbia, Canada, within which lies a 50 km-long submarine channel-lobe system (Figure 3.2a; Prior et al., 1986; Zeng et al., 1991). The submarine channel-lobe system extends from the prodeltas of the two feeding rivers (Homathko and Southgate), to a terminal lobe at 650 m water depth (Figure 3.2b). The channel has an average gradient of 0.6° and sinuosity of 1.4. The uppermost channel may reach slopes of up to 3°, while the gradient at the lobe is around 0.1° (Zeng et al., 1991; Gales et al., 2019). The channel floor is composed of sand, while overbank areas are dominantly silty at the surface, but sandy turbidites are found in the subsurface (Zeng et al., 1991; Hage et al., 2020). The Homathko river is responsible for 70 – 80% of the freshwater input, the Southgate for 15 – 25% and small rivers and streams coming in from the sides of the fjord for 5% (Syvitski and Farrow, 1983; Zeng et al., 1991).

Tens of turbidity currents occur yearly during the summer freshet, when the Homathko River discharge rises above 200 m^3/s as a result of increased glacier melt (Prior et al., 1987; Zeng et al., 1991; Bornhold et al., 1994). The system is inactive during the winter months, when the river discharge is typically below 100 m^3/s. These turbidity currents can dramatically shape the seafloor. Repeated seafloor surveys a few years apart have shown how over 20 m of vertical erosion can occur in various stretches of the submarine channel (Conway et al., 2012; Heijnen et al., 2020). Much of this vertical erosion is linked to upstream-migrating knickpoints.

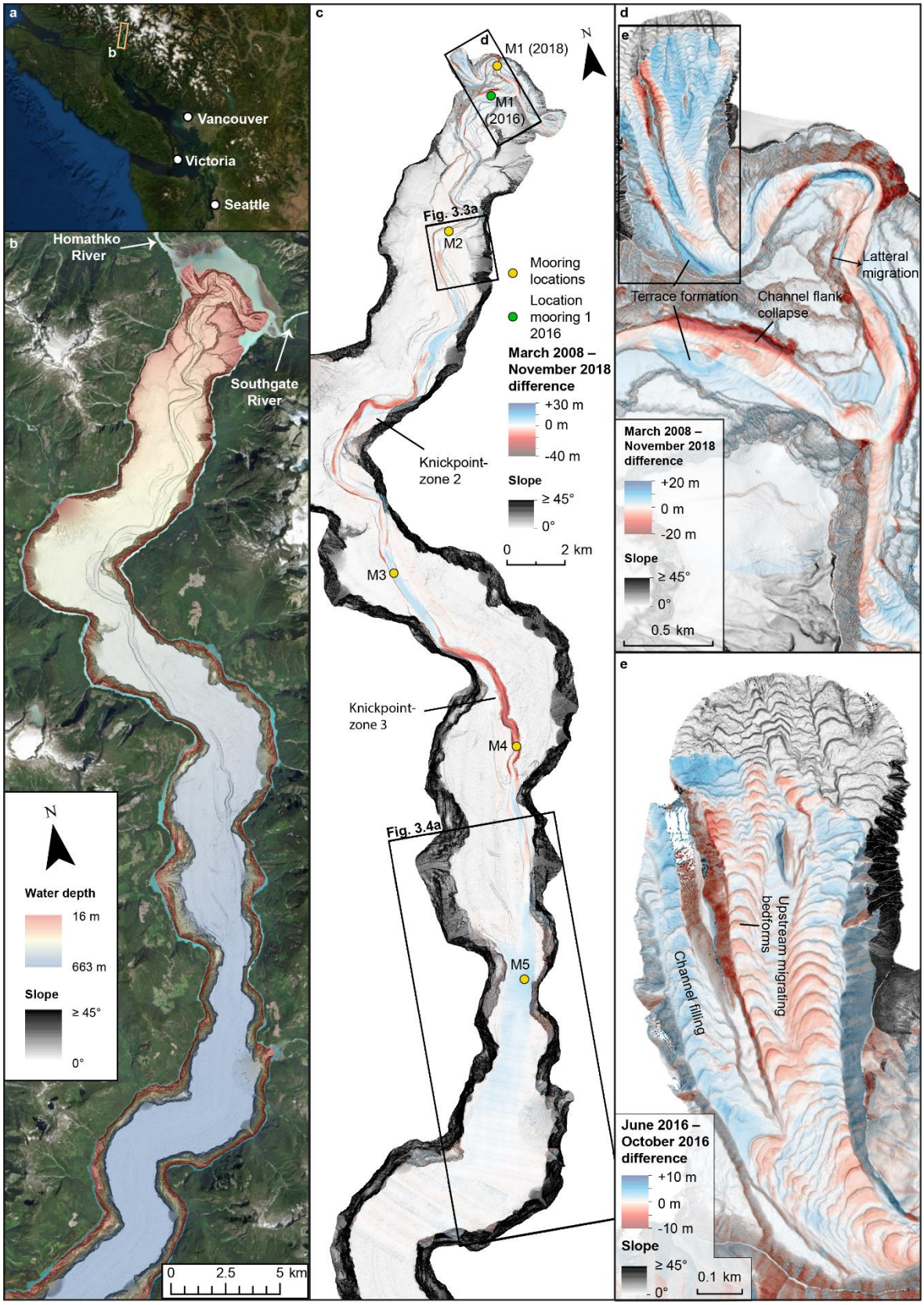

Figure 3.2: Location, morphology, and change of the Bute Inlet submarine channel-lobe system. Source satellite data: Esri, DigitalGlobe, GeoEye, Earthstar, Geographics, CNES/Airbus DS, USDA, USGS, AeroGRID, IGN, and the GIS User Community. a) Location of Bute Inlet. b) Overview of the submarine channel-lobe system in Bute Inlet as monitored in March 2008. Data is presented as a

slope map overlain by a transparent bathymetry map. c) 2008 slope map overlain by a March 2008 – November 2018 difference map. Location of moored instrument stations are shown. Note the along channel alternation of erosional and depositional areas controlled by knickpoints. d) Detailed difference map of the upper channel. Location shown in panel c. Note patterns of erosion and deposition cause by a variety of different processes. e) Detailed difference map over June–October 2016 of the Homathko River prodelta. Location shown in panel d. Note the upstream-migrating bedforms dominating the evolution of the prodelta on the short timescale.

3.5 Methods

The monitoring approach presented here integrates repeat seafloor surveys, and flow monitoring, along the entire length of the system, as well as discharge measurements of the main feeding river.

3.5.1 Repeat seafloor surveying

The submarine channel system in Bute Inlet was surveyed ten times between March 2008 and November 2018 to determine changes in elevation and planform geometry. The surveys were performed in March 2008; November 2010; June 2014; February 2015; June 2016; October 2016; June 2017; October 2017; May 2018; November 2018. The surveys vary in coverage from the entire width of the fjord, to just the main channel. All surveys except the survey in June 2014 were obtained using the *CCGV Vector*. This vessel was equipped with a Kongsberg-Simrad EM 1002 (100 kHz) multibeam echosounder in 2008. It was updated with a Kongsberg EM 710 (0.5x1.0 degree, 70-100 kHz) from 2010 onwards. The survey from 2014 was obtained using the *CSL Heron*, equipped with a Kongsberg EM 710 (1x2 degree, 70-100 kHz) multibeam echosounder. All multibeam echosounders were operated using Kongsberg Maritime SIS Software. Heave, roll, and pitch corrections were incorporated in the acquisition process using motion sensors. Data were then processed in CARIS HIPS and SIPS software. Tidal corrections were performed using predicted tides. The surveys were processed in grids varying from 5x5 m to 1x1 m horizontally. Typical vertical accuracy of the surveys is around 0.5% of the water depth (Heijnen et al., 2020). Changes to the submarine channel-lobe system are visualised using difference maps, which are constructed by subtracting surface elevations of an older survey from a newer survey.

3.5.2 Turbidity current monitoring

Flow monitoring campaigns were performed in Bute Inlet over the summers of 2016 and 2018. Instruments were moored in the channel at five different locations, ranging from 3 to 42 km from the Homathko river mouth, numbered as moorings 1 to 5 from upstream to downstream (Figure 3.2b). Locations of the moorings were the same in 2016 and 2018 apart from the most upstream mooring, which was positioned further upstream in 2018 than in 2016. The moorings recorded from the 9th of June until the 23rd of September in 2016, and from the 14th of May through the 8th of November in 2018. The Acoustic Doppler Current Profiler (ADCP) on mooring 1 failed in 2016 from the 31st of July onwards. The moored instruments included a downward looking Teledyne Workhorse ADCP suspended above the channel. Moorings 1 to 3 consisted of a 600 kHz ADCP suspended 30 m above the seafloor in 2016. Moorings 4 and 5 were equipped with a 300 kHz ADCP in 2016. Moorings 2 to 5 in 2018 included a 600 kHz ADCP suspended 25 m above the channel. Mooring 1 in 2018 was equipped with a 1200 kHz and 300 kHz ADCP suspended at 12 m and 40 m above the channel floor respectively.

3.5.3 River discharge

River discharge of the Homathko River, near the river mouth is monitored and available for the entire survey period (https://wateroffice.ec.gc.ca; station 08GD004).

3.6 Results

3.6.1 Evolution of the entire system between 2008 and 2018

A difference map of the entire submarine channel system in Bute Inlet reveals that it is very active, with 30% of the system undergoing >5 m elevation change over these ten years (Figure 3.2c). Erosion locally exceeds 30 m, and deposition locally exceeds 10 m. There are no large areas of the channel or lobe which were characterised by no change. The upper parts of the channel and the prodeltas show complex patterns of erosion and deposition (Figure 3.2d,e). The channel is dominated by an along-channel alternation of erosion and deposition. This alternation is the result of upstream-migrating knickpoints that dominate the main channel (Heijnen et al., 2020). The lobe is characterised by up to 10 m of deposition. The overall volume of the deposits in the channel and on the lobe, over the entire survey period, exceeds that of the erosion by around 9 million m^3 (*Table 3.1*). This is equal to around 20 – 30% of the total amount of sediment input by the main feeding river.

System component	Available sediment	Sediment deposited
Homathko River (based on annual range of sediment discharge to Bute Inlet from (Syvitski and Farrow, 1983))	28.0 – 48.0 million m^3 (i.e. sediment supplied by the Homathko River)	-
Prodeltas & Channel (based on the volume of sediment eroded or deposited within these areas during the timelapse surveys)	41.0 ± 9.7 million m^3 (i.e. eroded volume)	18.9 ± 8.3 million m^3 (i.e. deposited volume)
Lobe (based on the volume of sediment deposited on the lobe)	- (no discernible erosion detected)	29.9 ± 37.9 million m^3 (i.e. deposited volume)
Total	69.0 – 89.0 million m^3	48.8 million m^3
	Overall removal/bypass of 20.2 – 40.2 million m^3 of sediment over the entire system.	

Table 3.1: Sediment budgets in Bute Inlet between March 2008 and November 2018. Sediment input combines the sediment exhumed through erosion, and sediment delivered by the Homathko river. Sediment volume delivered by the Homathko river is represented as the volume if it were deposited with a porosity between 0.3 and 0.6 (Beard and Weyl, 1973; Houston et al., 2011). This sediment input is the sediment that is made available for deposition in the system. Sediment deposited is the volume of the deposits in the difference map, excluding the overbanks. Uncertainty in the volumes derived from the difference maps are based on a vertical accuracy 0.5% of the water depth.

3.6.2 Prodelta and uppermost channel

A complex pattern of erosion and deposition occurs in the prodelta and most upstream part of the channel. Crescentic bedforms are abundant on the prodelta and in the upper channel, and their migration reworks the substrate (Figure 3.2e). Furthermore, small channel-bank collapses,

and the formation of terraces and local avulsions of the thalweg within the channel confinement are observed (Figure 3.2d).

3.6.3 Main channel

The main channel is dominated by upstream-migrating knickpoints. Sediment directly upstream of knickpoints is eroded when knickpoints migrate upstream. Sediment is then deposited further downstream. This creates a pattern of alternating erosion and deposition along the channel (Figure 3.2c; Heijnen et al., 2020). However, this deposition and erosion migrates along the channel, as knickpoints migrate. So, a certain area in a knickpoint-dominated channel might be depositional at one time, and erosional at another. Detailed observation of the most upstream area of knickpoints shows that this deposition and erosion can balance over time (Figure 3.3).

The timescale of our repeat surveys is too short to observe whether upstream-migrating knickpoint-zones result in the generation of larger bypass zones in the channel (Figure 3.2). However, we can estimate an erosion rate based on the height of the knickpoints, distance to the next knickpoint-zone, and migration rate. We can compare this to the amount of deposition just upstream of the knickpoint-zone to estimate the balance between erosion and deposition over longer timescales. The deposition rate upstream of knickpoint-zone 2 is 0.9 m/yr and the erosion rate associated with the migration of knickpoint-zone 2 is 1.7 m/yr on average. The deposition rate upstream of knickpoint-zone 3 is 0.6 m/yr and the erosion rate associated with the migration of knickpoint-zone 3 is 0.7 m/yr on average. These estimations show that the knickpoint erosion and deposition are almost balanced around knickpoint-zone 3, and the erosion seems to exceed the deposition around knickpoint-zone 2.

3.6.4 Lobe

Deposition of up to 10 m was recorded on the lobe between March 2008 and November 2018 (Figure 3.4a, b). This deposition almost exclusively occured between November 2010 and February 2015. The highest average deposition rate was up to 3 m/y between June 2014 and November 2015, however the temporal resolution varies. No deposition greater than the vertical accuracy of the multibeam is detected on the lobe after November 2015. So, major sediment delivery to the lobe appears to occur within 40% of the years observed. A 15 m-high knickpoint was present in 2008 2.5 km upstream of the main depositional area of the lobe. It can be traced to November 2018, and has migrated 2.1 km upstream (Figure 3.4). This migration almost exclusively occurred during periods of deposition on the lobe.

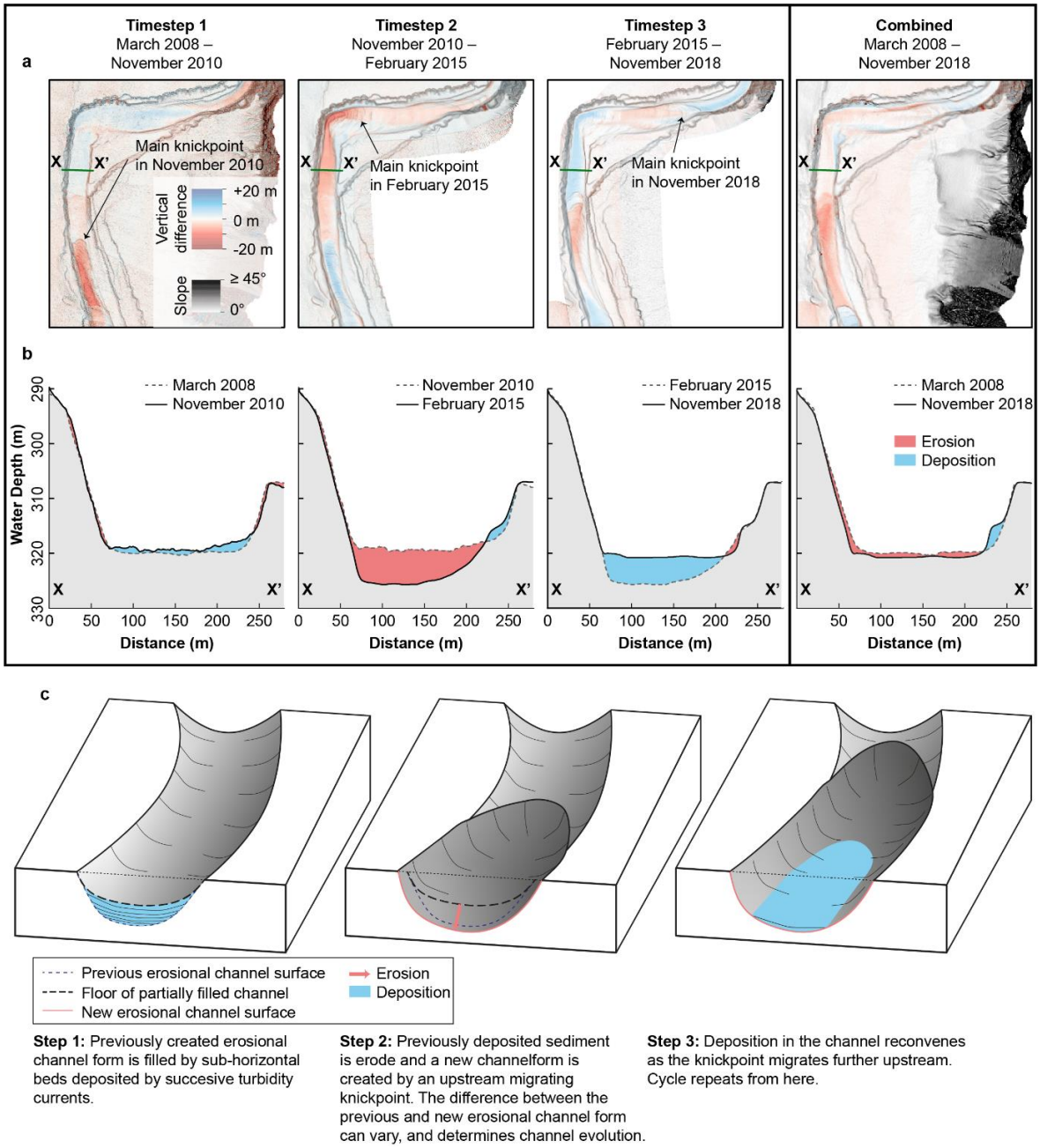

Figure 3.3: Timelapse difference maps and cross sections of an area affected by knickpoint related erosion and deposition. a) Difference maps over three time intervals compared to the difference map over the entire survey area. Location shown in Figure 3.2c. Note how the erosional and depositional area shift over time as the knickpoint migrates. b) Cross section through the channel showing changes over time compared to the change over the entire survey. Location shown in panel a. Note how the area of cross section is characterised by both phases of erosion and deposition that balance out over time. d) Schematic model showing how knickpoint related erosion and deposition can cause channel bypass over longer timescales.

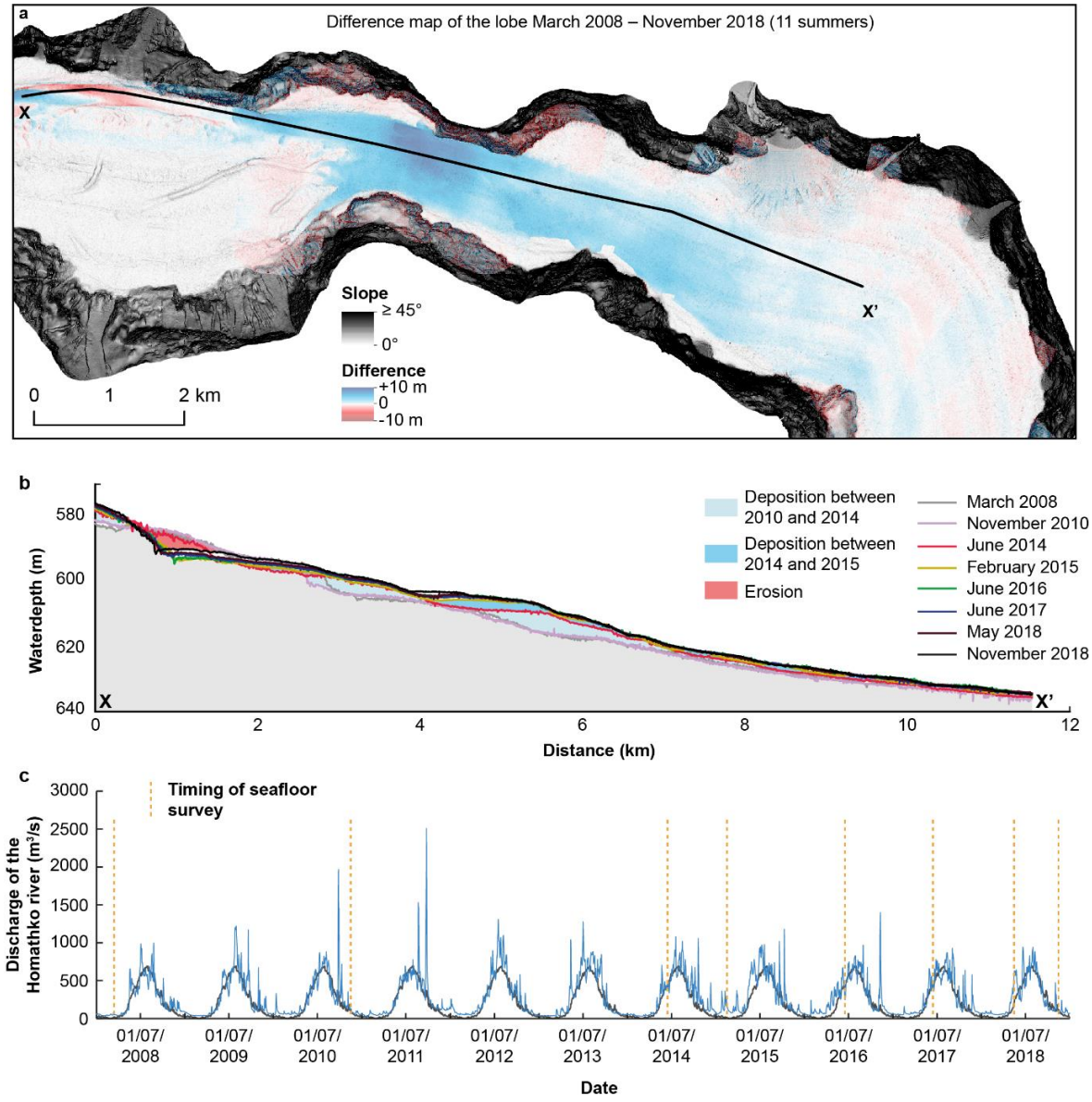

Figure 3.4: Deposition on the lobe and discharge of the system's feeding river. a) Difference map showing deposition on the lobe over the entire survey. Location shown in Figure 3.2c. b) Cross section showing deposition on the lobe over time. Note the deposition occurs almost exclusively between November 2010 and February 2015. c) River discharge of the Homathko River, which feeds the submarine channel-lobe system in Bute Inlet. Timings of the seafloor surveys are indicated. Two main surges occurred over the survey period, in 2010 and in 2011.

3.6.5 Turbidity current runout distances determined from ADCP monitoring

Turbidity currents typically last around 1 – 2 hours at mooring 1 and their velocities range between <1 m/s to several m/s (Figure 3.5). The ADCPs recorded 113 turbidity currents over the summers of 2016 and 2018 (Figure 3.6a). Most flows were recorded in 2018 (N=95). This difference might be partly attributed to mooring 1 being located further downstream in 2016, as well as mooring 1 failing halfway through its deployment in 2016. Six flows in 2018 were recorded at mooring 2, and not at mooring 1. This can be attributed to flows starting at the Southgate River, since the mooring is located upstream of the Homathko and Southgate confluence. These two flows are not taken into consideration in this analysis, as including these flows would over-represent the amount of flows reaching mooring 2. There was a decrease in the number of flows recorded with distance along the channel (Figure 3.6b). Most flows dissipated within the proximal part of the channel. Six flows reached mooring 3, and only 2 out of the 113 flows reached the lobe.

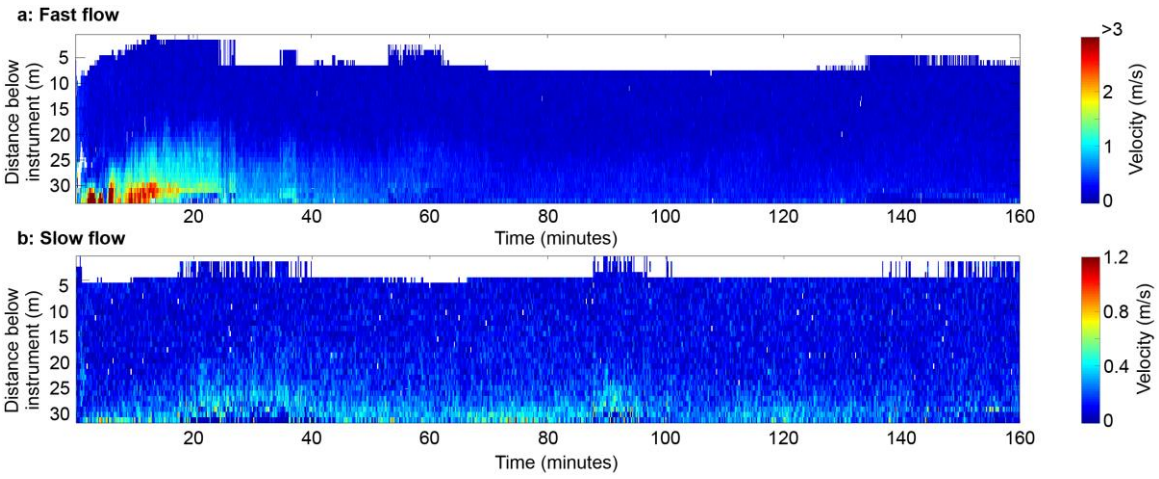

Figure 3.5: Examples of a fast (a) and slow (b) turbidity current in Bute Inlet. Measurements are from mooring 1. (a) occurred on 20-08-2018 at 15:26 (GMT), and (b) occurred on 26-06-2018 at 18:10 (GMT).

3.6.6 River discharge

Discharge of the Homathko River was seasonally variable (Figure 3.4c). Discharge in winter was typically below 100 m^3/s, while discharge in summer was typically above 500 m^3/s, with several peaks yearly above 800 m^3/s. The river discharge over the entire survey period showed a fairly consistent profile with annual discharges varying between 7.8 km^3/yr and 9.8 km^3/yr. However, much larger variations between years occurred on daily to weekly timescales, with the average daily percentile variation being 48%. Furthermore, two big peaks in river discharge (> 1500 m^3/s) occurred in September 2010 and September 2011.

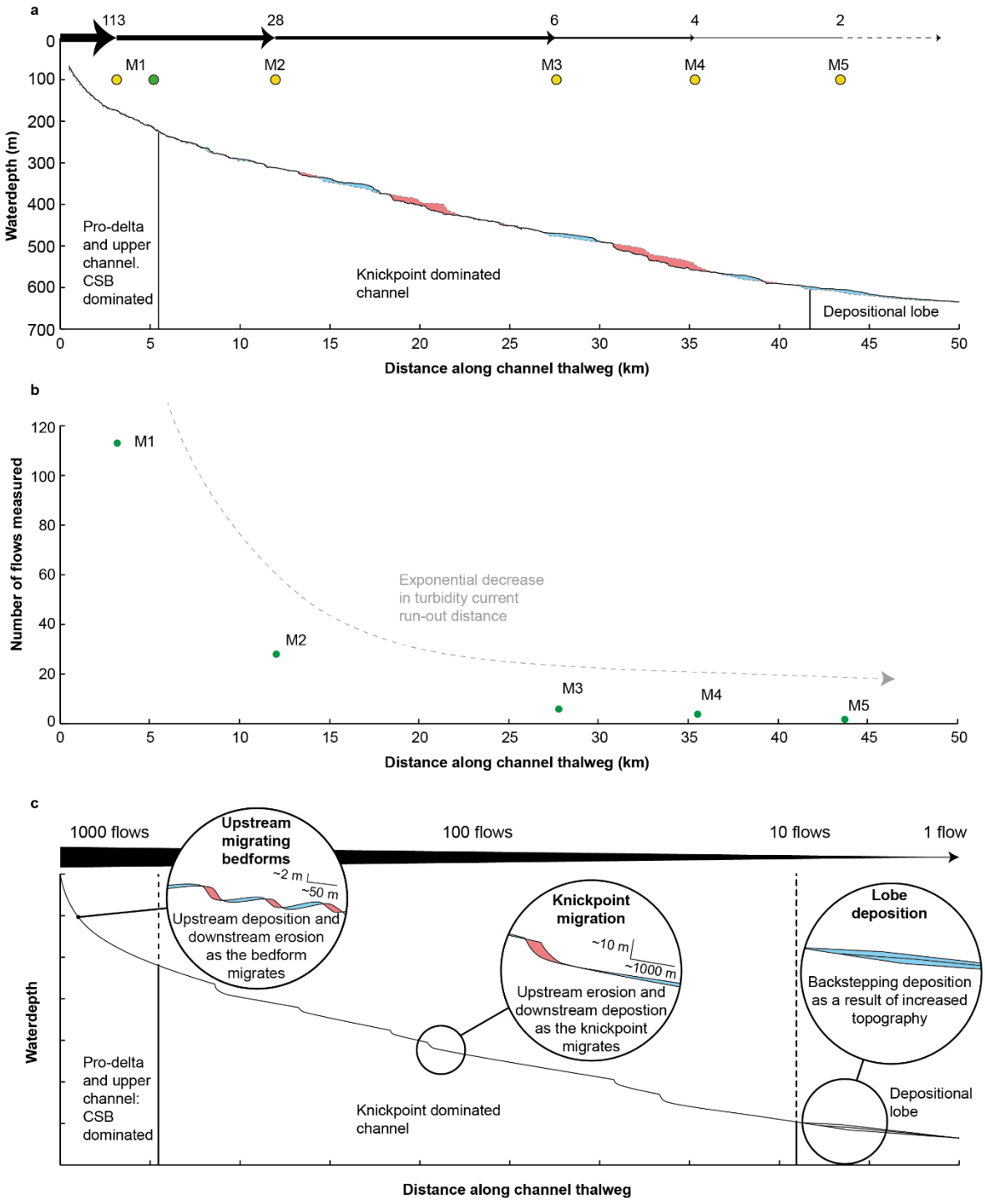

Figure 3.6: Turbidity current monitoring and longitudinal channel profiles. a) Amount of flows recorded by the ADCP at each moored station. Locations of the moorings are shown on a longitudinal profile along the channel thalweg and over the lobe. The longitudinal profile also shows the bathymetric difference between March 2008 and November 2018. b) Amount of flows recorded at each mooring plotted against the distance along the channel thalweg. There is an exponential decrease in the amount of flows with runout distance. c) Schematic diagram showing the relative flow frequency and the dominant depositional and erosional processes along a knickpoint-dominated channel.

3.7 Discussion

Here we use the observations from Bute Inlet to discuss how sediment is transported through a knickpoint dominated submarine channel and onto the lobe. We then compare this to previous models of sediment transport through submarine channels. This is followed by the presentation of a new model that can explain how the upstream migration of knickpoints can generate bypass zones in submarine channels, and lastly we discuss the implications for how submarine channel systems bury land-derived material, and how they record past environmental signals.

3.7.1 Stepwise sediment transport through a submarine channel and discontinuous sediment delivery onto the lobe

Observations from the active submarine channel in Bute Inlet reveal new mechanisms of how sediment is transported through submarine channel systems. Here, we discuss these mechanisms and present a new model explaining how submarine channel systems fill and flush and how lobes are built. In this model, sediment is transported downstream through several steps of upstream-migrating crescentic bedforms and knickpoints and the resulting sediment delivery to the lobe is discontinuous (Figure 3.4; Figure 3.6).

Sediment is transported and reworked in the upper part of the system by small flows that occur frequently (10s of flows a year). Most flows dissipate over relatively short runout distances (< 12 km), depositing their sediment in the proximal part of the system. This sediment is transported and reworked in the proximal part of the system, which is characterised by migration of crescentic bedforms (Covault et al., 2017; Vendettuoli et al., 2019), terrace formation and channel avulsions within the main channel confinement, and channel-flank failures (Figure 3.2d, e).

Sediment is then transported further downstream by less frequent flows (~10 flows per year) with longer runout distances that dissipate somewhere in the channel, past the upstream-most part, but before the channel to lobe transition zone, between around 5 and 40 km from the river mouth in Bute Inlet. These flows trigger the upstream migration of knickpoints, the morphodynamic process dominating the main part of the channel (Heijnen et al., 2020). Sediment is eroded upstream of knickpoints as they migrate, and then deposited downstream of knickpoints. These zones of erosion and deposition migrate as knickpoints themselves migrate. So, sediment deposited downstream of knickpoints is later eroded by the next zone of upstream-migrating knickpoints. Most of these flows also do not reach the lobe, depositing all of their sediment in the channel.

An even less frequent type of flow (1 observed in each year of monitoring) occurs that eventually carries sediment past the channel and onto the lobe. However, these two observed flows did not leave resolvable deposition on the lobe. Our results show that events of major sediment delivery to the lobe occur more sporadic than can be observed in only two seasons (summers 2016 and 2018) of flow monitoring. The lobe has grown by up to 10 m vertically over the study period. This growth occurred almost exclusively within 4 of the 11 monitored years, between November 2010 and February 2015. This suggests there is an even larger type of flow event, not captured during in our flow monitoring results, that occurs in Bute Inlet in the order of once every 10 years.

The flows responsible for the high amount of sediment accumulation observed between November 2010 and February 2015 on the lobe cannot be clearly linked to external triggers. A big surge on the feeding river occurred in 2011, which could explain the 6 m of deposition on the lobe. However, the second biggest surge, which occurred in 2010, is not represented on the lobe. Furthermore, the period between June 2014 and February 2015 accounts for the highest aggradation rate, but there is no clear signal in the river discharge data that can be linked to this (Figure 3.4). We propose that these flows are not generated by external triggers, but by internal processes. A first possibility is that the upstream channel needs to be preconditioned with enough sediment to enable flows to ignite and bring sediment to the lobe. This has also previously been suggested to be a controlling factor for initiating turbidity currents and for the generation of long runout turbidity currents (Hage et al., 2019; Heerema et al., 2020). However, the upper part of the system does not show a clear depositional pattern (Figure 3.2d, e) Secondly, it could be possible that a certain knickpoint configuration could favour turbidity currents to reach longer runout distances. Turbidity currents potentially ignite when they flow down a knickpoint, whereas the flatter reaches between knickpoints cause turbidity currents to decelerate. A configuration in which the flatter reaches are shortest might favour flows reaching the lobe. However, no clear patterns in the knickpoint configurations in November 2010, June 2014, or February 2015 are found. Longer term monitoring in Bute Inlet is needed to reveal how a new period of sediment delivery to the lobe is generated. Furthermore, coring of the lobe to reveal the structure of the 10 m thick sediment accumulation could reveal insights into the nature and controlling process of sediment delivery to lobes. Simple observations such as the number of beds in this accumulation could give significant insights.

Overall volumes of seafloor change, combined with estimations of sediment input by the main feeding river suggest that 10 million m^3 of sediment, around 20% – 30% (depending on the assumed porosity of the sediments) of sediment input from the main feeding river, is buried by the submarine channel system between March 2008 and November 2018. However, the remaining 70 – 80%, which equates to 19.2 – 39.2 million m^3 of sediment, that was delivered to

the system between March 2008 and November 2018 in the system, cannot be traced based on the difference maps. Additionally, sediment input from the Southgate River and other small sediment input sources are not accounted for in the deposits either, since no data for their sediment input are available. Deposition of sediment thicknesses that are below the resolution of the multibeam echosounded outside the channel and further beyond the main depositional lobe may account for much of this apparently missing sediment budget. If the complete remainder of sediment would be deposited in overbank areas and up to 10 km past the proximal lobe, these deposits would be 20 – 40 cm thick on average across the fjord width. Although fjords can experience very high sedimentation rates (Syvitski et al., 1987), sediment transport further out of the system, and storage in the prodelta upstream of the survey coverage, might account for the missing sediment in the submarine channel system.

3.7.2 Comparison with other models of sediment transport through submarine channels

Our model, synthesised from observations of sediment transport through the submarine channel-lobe system in Bute Inlet, differs from previously described models in three main respects. First, turbidity currents in our model occur with a range of runout distances spanning the entire system. The frequency of flows decreases with runout distance (Figure 3.6b). Previous models predicted a unimodal or bimodal flow distribution in which flows either would reach the terminal lobe, or would fill the proximal part of the system (Stevenson et al., 2013; Allin et al., 2016; Heerema et al., 2020). Second, we observe that turbidity currents interact with the substrate along the entire system. This interaction is mainly expressed as migrating zones of erosion and deposition associated with the upstream-migration of knickpoints. We do not see long sections of the channel that do not experience change, as would happen if turbidity currents reached a state of autosuspension over long areas of the channel (Stevenson et al., 2013). Nor do we see a binary pattern of frequent small flows filling the proximal part of the system with sediment, which is then episodically flushed out by a large flow (Mountjoy et al., 2018). Finally, in our model sediment delivery to the lobe does not necessarily require flows triggered by catastrophic external events such as earthquakes or floods. Our observations and resulting model have similarities with the modified ‘fill and flush model’ of stepwise downstream transport of sediment (Paull et al., 2005). However, no clear preconditioning in the upper part of the channel is observed. Furthermore, in our model, a full spectrum of flow runout lengths from proximal to distal is present that continuously reworks sediment all along the system, whereas the modified ‘fill and flush model’ suggests less activity than observed here in the distal part of the channel outside of occasional big flushing events.

This study offers the first observations of how the upstream-migration of knickpoints can be a controlling process in filling and flushing submarine channel systems. We recognise that other systems have different morphologies and can be dominated by other processes such as lateral migration of channel bends (e.g. Sylvester et al., 2011; Covault et al., 2019). However, we anticipate similar sediment transport mechanisms to occur in systems, or parts of systems, that are relatively straight and contain knickpoints. Similar systems could include parts of Monterey Canyon, offshore California; the channel in Lake Geneva, Switzerland; and Capbreton Canyon, Bay of Biscay (Paull et al., 2011; Corella et al., 2016; Guiastrennec-Faugas et al., 2020a).

3.7.3 Sediment bypass in submarine channels

Submarine channels are often recognised as sediment bypass zones, which is often interpreted to be the result of successive bypassing flows (e.g. Stevenson et al., 2015; Hubbard et al., 2020). However, here we show that bypass zones are not necessarily generated by successive bypassing flows. We show how erosion and deposition associated with upstream-migrating knickpoints can generate bypass zones in Bute Inlet. In this model, erosional and depositional areas that migrate along the channel, and create a series of cut-and-fill episodes that can balance out and result in bypass over longer timescales. Here, a given location is most of the time depositional, until a knickpoint migrates through, eroding these deposits, and re-incising the channel. Deposition reconvenes after the knickpoint has passed (Figure 3.3c). Therefore, on the shortest timescale, most parts of the channel are depositional zones. Also, most flows are depositional during most of their path downstream. Net bypass in a knickpoint dominated system is thus only formed over longer timescales. This net bypass is created by long-lived deposition (fed by depositional flows) alternating with short lived erosional episodes. Fully bypassing flows (that do not deposit over long stretches of the channel) are very uncommon in this type of system and are not required to create bypass in the depositional record.

Repeated erosion and fill cycles are commonly observed in outcrop and in the subsurface (Mutti and Normark, 1987; Maier et al., 2012; Hubbard et al., 2014, 2020). This pattern has been attributed to sediment bypass, but lacked a consistent process explanation until recently. These cycles have previously been attributed to externally controlled fluctuations in turbidity current energy (e.g. McHargue et al., 2011). However, recent repeat seafloor mapping studies have suggested that knickpoints might be able to generate repeated cycles of erosion and filling and associated sediment bypass (Guiastrennec-Faugas, et al., 2020a; Heijnen et al., 2020). Here we prove this by demonstrating for the first time how the erosion associated with the upstream migration of a knickpoint can be balanced by phases of deposition before and after knickpoint migration.

3.7.4 Implications for stratigraphic completeness, signal preservation, and burial of organic carbon and pollutants

Prior studies have used submarine channel and lobe deposits to reconstruct past environmental signals, turbidity current frequency, organic carbon burial potential and other applications (e.g. Prins and Postma, 2000; St.-Onge et al., 2004; Baudin et al., 2010; Jobe et al., 2018). Indeed, our results suggest that Bute Inlet actively buried sediment on the lobe during the 11-year monitoring period. However, better understanding of how these deposits are reworked after initial deposition, and how they are eventually preserved is required to correctly interpret these important records.

Previous studies have already investigated stratigraphic completeness and signal preservation in different parts of submarine channel-lobe systems. The term stratigraphic completeness is used here to describe the preservation of deposited sediment (Sadler, 1981; Strauss and Sadler, 1989; Straub and Esposito, 2013; Vendettuoli et al., 2019). Areas in which deposits are later partly reworked have a low stratigraphic completeness. We use the term signal preservation to describe how well deposits represent environmental patterns observed upstream in the system, such as discharge of the feeding river and the amount of flows that occurred in the system (Romans et al., 2016; Burgess et al., 2019). First, prodelta systems have been shown to have a low stratigraphic completeness (<10%) as a result of the migration of crescentic bedforms (Vendettuoli et al., 2019). Similar bedforms and associated reworking are observed here in Bute Inlet (Figure 3.2e). Second, previous studies suggested lobes may have a low signal preservation, as a result of the autogenic process of compensational stacking (Burgess et al., 2019; Ferguson et al., 2020). The timescale of our study is too short to observe compensational stacking, but we can already observe a shift in the location of the maximum deposition on the lobe. The maximum depositional thickness between 2014 and 2015 is further upstream than that of 2010 and 2014. This upstream movement of depositional focus on the lobe might resemble lobe back-stepping observed in laboratory experiments (Straub and Pyles, 2012; Fernandez et al., 2014; De Haas et al., 2016; Ferguson et al., 2020).

Our data reveals additional processes that cause lower stratigraphic completeness and signal preservation in submarine channel-lobe systems. Firstly, we show how the upstream migration of knickpoints reworks almost the entire channel fill, and recycle recent deposits. This process suggests that stratigraphic completeness is very low in knickpoint-dominated channels. Indeed, our results demonstrate that depositional zones accumulate up to 1 m of sediment a year, yet such systems are modelled to aggrade only 1-5 cm a year over longer timescales (Syvitski et al., 1988). This suggests a stratigraphic completeness of 1–10% for channel deposits in Bute Inlet. This

is even lower than the values found for channels dominated by migrating crescentic bedforms on the Squamish Delta (Vendettuoli et al., 2019). Furthermore, this reworking can re-excavate organic carbon and pollutants stored in submarine channel deposits. Recent studies have shown high organic matter content in modern turbidity current deposits (Baudin et al., 2017; Hage et al., 2020), however our data shows that these deposits may be recycled and potentially oxidized several times before final burial. Secondly, we show that 98% of the flows do not reach the lobe. Two flows reached the lobe in the summers of 2016 and 2018. The deposits of these two flows are too thin to be resolved in our repeat surveys. These two thin beds on the lobe thus represent an upstream system in which over a hundred flows occurred and in which the channel is characterised by tens of meters of incision locally and widespread deposition. So, lobe deposits, on shorter timescales than on which compensational stacking occurs, also do not give a good representation of the activity of the system. Finally, these data also show that deposition on the lobe cannot clearly be linked to signals in the river discharge. This suggests that sediment accumulation rates on the lobe can be dominated by internal processes rather than external signals.

3.8 Conclusions

We present the first integrated monitoring of an active submarine channel-lobe system along its full length, consisting of: 1) repeat seafloor surveying, 2) turbidity current monitoring, and 3) discharge of the feeding river. This allows a source to sink analysis of how sediment is transported through submarine channel-lobe systems. We show how sediment transport through submarine channel-lobe systems is controlled by upstream-migrating knickpoints and is characterised by several steps of reworking. The resulting sediment delivery to the lobe is discontinuous and cannot be directly linked to the main feeding river. This knickpoint-related reworking in the channel also offers a process that can generate sediment bypass zones, which are so characteristic in submarine channels, without the flows having to be in a state of bypass themselves. Lastly, the high levels of reworking and internal processes observed here result in low stratigraphic completeness in channels and low signal preservation on lobes. This high amount of reworking also shows the potential for re-excavation of organic carbon and pollutants deposited in submarine channels.

Chapter 4 First detailed time-lapse surveys from a major submarine canyon-channel system reveal a spatially-variable modulation of sediment transport to the deep sea

This chapter is being prepared for submission to a peer-reviewed journal, and is co-authored by Maarten S. Heijnen, Ed L. Pope, Peter J. Talling, Michael A. Clare, Matthieu J.B. Cartigny, D. Parsons, Megan L. Baker, Florian Pohl, Sean Ruffell, M. Hasenhündl, Catharina J. Heerema, Sophie Hage, Stephen M. Simmons, Claire McGhee, Morelia Urlaub, Arnaud Gaillot, Bernard Dennielou, and Ricardo Silva Jacinto.

M.S.H. is the main author of the manuscript and performed the majority of the data analysis. M.S.H. designed and acquired the 2019 seafloor surveys. M.A.C., M.J.B.C., P.J.T., assisted with writing the manuscript. M.S.H., E.L.P., S.R., S.H., and A.G. were involved in data analysis. M.S.H., E.L.P., P.J.T., S.H., M.L.B., S.R., M.H., C.J.H., S.M.S., C.M., and R.S.J. were involved in data collection. P.J.T., and R.S.J. were in charge of the 2019 expedition. M.A.C., M.J.B.C., P.J.T., R.S.J., M.U., and B.D. designed the overall project, and secured funding. R.S.J. provided the 1998 – 2000 bathymetric surveys. Only M.A.C., M.J.B.C., and P.J.T. reviewed this chapter.

4.1 Abstract

Large submarine canyon-channel systems are a primary conduit for land-derived sediment, nutrients, organic carbon, and pollutant transport to the deep-sea. However, these systems are difficult to monitor due to their inaccessible location and the destructive and episodic nature of the seafloor sediment flows (such as turbidity currents) that flow through them. Understanding how these flows transport, deposit, and re-excavate land-derived material across submarine channel systems is important for understanding how efficiently submarine channel systems bury organic carbon, and where and to what extent pollutants and nutrients affect deep-sea ecosystems. Furthermore, visualising the seafloor response to turbidity currents is important in assessing geohazards for seafloor infrastructure. Here we present the results of a seafloor survey performed in 2019 along ~475 km of the full margin-scale Congo Fan submarine channel system, and compare this survey to a set of surveys acquired in 1998 and 2000. This study, that spans two decades, presents the first repeated surveying of a large active submarine channel system, documenting how erosion and deposition by turbidity currents varies along the channel system.

We show that the system can be divided into three different zones based on distinct erosional and depositional patterns that affect the channel. First, canyon flank collapses and associated deposits occur commonly in the upstream part of the system. Large collapses can cause meander bend-cut-offs and blockages that trap sediment in the canyon. Second, the intermediate reach of the channel is dominated by outward expansion and downstream translation of bends, similar to meandering rivers. Third, the most distal channel is straighter and dominated by upstream-migrating knickpoints. The transition between the flank-collapse dominated canyon to the meandering channel coincides with the base of the continental slope. The transition from a meandering regime to a knickpoint-dominated regime coincides with the location of a recent avulsion. This suggests that the occurrence of the different zones is controlled by basin structure (i.e. regional slope) and channel maturity, and that a section of a channel can evolve through these different zones as it matures. Finally, I synthesise a generalised model of how submarine channels work. This model shows that sediment can be stored and re-excavated along the entire system, albeit through a range of different processes.

4.2 Introduction

Submarine canyons and channels are common features on the seafloor, and they are formed by often powerful sediment-laden flows called turbidity currents (Harris and Whiteway, 2011). Here I use the term canyon to refer to the net-erosional parts of these systems which are largely fixed in place and are commonly incised into the continental shelf and slope (e.g. Micallef et al., 2014). We refer to the more distal parts of these systems as channels, which can exhibit a combination of erosion and deposition and can migrate over time (e.g. Maier et al., 2012). Submarine canyon-channel systems form some of the largest sediment accumulations on our planet, known as submarine fans (Normark and Carlson, 2003). Submarine channel systems thus play an important role in the global transfer of sediment, nutrients, organic carbon, and pollutants (Quadfasel et al., 1990; Baudin et al., 2017; Kane and Clare, 2019; Azaroff et al., 2020). Furthermore, the sediment flows that traverse these canyons and channels pose a hazard to seafloor infrastructure, including telecommunication cables that now carry over 95% of global data traffic (Heezen and Ewing, 1952; Carter et al., 2009; Pope et al 2017a, b). Therefore, understanding how submarine channel systems evolve, and how they are filled and flushed by sediment flows, is important for understanding how sediment, organic carbon, nutrients and pollutants are redistributed and buried in the deep-sea, and for assessing offshore geohazards.

The evolution of large ocean-scale submarine canyons and channels is poorly understood, because these systems are hard to monitor, resulting in a lack of direct observations. Offshore satellite-based mapping is limited to very shallow waters, so imaging submarine canyon-channel

systems relies on surveying using ships or underwater vehicles (e.g. Babonneau et al., 2002; Dennielou et al., 2017; Traganos et al., 2018). Due to recent advances in technology, detailed mapping of the modern seafloor is becoming more commonplace (Paull et al., 2010; Hughes Clarke, 2018; Vendettuoli et al., 2019; Guiastrennec-Faugas et al., 2020a). Various mechanisms have been proposed to be important for how submarine canyon-channel systems evolve. One of the best-known models for submarine channel evolution is similar to that of meandering rivers (Sylvester et al., 2011; Covault et al., 2019). In this model channels evolve through outward expansion and downstream translation of channel bends. This bend migration is the result of secondary helical flow (Dietrich et al., 1979). However, recent time-lapse surveying has shown that the upstream-migration of steep steps called knickpoints, can also be important for how channels evolve (Guiastrennec-Faugas, et al., 2020a; Heijnen et al., 2020). Sediment is eroded as the knickpoint migrates upstream, and then this sediment is deposited downstream of the knickpoint. Other studies have shown how the floors of submarine channels consist of crescentic bedforms (Covault et al., 2014, 2017; Hughes Clarke, 2016; Vendettuoli et al., 2019). These bedforms also migrate upstream as a result of overpassing turbidity currents. Their migration is associated with erosion and deposition, which has also been shown to be important for the evolution of submarine channels and the deposits they leave behind. Lastly, submarine slope failures can be extremely large, occur on much lower gradients than on land, and travel for much longer distances (Talling, 2014). Several studies have shown that landslides on submarine channel-flanks may play an important role in their evolution (Armitage et al., 2009; He et al., 2014; Mountjoy et al., 2018; Pope et al., in prep).

However, most repeat seafloor mapping efforts in submarine canyon-channel systems up to now have been made within small systems that do not span continental margins, or are limited to a small part of a bigger fan system (e.g. Paull et al., 2011; Vendettuoli et al., 2019; Guiastrennec-Faugas, et al., 2020a; Heijnen et al., 2020). This is because surveying margin-scale systems is particularly costly and time consuming, and large water depths limits the resolution of imagery. Thus, the erosional and depositional processes in large, active, margin-scale systems, such as the Congo Canyon and Channel, have not yet been documented. Therefore, the relative contribution of different erosional and depositional processes along large scale systems remains unclear, as do the processes that influence the sediment transport of land-derived material to the deep sea.

Here we present a new detailed seafloor survey along the active channel of the Congo Fan, obtained in 2019. The 2019 survey spans 75 km of the upper Congo Canyon length, and 400 km of the downstream channel of this large submarine fan system. We then compare this survey to previous surveys obtained in 1998 and 2000 (Babonneau et al., 2002), resulting in the first ever difference maps covering a large submarine canyon-channel. This long duration (20 years)

between the two sets of surveys results in substantial, and thus resolvable, morphological changes which help to overcome the lower resolution associated with seabed surveying in deeper-water.

4.3 Aims

We use the detailed time-lapse surveys from a major submarine fan to address the following aims. Our overarching aim is to understand how submarine canyons and channels work. The first specific aim is to identify the different processes that control how channels evolve, and their associated canyon-channel morphologies. Secondly, we analyse how these different processes, morphologies, and their relative importance, are distributed along the canyon-channel system, and what determines this distribution. Lastly, we synthesise generalised models for the behaviour and long-term evolution of submarine canyon-channels, and discuss how this behaviour might impact the delivery of land-driven material into the deep-sea.

4.4 Geographic and oceanographic setting

The Congo Fan is located offshore West Africa. The submarine canyon that feeds the fan is directly connected to the mouth of the Congo River, the second largest river in the world by discharge (Milliman and Farnsworth, 2011). The currently active canyon-channel system is over 1,200 km long (measured along channel) and reaches water depths of over 4,800 m (Figure 4.1). The sediment accumulation created by this system is one of the largest on Earth (Droz et al., 1996, 2003; Normark and Carlson, 2003; Reece et al., 2011). The fan is located on the passive East Atlantic margin, where it has developed since the Oligocene (Brice et al., 1982). Although on a passive margin, the Congo Fan is affected by salt tectonics, which locally control the geometry of the West African margin (Marton et al., 2000). The Congo Fan consists of several laterally stacked sub-fans, with the development of the currently active part of the fan starting 210,000 years ago (Droz et al., 2003). This modern part of the fan has experienced 49 individual channel avulsions in the last 210 kyr (Picot et al., 2016, 2019). Many of the abandoned channels can still be observed on the seafloor (Babonneau et al., 2002). Flow monitoring studies have shown that the canyon and most recent channel are active, with multiple turbidity currents each year, which can sometimes last for more than 10 days and can transport up to 5.5 Mt of sediment (Heezen et al., 1964; Khripounoff et al., 2003, 2009; Azpiroz-Zabala et al., 2017a; Simmons et al., 2020). One moored instrument, which was deployed in the upper part of the canyon at 2 km water depth, demonstrated that turbidity currents were active for one third of a three-month monitoring period (Azpiroz-Zabala et al., 2017a). The upper canyon is up to 1200 m deep and 15 km wide

(Babonneau et al., 2002). Canyon depth and width gradually decrease in the distal channel to <150 m and 1000–1500 m, respectively. The canyon has an average sinuosity of 1.3. The sinuosity in the channel (measured over a length scale of 10 km) varies from 1.7 in highly meandering parts of the middle parts of the channel, to 1.14 in the distal channel. Channel gradient ranges between 0.7° and 0.1° over the whole system (Babonneau et al., 2002).

4.5 Methods

A seafloor survey of parts of the canyon and distal channel (Figure 4.1) was acquired between 9 September and 2 October 2019 using the *James Cook*, and its hull-mounted Kongsberg EM122 (1 x 1) multibeam echosounder, controlled by Kongsberg SIS software. The multibeam echosounder was configured to obtain the highest resolution data possible by setting the swath to a minimum fixed angle of 90°. Three sound velocity profiles were obtained approximately 24 km apart in the upstream canyon, and five in the distal channel spaced 40 – 120 km. The ship's position was tracked using two independent GPS systems, corrected by a CNav system which provides differential GPS data for the two systems, resulting in a positioning accuracy of < ±1 m. Data was then processed in Caris HIPS and SIPS software, and analysed using ArcGIS software.

The survey covers part of the upstream canyon and the distal part of the channel (Figure 4.1). The survey was designed to acquire high resolution data, rather than to cover a large area. The survey design consists of a line along the channel, followed by lines across channel, with at least 67% overlap with the previous line (Figure 4.2). Performing such a survey at 5 knots ensured that the entire studied canyon reach was surveyed in detail from 3 different angles. This resulted in a spacing of soundings in the upper canyon that is finer than the footprint (~25 m) of the individual beams. The channel survey was performed using the same multibeam settings and at the same speed. However, the survey resolution in the distal channel varied as a result of variable survey lay-out. Some areas are covered by a similar pattern as in the upper canyon, comprising a line along the channel, followed by across-channel lines with 67% overlap. However, other areas are covered by either a single or double line along the channel (Figure 4.3). This resulted in average sounding spacing comparable to or higher than the beam footprints (>72 m). To show this high resolution data, digital elevation models (rasters) were generated with a bin size smaller than the footprint of individual beams. This means that individual horizontal features smaller than 20 m in the upstream canyon, and 70 m in the distal channel, still cannot be visualised. However, by gridding finer than the size of the beam footprints, the grid works as a fine moving average of a high amount of strongly overlapping coarser data points. This can approximate patterns in slopes of larger features, such as the canyon and channel walls, at a resolution lower than the footprint of the individual beams. This approach is applied here as the canyon survey has a horizontal

resolutions of 5 m, and the channel survey has a horizontal resolution 20 m. The survey obtained in 2019 has a vertical accuracy of ± 0.2% of the water depth.

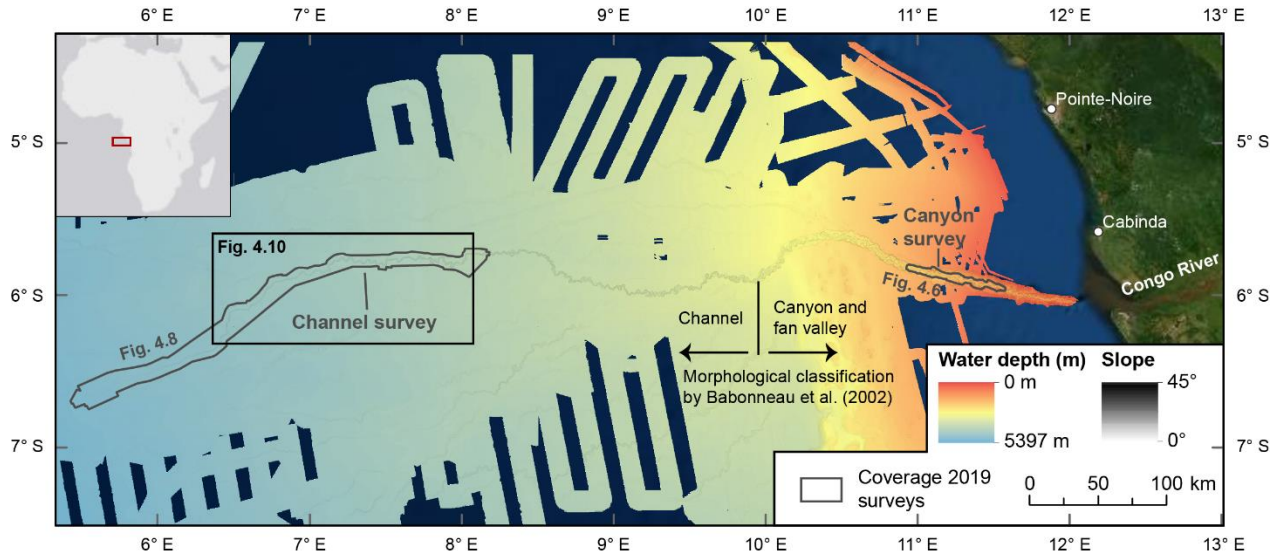

Figure 4.1: Location and survey coverage of the active part of the Congo submarine fan. Shown bathymetry is a combination of surveys acquired between 1998 – 2000 (Babonneau et al., 2002). Location of the boundary between the channel and the canyon and fan valley from Babonneau et al. (2002). Outline of the coverage of the canyon and channel surveys acquired in 2019 is shown. Source satellite date: Esri, DigitalGlobe, GeoEye, Earthstar Geographics, CNES/Airbus DS, USDA, AeroGRID, IGN, and the GIS User Community.

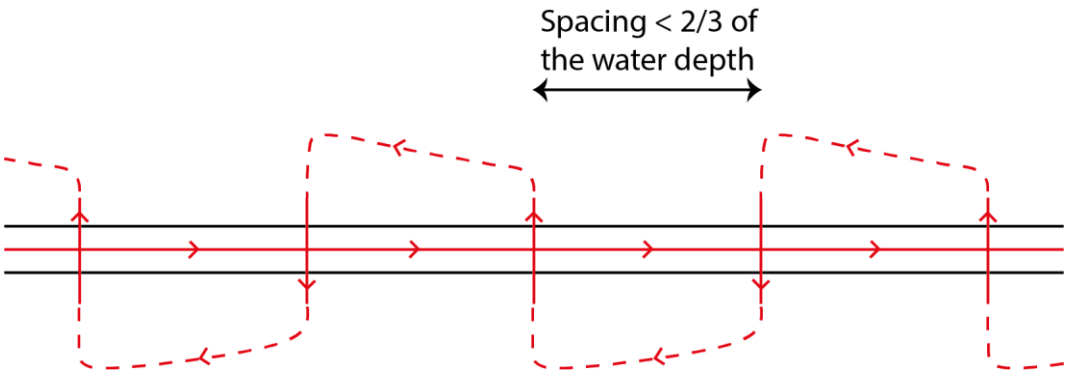

Figure 4.2: Cartoon of the 2019 survey design. A single line along the channel, followed by lines across the channel. Dashed lines represent the ship's track between the lines.

This new 2019 survey was then compared to bathymetric surveys obtained between 1998 and 2000 (Babonneau et al., 2002). The canyon was surveyed in 2000 in detail using a EM3000 multibeam echosounder during the ZAICAR cruise on research vessel *Le Suroît*. The resulting bathymetry model has a grid size of 50 m with a vertical accuracy of ± 5 m. The channel was surveyed 1998 using a EM12 multibeam echososunder during the ZAIANGO cruises on research vessel *L'Atlante*. The resulting bathymetry model has a grid size of 100 m with a vertical accuracy of ± 10 m. The ship's navigation in both the ZAICAR and ZAIANGO cruises were tracked using dGPS with an accuracy of ± 3 m (Babonneau et al., 2002). Comparisons between these surveys and the new survey allow analysis of how the channel has changed over the last few decades.

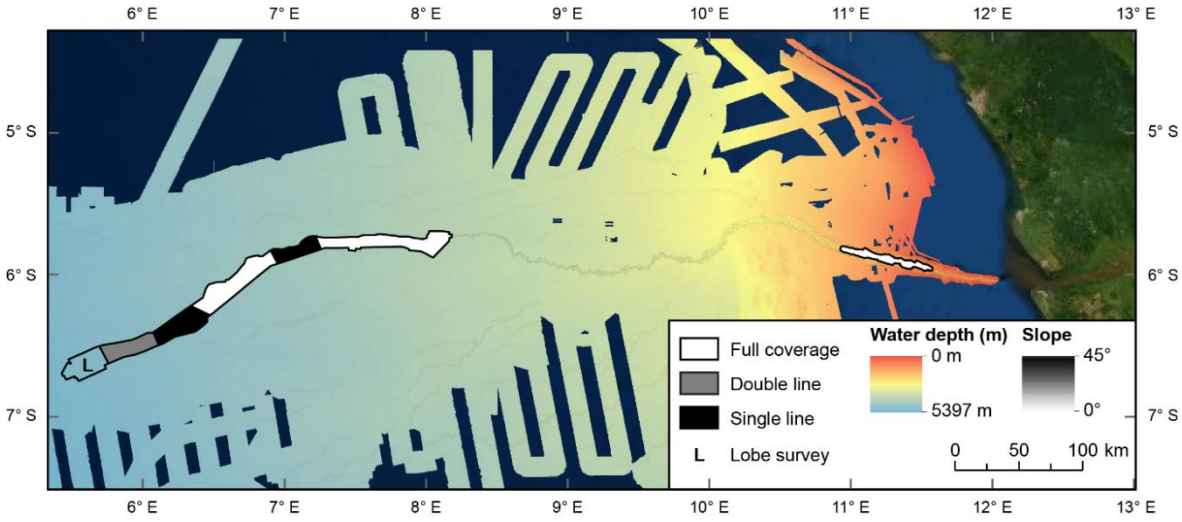

Figure 4.3: Overview of the different resolutions of the survey along the channel. Full coverage represents the design shown in Figure 4.2.

Difference maps are made to visualise the change in seabed elevation between the 2019 survey and the 1998 – 2000 surveys. These difference maps are constructed by subtracting the elevations recorded by older survey depths from the newer survey. Difference maps spanning such long times (20 years) are prone to vertical errors, due to differences in the equipment used and design of surveys. Data at the outer edges of the swath, and areas of steeper slope (more than a few degrees) are especially prone to errors. Here we use relatively flat areas such as terraces and overbank areas to estimate the magnitude of the vertical error. We then only display changes that are above this error. This background error was determined at 10 m for the channel survey, which is equivalent to around two standard deviations (Figure 4.4). The difference map of the canyon survey is characterised by a systematic error that increases in magnitude towards the outer limits of the survey area (Figure 4.5), which appears to be caused by a roll error. This error mainly affects the outer terraces, rather than the canyon floor. We display any change between -25 and

+25 m, as this sufficiently removes most of the error, but does not obscure erosional and depositional patterns within the canyon, which commonly exceed ±25 m. The outermost edges of the error have been removed manually. This high error in the proximal survey is mainly the result of high errors that occur along the outer edges of the difference map. Some of this error even exceeds 25 m, and is eventually removed manually (Figure 4.5).

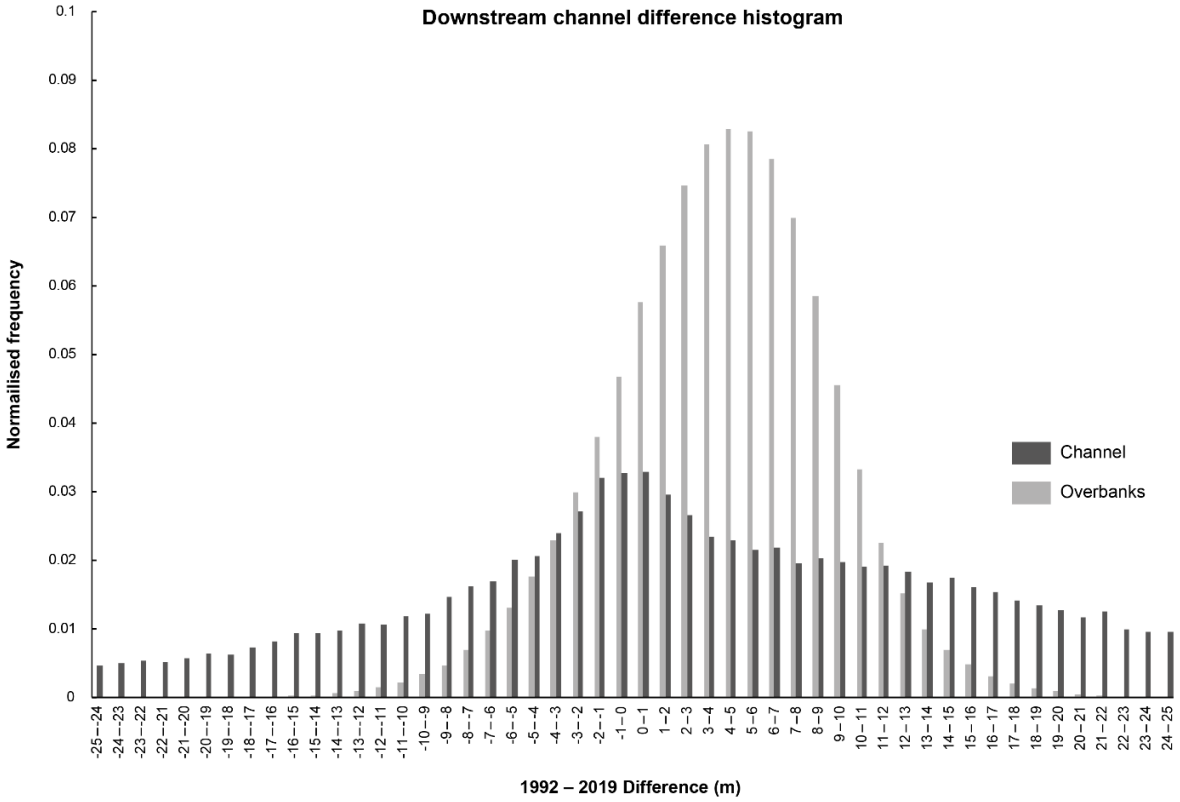

Figure 4.4: Histogram of the magnitude of change observed in the distal channel and on the overbanks. The overbanks are assumed to be subject to minimal change and mainly showing noise. This suggests that most noise in the difference maps is between -10 and 10 metres.

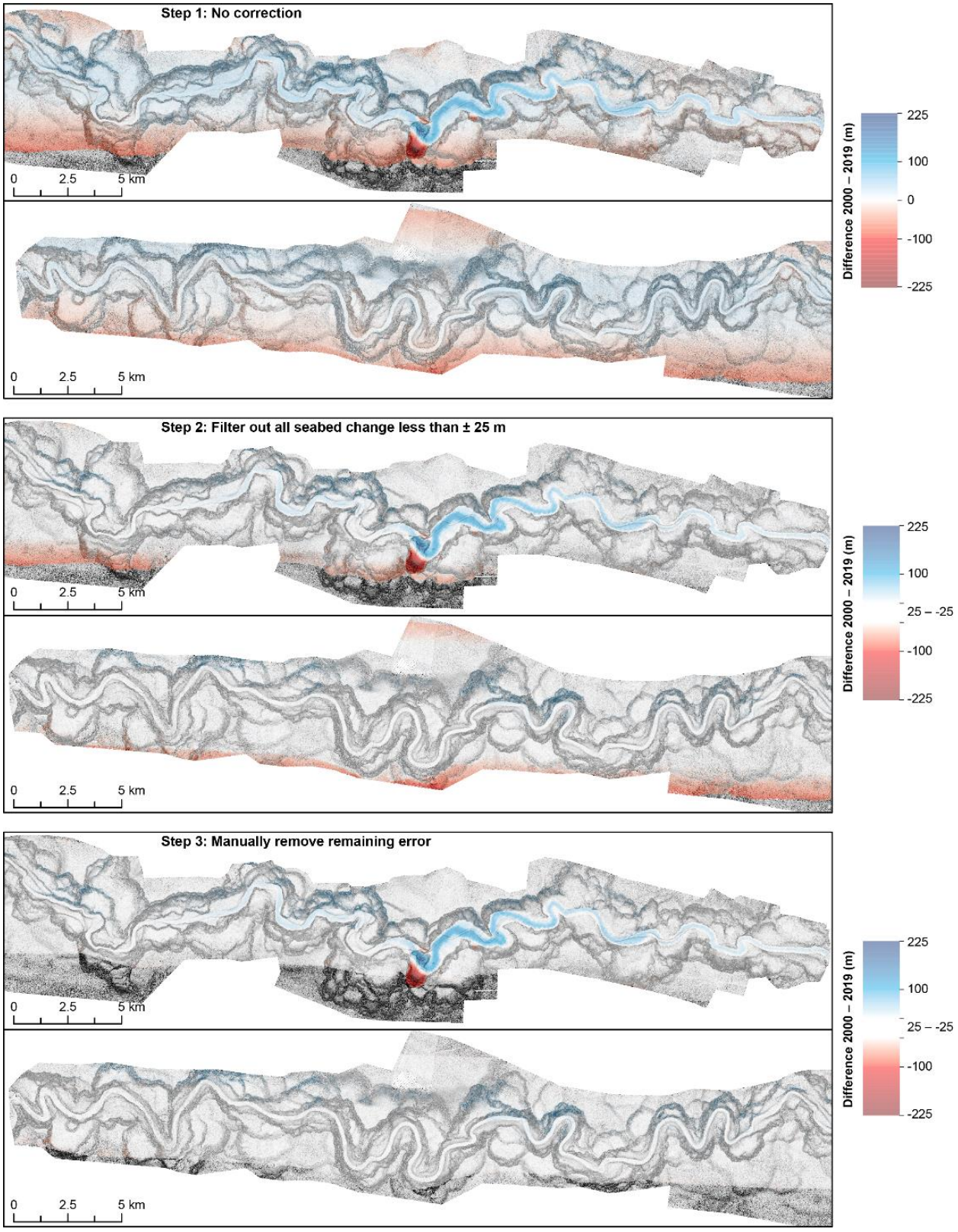

Figure 4.5: Correction procedure of the offset observed in the difference map of the canyon survey. There is an error in the difference maps that increases in magnitude towards the outer edges of the survey. This error is removed by filtering out all vertical change < ± 25 m (step 2). Remaining error is than manually removed (step 3).

4.6 Results

4.6.1 Canyon Survey

The upper canyon was surveyed in 2019 between 11° 35’ and 10° 36’ E , between 1300 and 2300 m water depth (Figure 4.1; Figure 4.6). In this area, the canyon is 850 – 1400 m deep, and has an overall sinuosity of 1.5. The upper canyon contains several levels of terraces. The shape of the terraces could be the result of previous channel bends (Figure 4.6), or headscarps of canyon-flank collapses (Babonneau et al., 2002; Pope et al., in Review). A clear example of a deposit related to such a canyon-flank collapse is present in the upstream part of the studied reach of the canyon (Figure 4.6; Figure 4.7; Pope et al. in prep). The channel floor upstream of this landslide-blockage is wide and flat (500 – 1,000 m), with a small (100 m wide, 10 m deep) discontinuous channel (Figure 4.6; Figure 4.7). The channel floor downstream of the landslide-dam is narrower (200 – 400 m), and it is locally characterised by bars at the inner bends. Several 5 – 100 m high knickpoints are present adjacent to, and upstream of, the landslide-dam.

A difference map showing change in seabed elevation between 2000 to 2019 records locally-variable morphological change in the canyon (Figure 4.6). The main change is related to the canyon-flank collapse and its related deposit. The excavated volume associated with the collapse is around 0.1 km^3 and has resulted in over 200 m of erosion locally. The associated deposit is up to 180 m thick and dammed the canyon, causing the trapping of sediment in the canyon. This trapping has resulted in the deposition of a wedge of sediment upstream of the landslide-dam, which is up to 140 m thick near the dam, and up to 40 m thick at the eastern edge of the survey (Figure 4.6; Figure 4.7). The total deposition associated with the landslide and subsequent trapped wedge of sediment is around 0.6 km^3. The deposit is also subject to erosion, as the knickpoints associated with the landslide dam migrate upstream. This erosion has resulted in a 100 – 150 m wide and 60 m deep channel incision through the landslide-dam, laterally offset from the original channel, effectively cutting off the original channel bend. The rate of knickpoint migration is unclear since the timing of the canyon-flank collapse is unknown. An additional smaller canyon-flank collapse is also present further upstream (Figure 4.7).

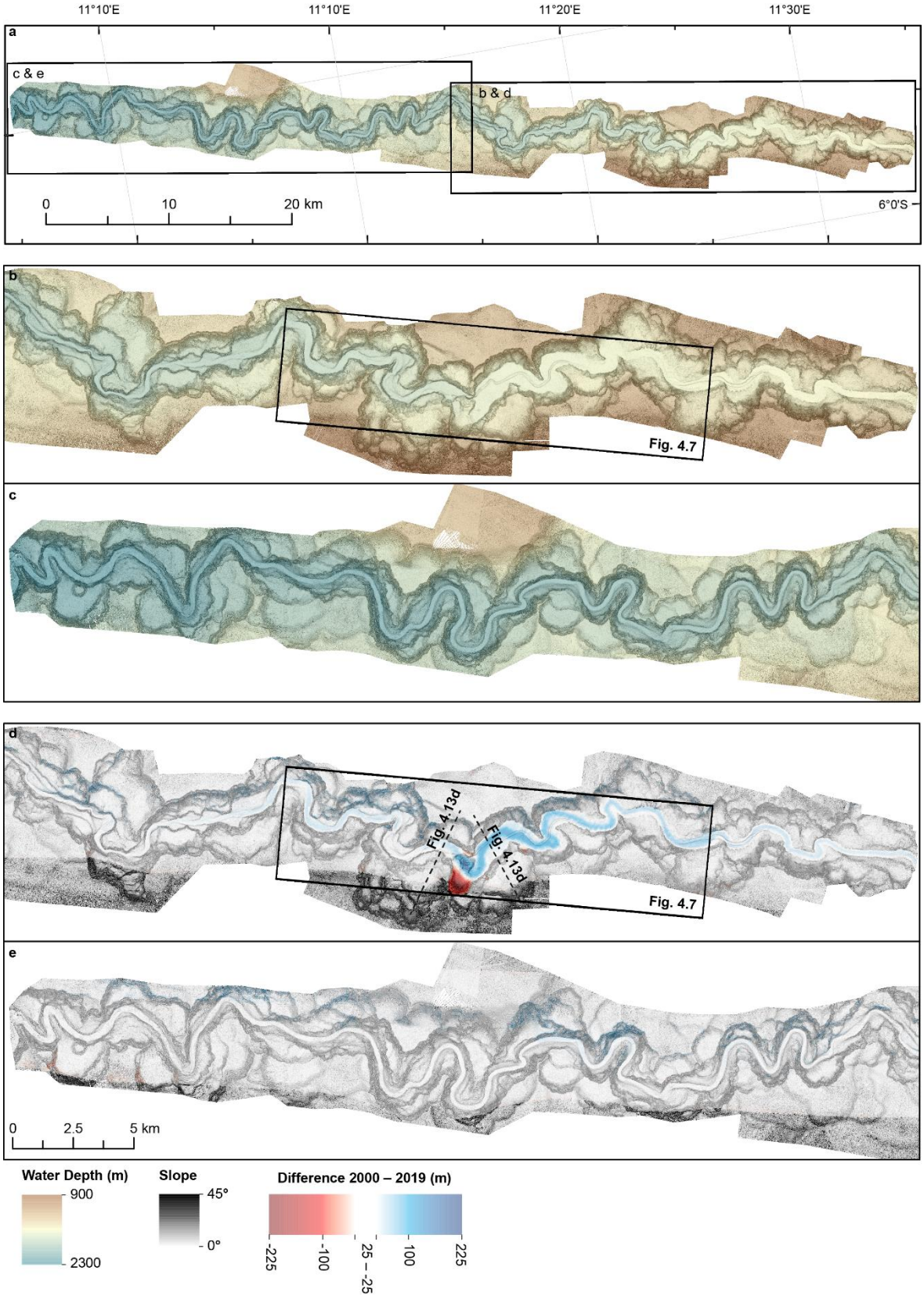

Figure 4.6: Bathymetry of the surveyed reach in the upper canyon and difference in bathymetry between 2000 and 2019. Location of the surveyed reach is shown in Figure 4.1. a) Overview of the entire surveyed reach in the upper canyon. b-c) Bathymetry of the upstream canyon in 2019. d-e) Difference map 2000 – 2019 in the upper canyon. Note that most change is located in the upper part of the canyon survey. Difference on steep slopes are interpreted as error.

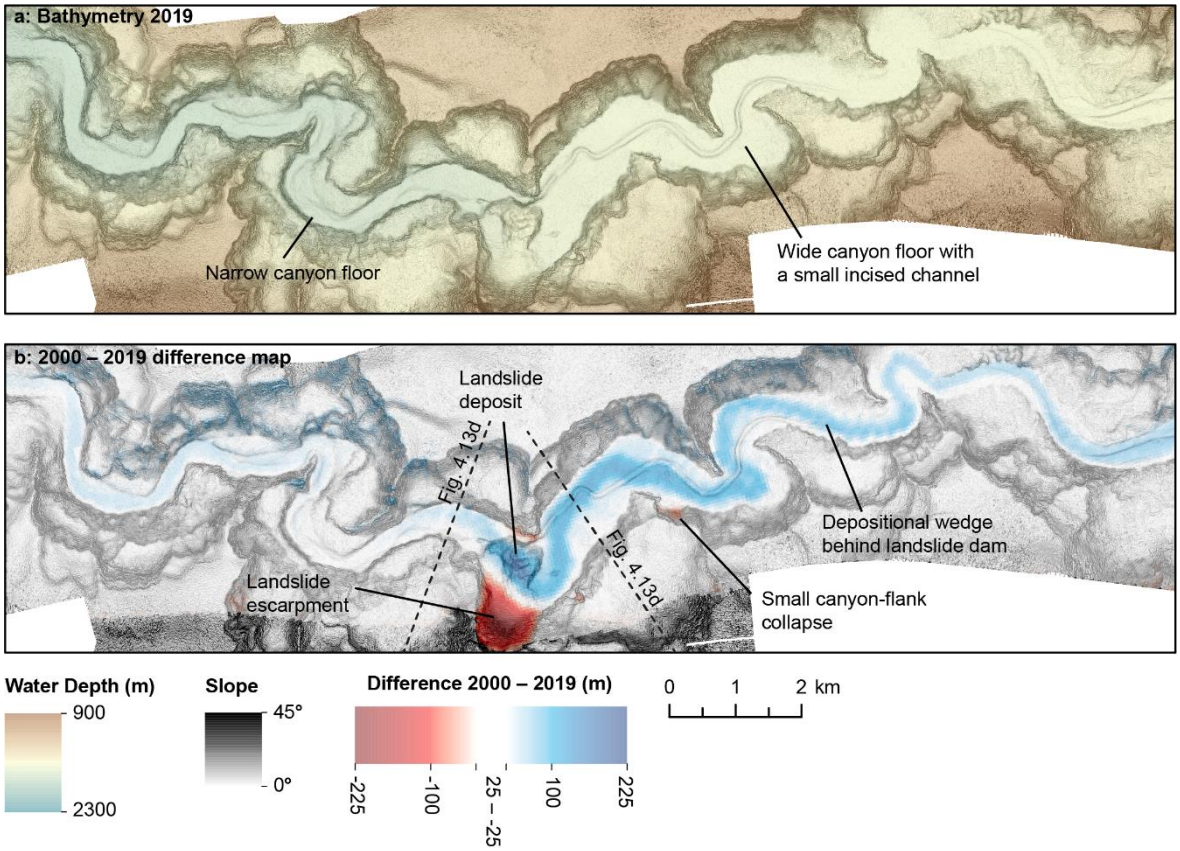

Figure 4.7: Detailed bathymetry and difference maps around the canyon-flank collapse in the canyon survey. Location shown in Figure 4.6. a) Bathymetry of the canyon around the major canyon-flank collapse. Note how the channel floor is wide and has a small channel incised in this wide floor upstream of the flank collapse, while the canyon floor is narrower downstream of the collapse. b) Difference map showing the difference in seabed elevation between 2000 and 2019. The canyon-flank collapse erodes up to >200 m and the landslide deposit is >100 m high. Note the small passage eroded in the northern edge of the landslide deposit. An additional small canyon-flank collapse is also present upstream

4.6.2 Channel survey

The downstream channel was surveyed between 8° 11’ E until the lobe at 5° 26’ E , between 4000 and 5000 m water depth (Figure 4.1; Figure 4.8), and a difference map shows seafloor change from 1998 – 2019 (Figure 4.9). The channel is 150 m deep at the most upstream part of this survey, and decreases in depth downstream until the terminal lobe, where the confinement fades. The upper part of the channel has a sinuosity of 1.4, which abruptly decreases to a sinuosity of about 1.1 halfway along the surveyed channel reach - at around 6° 54’ E 5° 54’ S (Figure 4.8; Figure 4.10). The sinuous channel upstream of this point is characterised by terraces that resemble patterns of downstream translation and outward expansion of channel bends, as observed in meandering rivers (Figure 4.8; Figure 4.10). The channel is asymmetric in this area, as

the thalweg is located towards the outer bend and bars are present on the inner bends (Figure 4.8; Figure 4.10). A series of disconnected steep topographic steps is present between three bend apices along the northern part of the channel (Figure 4.8b). Furthermore, a less pronounced channel is present between two bends (Figure 4.8c). These overbank features suggest turbidity currents can spill over the main channel, and might generate future bend cutoffs. Terraces, bars, and asymmetry are less common further downstream, where the channel is straighter (Figure 4.8; Figure 4.10). A 10 m-high knickpoint is present in the straighter section of the channel (Figure 4.8d; Figure 4.10d,e). Another steep topographic feature is present further downstream, which might be another knickpoint, but survey resolution limits detailed analysis (Figure 4.8e).

The difference map that spans 1998-2019 shows significant (> ±10 m) change along most of the channel (Figure 4.4; Figure 4.9). However, there appears to be a systematic offset in the difference map, in which deposition is enhanced along the north side of channels, and erosion along the south. This pattern is not a simple horizontal offset as a result of error in the positioning, as there is not consistently a band of erosion along one side and a band of deposition along the other side of the channel present along the survey area. Furthermore, both crests of the channel thalweg are found to have a different average offset, indicating the offset is not a simple unidirectional shift (Figure 4.11). Lastly the positioning error of both the 1998 and 2019 survey are much smaller (± 3 m, and <± 1 m respectively) than the offset, which often exceeds 100 m. This rules out the offset being attributed to errors in ship's navigation. This pattern might be real, due to another error that is not easily resolvable, due to the difference in design and resolution between the surveys, or a combination of some or all of these issues. Despite this offset with unclear origin, patterns can be observed in the difference map that overprint this offset.

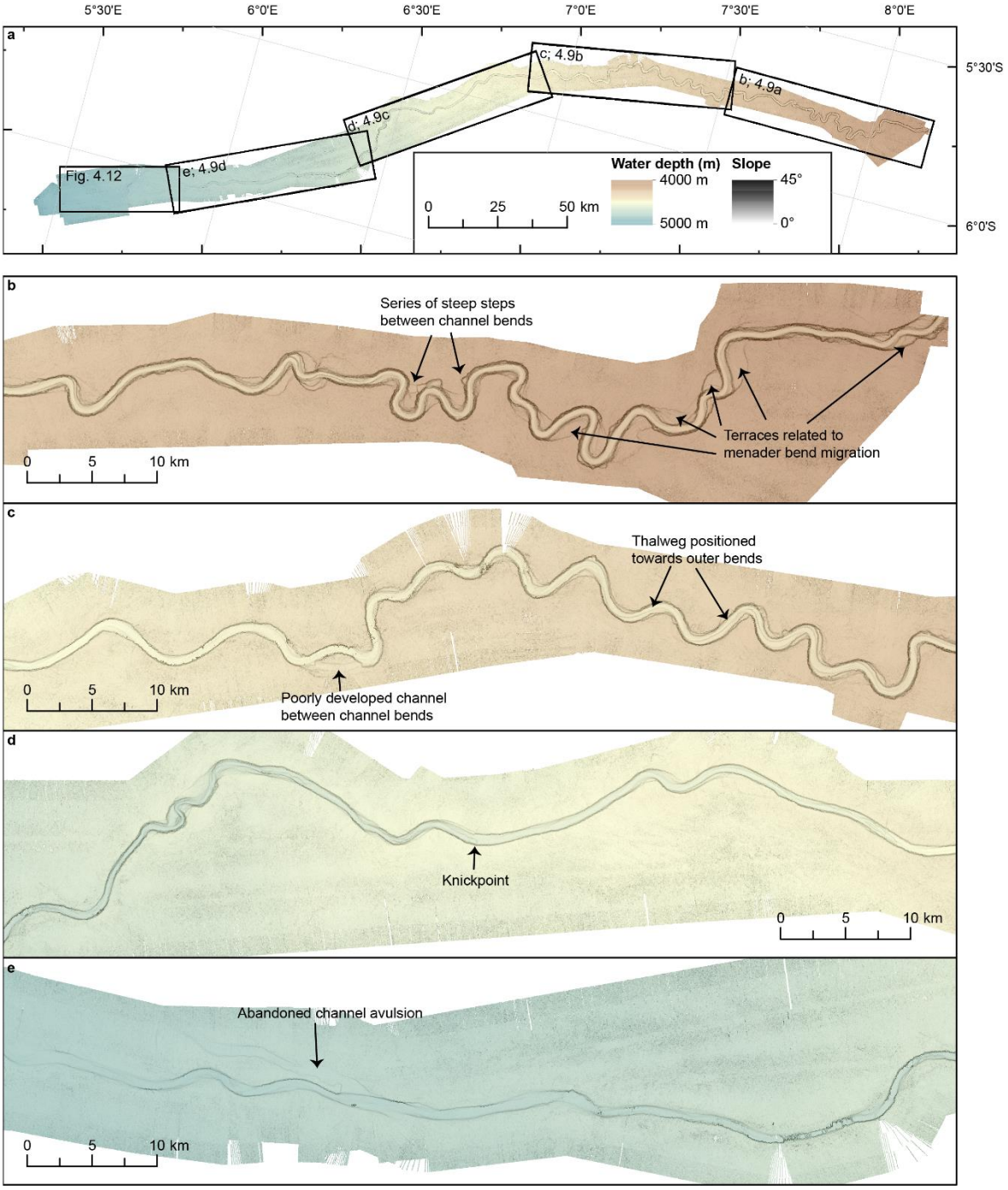

Figure 4.8: Overview of the channel survey. Location of the channel survey is shown in Figure 4.1. a) Overview of the complete survey. Note how the channel sinuosity abruptly decreases downstream of 6° 54' E. b) Most upstream part of the channel survey. The channel is sinuous and the terraces around the bends resemble past positions of the bends, suggesting the bends migrate through outward expansion and downstream translation of bends. c) This part of the channel is sinuous and the thalweg tends to be located toward the outer bends. Note the present of a poorly developed channel between two bends. d) This part of the channel is straight and contains a knickpoint. e) The most distal part of the channel is straight.

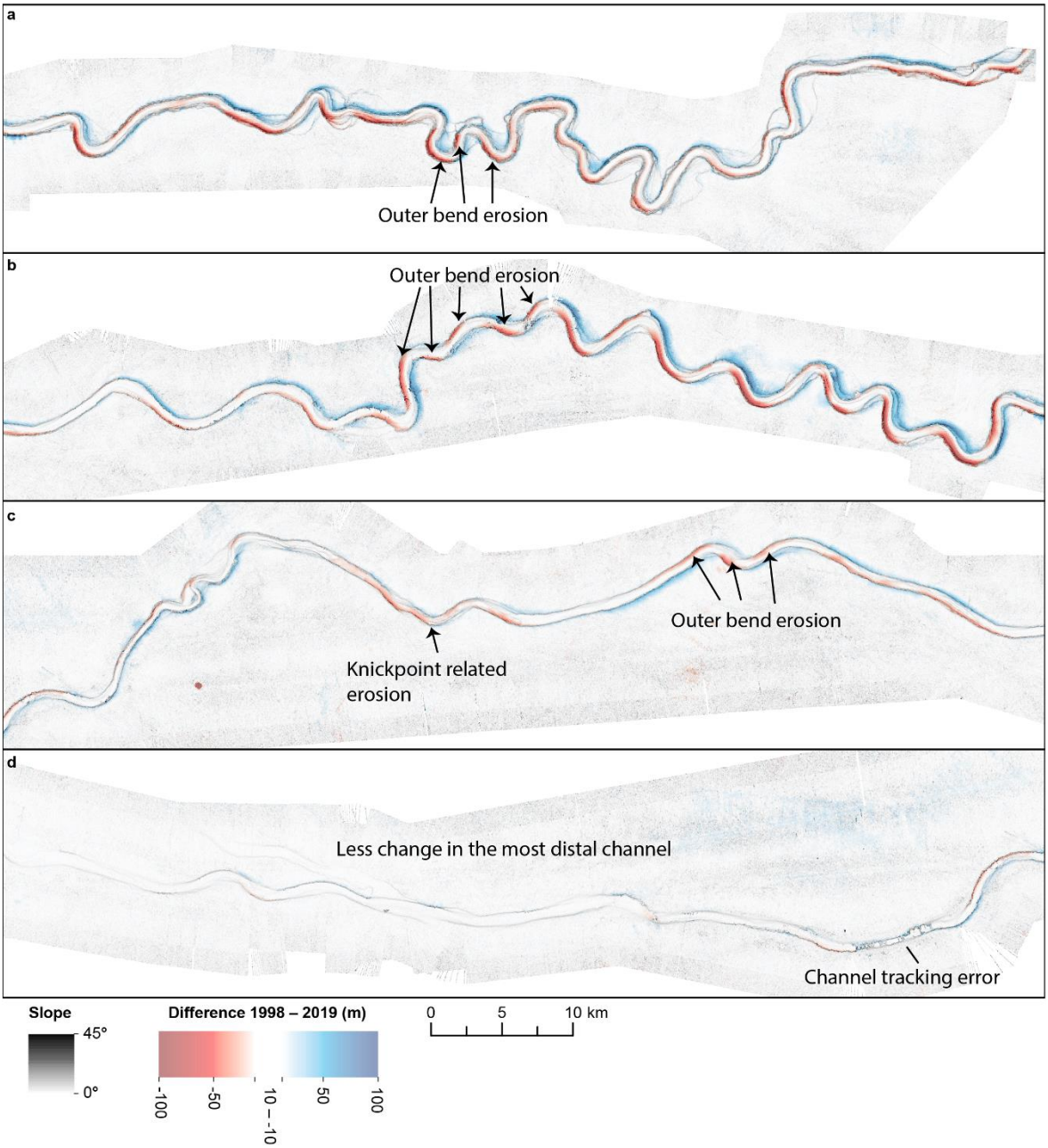

Figure 4.9: Difference maps of the channel survey spanning 1998 – 2019. Locations are shown in Figure 4.8. a-b) The sinuous upstream part of the channel survey is characterised by outer bend erosion. Inner bend deposition is also observed, but can be hard to distinguish from the offset present in the difference maps (Figure 4.11). c-d) The downstream part of the channel shows less change, but outer bend erosion is still observed locally. Channel wide erosion related to knickpoint migration is also observed.

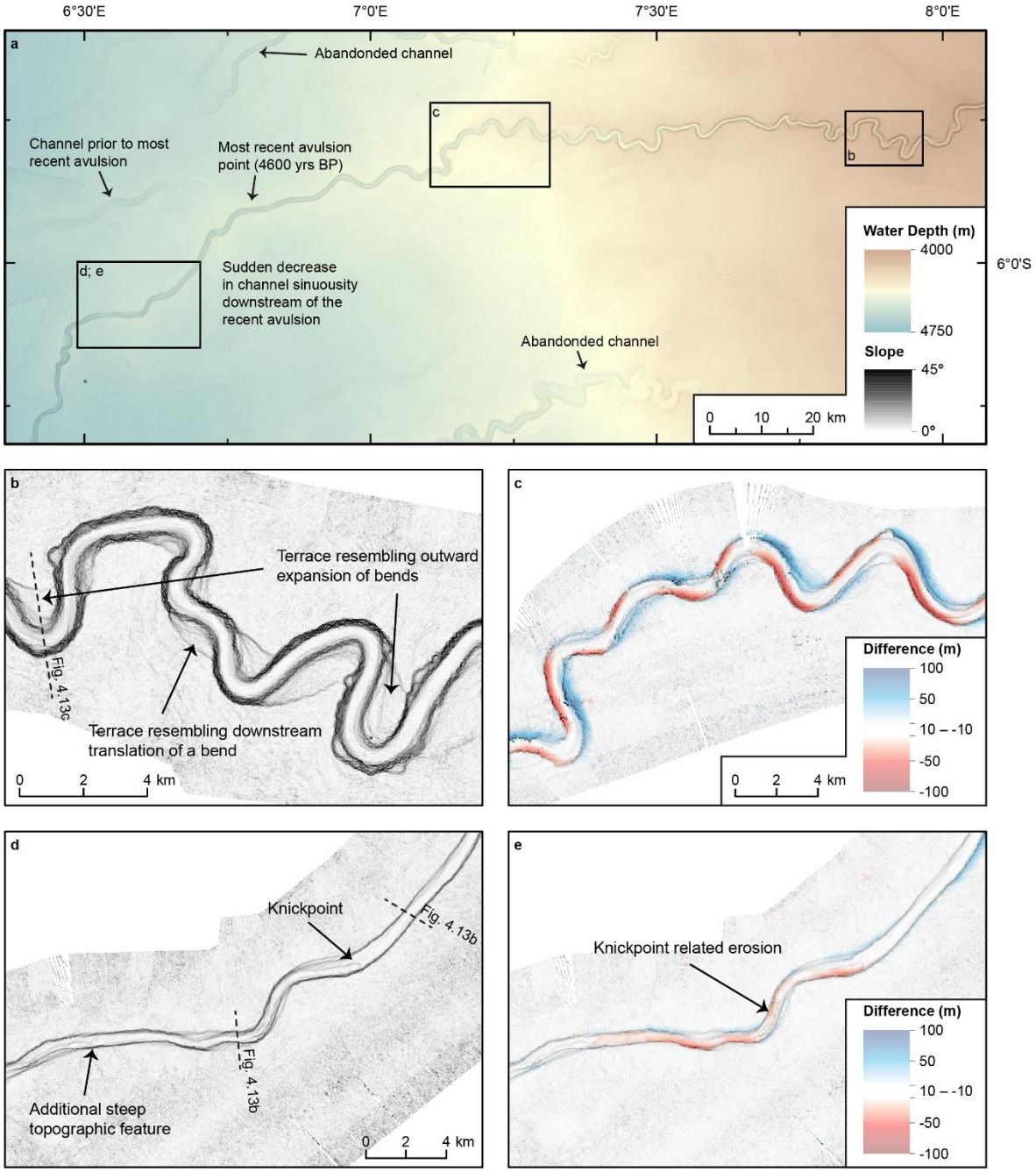

Figure 4.10: Overview and detailed morphology and change of the sinuous and straight part of the surveyed downstream channel reach. Location shown in Figure 4.1. a) 1998 bathymetry showing the transition from the upstream sinuous channel to the more downstream straight channel. This transition coincides with the most recent avulsion of the active channel (Picot et al., 2016, 2019). b) Slope map from 2019 showing terraces that resemble remnants of previous locations of the channel, indicating both downstream translation and outward expansion of channel bends. c) Map showing changes in seabed elevation between 1998 – 2019, showing erosion in outer bends and deposition in inner bends. Erosion is highest just downstream of the bend apex. d) straight channel with a knickpoint. e) erosion associated with migration of the knickpoint between 1998 and 2019.

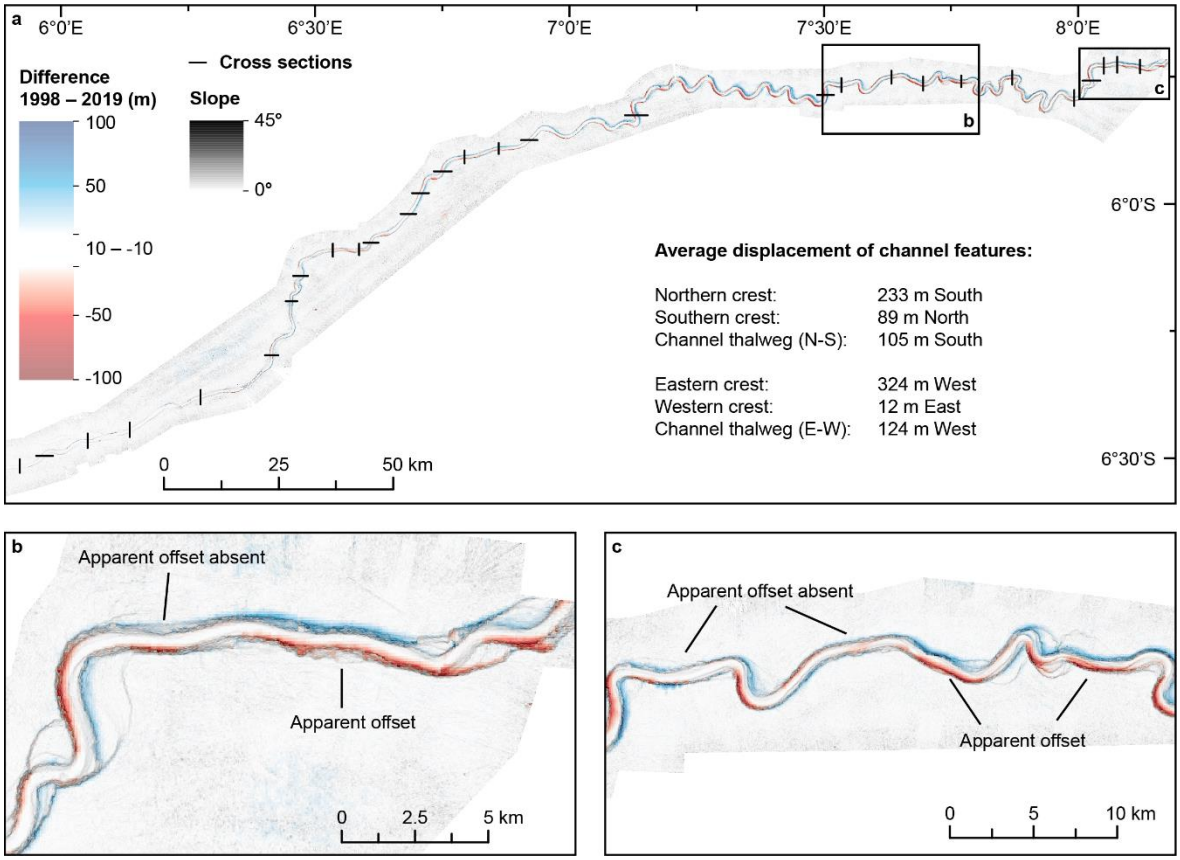

Figure 4.11: Analysis of the offset observed in the difference map of the channel survey. a) Offset of the channel crests and thalweg are measured for all shown cross sections. The results suggest that there is not a simple horizontal displacement present. b-c) Examples showing that this offset is not consistently present.

The more sinuous upstream part of the channel survey shows enhanced erosion at the outer bends (Figure 4.9; Figure 4.10). The majority of this erosion is predominantly located downstream of the bend apex. Deposition along the inner bends can be observed locally. Outer-bend erosion and inner-bend deposition is also observed in the downstream part of the system. However, a 15 km long stretch of the channel in the downstream area is associated with erosion that seems unrelated to channel bends (Figure 4.9d; Figure 4.10e). The areas immediately upstream and downstream of this erosion are characterised by less change. The upstream edge of this erosion coincides with the location of a knickpoint. This suggest that this erosion is related to the upstream migration of the knickpoint (Guiastrennec-Faugas et al., 2020a; Heijnen et al., 2020), which has migrated at an average rate of around 700 m/yr, based on the extent of the erosion.

4.6.3 Lobe

The lobe is located at the end of the channel, where the main channel loses its confinement (Figure 4.8; Figure 4.12). The area closest to the end of the main channel shows a poorly

developed channel, which is 1000 – 3000 m wide and around 10 m deep. A steep topographic feature is present, which resembles a knickpoint, but the data resolution prevents detailed analysis. This fading channel appears to be located between two steep edges with erratic crests. These features have been described and interpreted as landslide headscarps (Dennielou et al., 2017). No clear patterns of change are present on the lobe (Figure 4.12b).

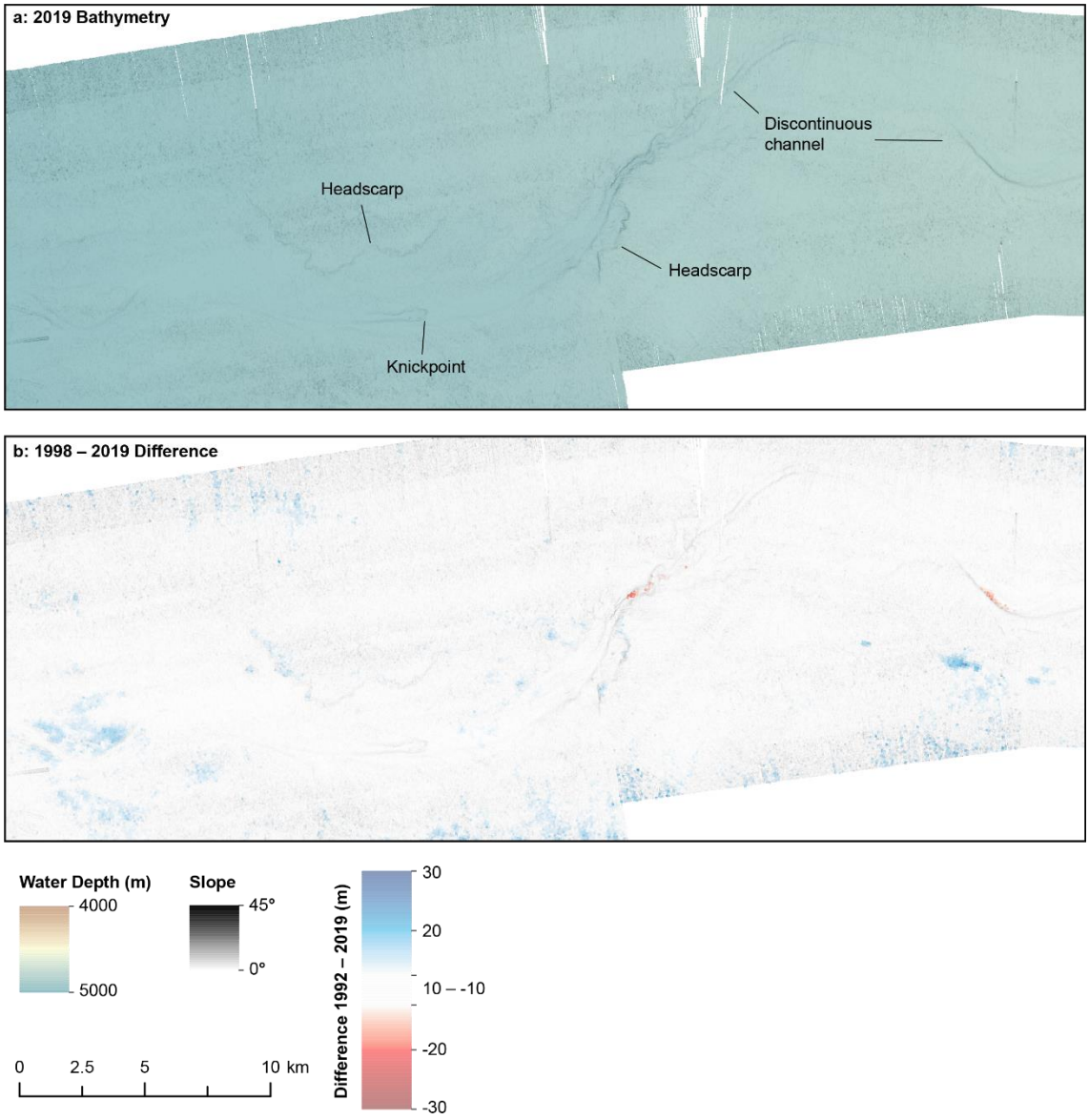

Figure 4.12: Morphology and difference on the lobe. Location shown in Figure 4.8. Scale of difference map is different from Figure 4.8. Note how there is no major consistent patterns of change on the lobe.

4.7 Discussion

Here we first summarise the different erosional and depositional patterns observed in the difference maps of canyon and channel surveys, and how they are distributed along the system. The main finding here is that the active canyon-channel system can be divided in three different

sections, which each store and re-excavate sediment in a different way, which is an advance from the previous division of channel zones based on morphology (Babonneau et al., 2002). We then continue by discussing what controls the distribution of these zones. Lastly we synthesise a general model of how submarine canyon-channel systems work, and consider the implications for longer-term channel evolution.

4.7.1 Different mechanisms dominate three distinct sections of the canyon-channel system

Time-lapse surveying of Congo Canyon-Channel system reveals that, over 20 years, the morphological evolution is controlled by distinctly different mechanisms, which create a highly spatially-variable pattern of erosion and deposition along the canyon-channel, with different mechanisms found to dominate in three distinct zones of the system (Figure 4.13). We now introduce these three zones and discuss the implications for the nature, rate and volume of sediment transfer along the canyon-channel and to the lobe at its deep-sea termination.

Upper canyon dominated by canyon-flank collapses, backfilling and re-incision: The dominant processes in this zone are canyon-flank collapses, canyon blockages, backfilling behind blockages, and subsequent re-incision (Pope et al., in prep). Large collapses (0.1 km^3) can be associated with meander bend cut-offs. Such blockages and associated backfilling of the canyon can result in areas of long (10s of km), thick (10s of m) deposition in the canyon, likely storing globally significant amounts of sediment, organic carbon, and potentially nutrients and pollutants (Pope et al., in prep). Backfilling results in a shallower wide and flat channel floor. This is then later re-incised through the upstream migration of knickpoints, which can generate a new channel within this backfill. This new channel can be located laterally offset from the location of the original channel, generating new terraces and bend cutoffs.

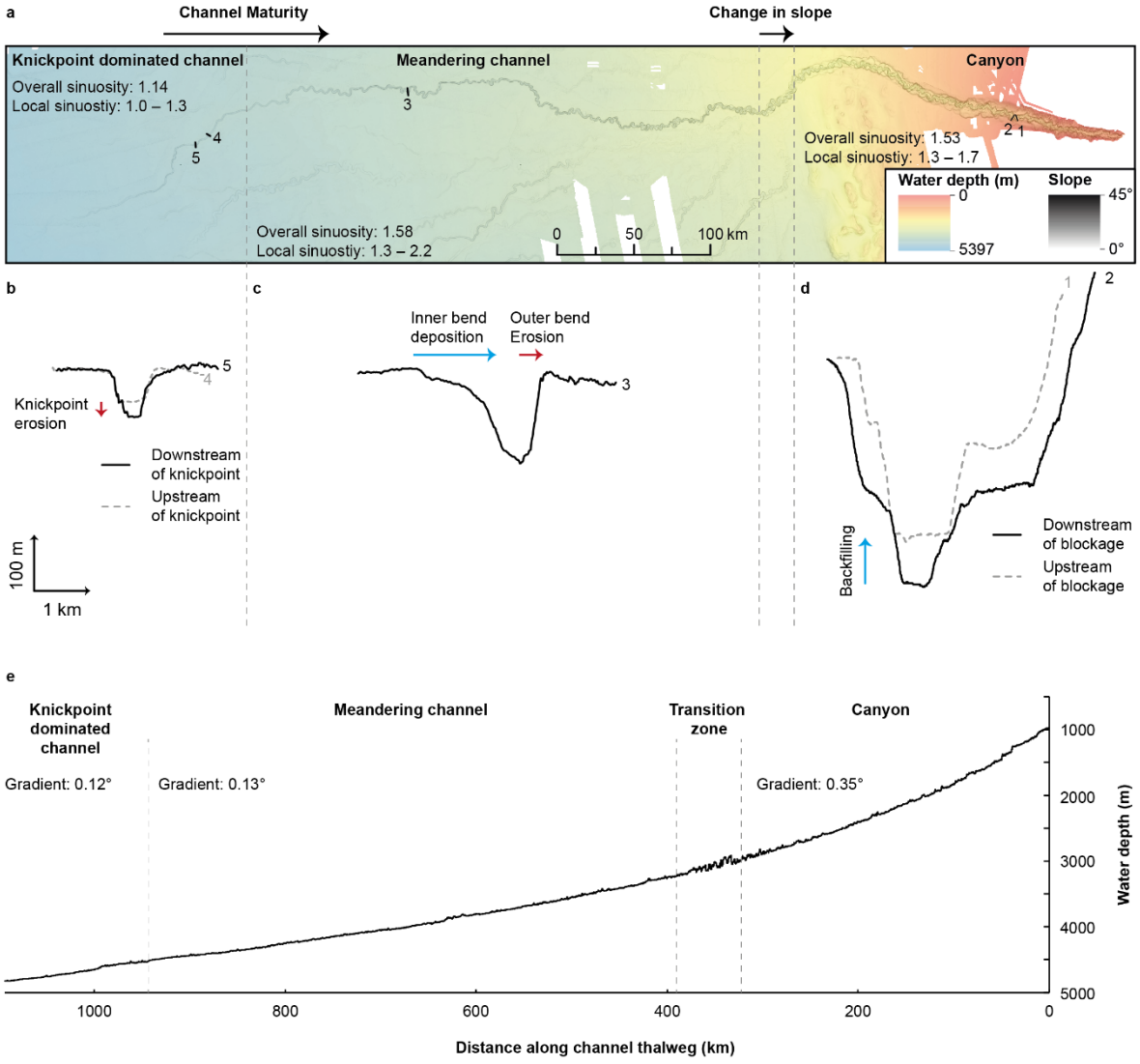

Figure 4.13: Overview of the different zones observed in the active canyon and channel of the Congo Fan. a) Overview of the system showing the locations and extent of each zone on the bathymetry from 1998-2000. b-d) typical cross sections showing the morphology of the channel and associated processes dominating each zone. Locations of the cross sections are shown in Figure 4.6; Figure 4.8. e) channel profile of the entire system showing a steeper concave profile along the canyon and a straighter profile along the channel.

Meandering channel dominated by expansion of channel bends: The evolution of the intermediate channel is characterised by outward expansion and downstream translation of channel bends (sweep and swing), similar to that observed in meandering rivers (Figure 4.9; Figure 4.10c). This evolution is observed both in the difference maps, as well as in the terraces that resemble remnants of previous positions of the bends (Figure 4.8; Figure 4.9; Figure 4.10). This swing and sweep process leads to the high sinuosity observed in this zone. The majority of the erosion in the outer bend appears to be located just past the bend apex, suggesting that these bends will both swing and sweep, rather than just swing, as suggested by previously (Peakall et al., 2000; Peakall and Sumner, 2015). Previous studies have suggested that downstream translation of bends is uncommon (Peakall et al., 2000); however, our results suggest that downstream translation does indeed occur in the active channel of the Congo Fan. Progressive bend migration can potentially lead to meander bend cut-off, but this is not observed in the areas covered by the 2019 surveys. However, locally steep steps or small channels are present that between bend apices, which might develop into future bend cutoffs. These features are outside the main channel, suggesting that turbidity currents are able to spill over the main channel (Figure 4.8b, c; Babonneau et al., 2002). Similar to river channels, the channel is asymmetric in cross section, with a steeper slope at the outer bend (Figure 4.8; Figure 4.10; Figure 4.13c).

Distal channel dominated by upstream-migrating knickpoints: This most downstream part of the channel is straighter (sinuosity 1.12) and contains segments that are characterised by hardly any change. The main change is associated with the upstream migration of a knickpoint that causes erosion across the channel's width as it migrates upstream. The most clear knickpoint has migrated upstream at around 700 m/yr, which is on the fast, yet of comparable order of magnitude to knickpoint migration in other systems (Guiastrennec et al., 2020a; Heijnen et al., 2020). This knickpoint has no clear origin, such as the knickpoints in the canyon survey that are related to the landslide-dam, or any external control knickpoints can have (Mitchell, 2006; Heiniö and Davies, 2007). This suggest that these knickpoints are generated internally by processes around the channel to lobe transition (Heijnen et al., 2020). This is the first time such internally generated knickpoints are reported in the distal parts of a large muddy system. Additional steep topographic features are present in the distal part of channel that resemble knickpoints, but the resolution of the surveys and lack of a resolvable erosional signature prevents decisive identification (Figure 4.8; Figure 4.12).

4.7.2 What controls the location of these zones along the canyon-channel system?

We now investigate what controls the distribution of these zones. The transition between the flank-collapse dominated canyon and the meandering part of the channel is not covered by the

new bathymetric surveys. Therefore, the transition cannot be based on until how far upstream outer bend erosion and inner bend deposition occurs. This transition is therefore based on morphological criteria. We define the transition between the canyon and meandering channel based on the uppermost clear traces of sweep and swing related terraces, and the lowermost place where a clear canyon with several steps of terraces is observed. This resulted in a transitional zone rather than a single point of transition (Figure 4.14). This transition zone coincides with a slope break, where the seaward limit of subsurface salt tectonics marks the transition from continental slope to continental rise (Figure 4.14; Babonneau et al., 2002). So the upper canyon zone develops on parts of the basin with a steep slope (0.3°), while the meandering channel develops on parts with lower slopes (~0.1°).

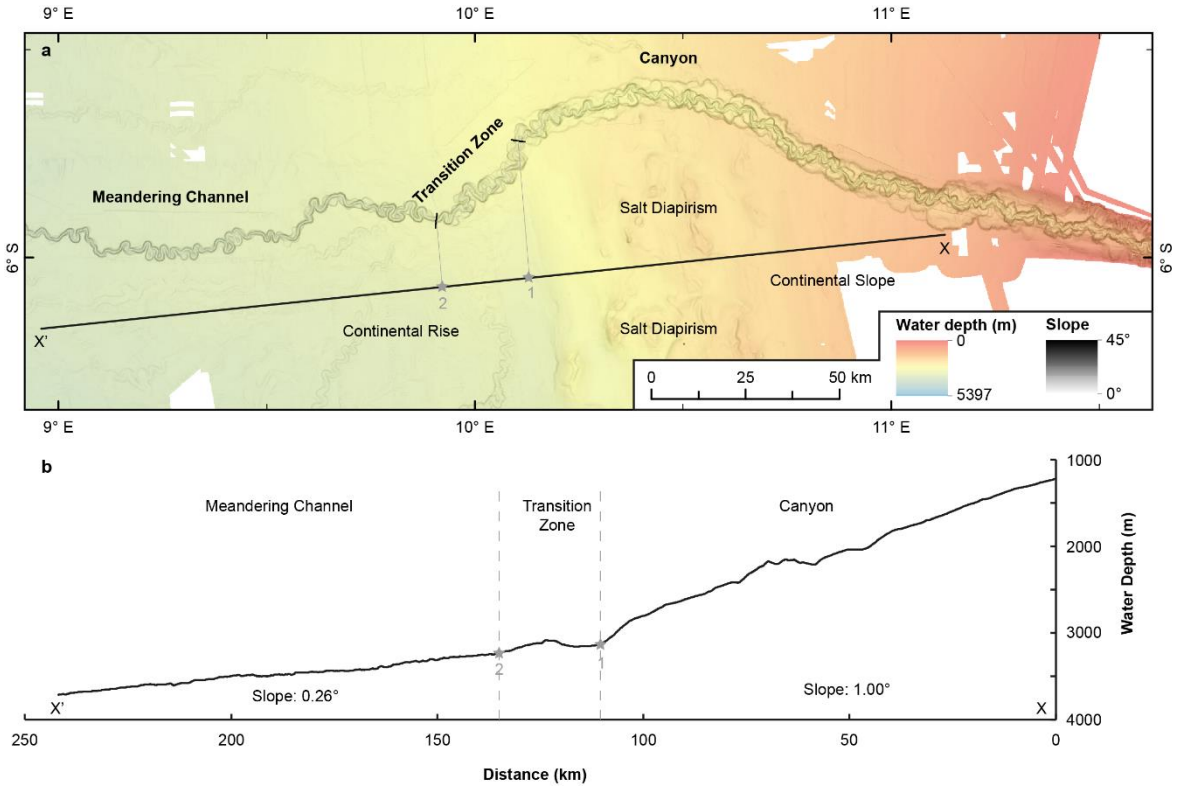

Figure 4.14: Profile along the basin floor outside the channel. a) Locations of the profile. b) profile along the basin floor outside the channel. It shows a change in slope that coincides with the transition between the canyon and the meandering channel.

The transition between the meandering channel and the knickpoint-dominated distal channel is well surveyed by the channel survey (Figure 4.10). This location does not appear to correspond to any regional morphologic or structural features, but is instead coincident with the location of the most recent avulsion of the channel, which occurred 4,600 years ago (Picot et al., 2019). This suggests that transition between the meandering channel and knickpoint-dominated channel is controlled by channel maturity. This transition is also characterised by a reduction in channel sinuosity and decrease in channel width. This suggests that a part of a channel that is knickpoint-dominated will develop in a meandering channel over time.

4.7.3 Generalised model of how submarine canyon-channel systems work

Based on the observations made here from the active Congo Canyon and channel, we synthesise a generalised model of how submarine canyon-channel systems work (Figure 4.15), and compare this with other seafloor systems. However, other high resolution imagery of submarine canyon-channel systems from source to sink is rare. High resolution surveys of the distal parts of submarine channels are especially rare. However, the well-studied Lucia Chica canyon and channels seem to fit our model very well (Fildani et al., 2020; Maier et al., 2020). A canyon is present upstream, followed by a meandering channel, while the most distal part of the systems is characterised by a straight channel with knickpoints. In contrast, several other systems appear to behave differently from our model. The submarine channels on the Squamish Delta are relatively straight, and lack different erosional and depositional zones (Brucker et al., 2007; Vendettuoli et al., 2019). This might be because the system is just a few km long, and was recently reset by human diversion of the river, therefore the system might not have matured enough yet. Other systems such as the Gaoping Canyon and the Monterey Canyon seem to have a less well developed intermediate meandering channel, but these systems have a strong structural control (Yu et al., 2009; Gardner et al., 2010).

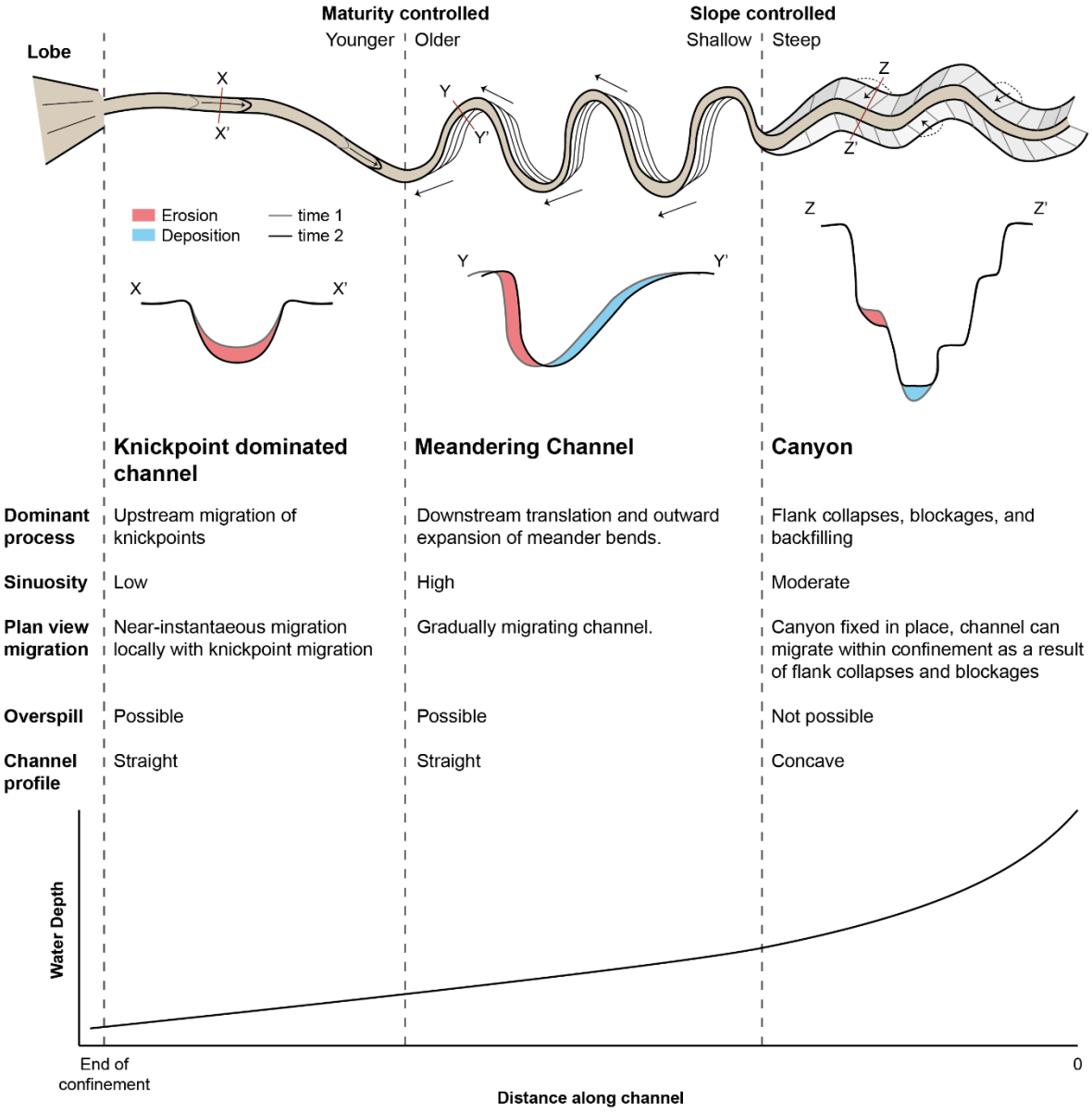

Figure 4.15: Schematic generalised model showing the different zones and associated processes in a submarine canyon-channel system.

4.7.4 Implications storage and re-excavation of land-derived material

Submarine canyons and channels have been proposed to be sites for efficient carbon burial (Baudin et al., 2017; Hage et al., 2020). However, most studies analyse only recent deposits, which might be just temporary storage locations that might be re-excavated by one of the many erosional patterns that occur in submarine canyon-channel systems.

Deposits in canyons might be related to dams further downstream in the canyon. Such deposits might be re-excavated, as we show here that these landslide-dam deposits are re-incised after the accommodation behind the dam is filled. Exact rates of deposition and re-incision of deposits behind landslide-dams are uncertain, due to a lack of constraint on the timing of the landslides, but may be on the order of 10s to 100s of years, as the landslide dam and depositional wedge behind show >10 m of erosion locally. Deposits formed in the meandering channel will be located in inner bends as point bars, or on the overbanks. Both types of deposits therefore have the potential to be the final sink for land-derived material. Meandering channels on submarine fans have the tendency to avulse, rather than create long lived flood plains that continuously rework previously generated channel bars and overbank (Normark, 1978; Paola, 2016; Picot et al., 2016; Foreman and Straub, 2017). However, overbank deposits directly outside outward expanding or downstream translating bends can be deposited readily. Inner bend deposits can be eroded trough downstream translation of the next upstream channel bend, if given enough time (100s – 1000s) years, given avulsion has not occurred yet. The more upstream extent of the meandering channel zone generates a longer lived meandering channel with the potential to rework previous deposits, since avulsions occur more often further downstream the meandering channel (Damuth et al., 1988; Picot et al., 2016). Lastly, deposits generated in sections of submarine channels that are dominated by the upstream-migration of knickpoints are not clearly observed here, but tend to be long (100s – 1000s of metres) and channel-wide (e.g. Guiastrennec et al., 2020a; Heijnen et al., 2020). Most of these deposits are likely to be reworked by subsequent knickpoints within years or tens of years (Guiastrennec-Faugas et al., 2020b).

4.7.5 Implications for longer term channel evolution and channel life cycles

If the different zones found in this study are indeed partly controlled by channel maturity, then channels can evolve through these different regimes over time (Figure 4.16). The evolution through these zones might offer some process explanation for channel life cycles, often observed in subsurface and outcrop data (Fildani et al., 2013; Maier et al., 2013; Hodgson et al., 2016). A typical channel life cycle consists of a phase of channel development, which is characterised by erosional steps, referred to as either scours, cyclic steps, or knickpoints (e.g. Fildani et al., 2013;

Toniolo and Cantelli, 2007). This results in a straight, wide, and shallow channel. This phase might be similar to the straight knickpoint dominated channel. As the channel matures over time, it becomes deeper and more sinuous, resulting in a meandering channel, similar to what is observed in the channel surveyed in this study. Channels eventually are abandoned, and are filled gradually. Our results show that the transition between the flank-collapse dominated canyon and the meandering channel is controlled by the structure of the basin, there may also be a component of maturity involved, as time is required to incise a deep canyon. Canyons develop as straight gullies, which have similar characteristics to the channel initiation phase of channel life cycle models (Lonergan et al., 2013; Micallef et al., 2014). It is possible that submarine canyons originate as knickpoint-dominated channels, and then develop into meandering channels. Immature channels consisting of a train of discontinuous scours suggesting canyons initiate this way are present on the slopes of Monterey and Lucia Chica Canyons (Fildani et al., 2006, 2013; Maier et al., 2013). Then lastly, if the slope is steep enough, incision continues and the channel evolves into a canyon. Whereas, if such a structural control is absent, the developed meandering on lower slopes lowers the energy of turbidity currents to prevent further incision (Toebes and Sooky, 1967). Instead of a deeply incised conduit, a channel maintained by both erosion and deposition develops, and continues to meander without deeply incising. This allows the meandering channel to reach a higher sinuosity compared to the upstream canyon (Babonneau et al., 2002). So maturity and a certain basin structure could also be seen as requirements allowing development of a certain zone, rather than a control. The last stage is channel abandonment, which can occur at any stage in the cycle, as a result of (internally generated) avulsions, removal of the sediment input, or changes to the basin structure. Both avulsions and changes to the basin structure have occurred on the Congo Fan in the past (Marton et al., 2000; Picot et al., 2016). Internally generated avulsions have been suggested to result from backfilling of a channel as a lobe grows (Armitage et al. 2012). Observations from submarine channels on the timescale of channel lifecycles also suggest that channels narrow as they get more sinuous, however we do not clearly see this in the Congo canyon-channel, apart from the very most distal part of the system (Dennielou et al., 2017).

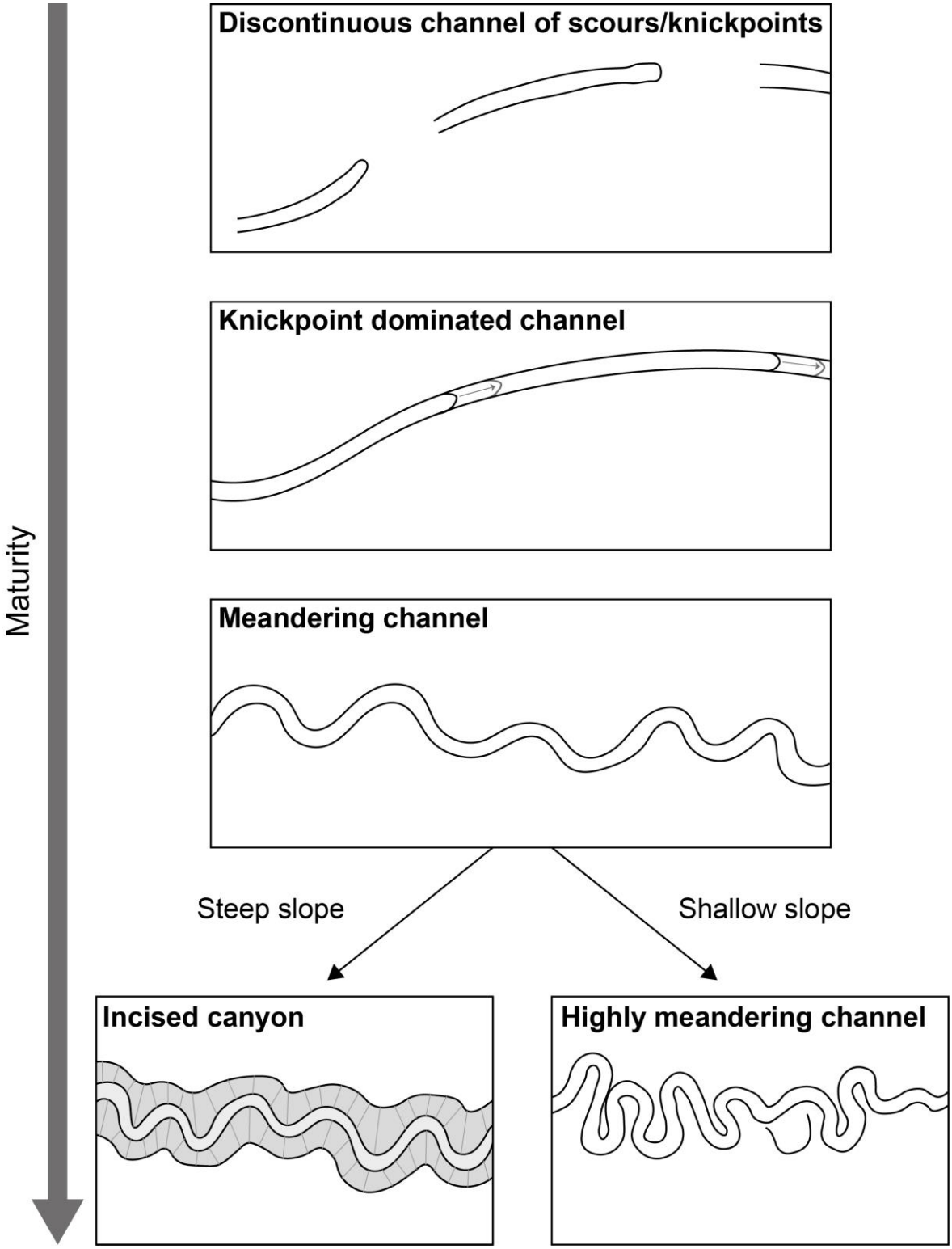

Figure 4.16: Schematic model of how a channel can evolve through the different zones outlined in this study. This evolution is controlled by maturity and the shape of the basin.

4.8 Conclusion

Here we present new bathymetric surveys over 75 km along the canyon and 400 km along the active canyon and channel of the Congo Fan. Comparison between these new surveys and a set of surveys obtained between 1998 and 2000, allows for the first ever time-lapse mapping of a major submarine canyon-channel system. This time-lapse mapping allows tracing the relative contribution of different erosional and depositional patterns along the system. We find that three different zones, characterised by a different set of erosional and depositional patterns are present, in which land-derived material is stored and re-excavated differently. The canyon is characterised by flank collapses that temporarily dam the canyon, followed by re-incision of those blockages. The middle part of the channel is dominated by meandering, in which material is eroded through the outward expansion and downward translation of bends, while sediment is deposited as bars on inner bends, and on the overbanks. Lastly, the most distal part of the channel is dominated by upstream-migrating knickpoints that generate deep, localised erosion as they migrate. The transition between the canyon and meandering channel is controlled by the slope, of the basin, while the transition between the meandering channel and the knickpoint dominated channel is controlled by channel maturity. These observations are then synthesised in a generalised model of how submarine canyon-channel systems work. This model demonstrates that sediment can be stored and re-excavated anywhere along a submarine channel system, through a range of different processes. Lastly we show that a section of a submarine channel can evolve through the different zones as it matures.

Chapter 5 Conclusions and future work

In this chapter, the main conclusions are presented by answering the three research aims defined in chapter 1. This is followed by a series of suggestions for future work, and then ends with summarising the potential implications of the key findings arising from this thesis.

5.1 Conclusions

The overarching aim of this thesis was to demonstrate how new high-resolution repeat seafloor surveys enable a better understanding of the processes that control the evolution of submarine channel systems and that modulate sediment transport into the deep sea. The surveys presented in this thesis consist of two sets of surveys that represent the most complete set of seafloor surveys of deep-sea submarine channel systems to date. The first set of surveys covered the submarine channel system in Bute Inlet and consisted of 10 surveys spanning 11 years. The second set of repeat seafloor surveys was the first to cover a large part of the margin-scale submarine channel system on the Congo Fan. These two sets of seafloor surveys were used to address three specific sub-aims.

5.1.1 Which processes control the evolution of submarine channels?

Previous studies had already established that meandering, migration of crescentic bedforms, and levee development can control the evolution of submarine channels. Chapter 2 used repeat seafloor surveys from Bute Inlet, British Columbia, Canada, to show that the upstream-migration of knickpoints can control the evolution of submarine channels. Knickpoints are steep steps in channel gradient that migrate upstream as a result of overpassing turbidity currents. This migration is associated with erosion upstream and deposition downstream of the knickpoint. This process generated an alternation of erosional and depositional zones along the channel in Bute Inlet. Knickpoint migration was found to be generated internally within the channel, without requiring external factors such as tectonics or base-level change. The rate of their migration was found to be two to six orders faster than that typically observed in rivers. Knickpoints can also migrate outside of the main channel confinement, and generate lateral migration of the channel, or excavate a channel in areas where no well-defined channel existed previously. The budgets of eroded sediment associated with knickpoint migration exceeded those associated with outer bend erosion by at least a factor of two. Knickpoints similar to those observed in Bute Inlet were found to be present in many other submarine channel systems around the world. We posit that the role of knickpoints in channel evolution may have been under-recognised by previous studies.

Indeed, studies published subsequent to that in Chapter 2 appear to confirm this point, showing that knickpoints play a key role in channel maintenance and evolution (Guiastrennec-Faugas et al., 2020a,b).

5.1.2 How is sediment transported through a submarine channel and onto the lobe?

Previous models of sediment transport through submarine channels suggested that either: i) small flows fill the upstream part of the submarine channel system with sediment which is then flushed down-stream by a subsequent larger flow; or ii) a more direct mechanism is responsible, wherein flows transfer sediment directly from the head of the system to the lobe, without significant interaction with the seafloor. In chapter 3, a modified model was proposed based on the monitoring results of the active channel system in Bute Inlet. This model was based on integration of repeat seafloor surveys with turbidity current monitoring and discharge measurements of the main river that supplies the sediment. In this new model, sediment is transported downstream in a stepwise manner by a range of flows that decrease in frequency with increasing runout length. The main differences between this new model and the pre-existing models are that there is no unimodal nor bimodal distribution in flow runout lengths, and that the entire channel is actively reworked by upstream-migrating knickpoints. This reworking is characterised by deep localised erosion and widespread deposition in the channel on the shorter timescale that we monitored on, but the analysis presented suggested that the erosion and deposition potentially balance out over longer timescales to generate a zone of sediment bypass. The resulting sediment delivery to the lobe in the new model is discontinuous and does not necessarily correlate with events that provide increased sediment input to the system.

5.1.3 How do different processes control channel evolution along the length of a margin-scale submarine channel system?

This aim was addressed in chapter 4 using a set of seafloor surveys that capture how the active channel system on the Congo Fan has changed over 20 years. This set of surveys covered a ~75 km long section along the canyon that is incised into the continental margin, and a ~400 km long section along the active channel on the fan. These surveys revealed that the system can be divided into three zones, based on the erosional and depositional patterns that are observed. The canyon was dominated by canyon-flank collapses that can block the canyon. These blockages led to subsequent backfilling. This deposition is temporary as the blockages and associated backfill are subsequently eroded. The middle part of the system, referred to here as the meandering channel, was dominated by the downstream translation and outward expansion of channel bends. This bend migration was associated with erosion in the outer bends and deposition in the

inner bends. The most downstream part of the channel was characterised by the upstream migration of knickpoints. The transition between the canyon and the meandering channel was controlled by the structure of the basin, and the transition between the meandering channel and knickpoint-dominated channel was controlled by maturity. Furthermore, all three zones are typified by a distinct set of different processes that can temporarily store and/or later re-excavate previously sequestered land-derived material.

These results have provided new insights into how submarine channel systems evolve and how these processes affect sediment transported through these systems. For example, the timelapse surveys from both Bute Inlet and the Congo Canyon show how upstream-migrating knickpoints and canyon-flank collapses can control how some channels, or parts of channels evolve, and how these processes rework sediment through temporary sediment storage and re-excavation. Furthermore, this thesis has demonstrated the variety and complexity of internal processes that occur in these systems. The work in Bute Inlet in particular has provided new insights into how sediment can be transported through several autogenic steps of reworking before reaching the lobe; hence deposits that build submarine lobes do not directly record episodic external events. Lastly, this thesis showed how technological advances, such as in seafloor mapping, can drive the discovery of new insights into the dynamics of submarine channels that play a globally important role in sediment transfer.

5.2 Future work

The outcomes from this thesis also stimulate many new questions for future research. This section now proposes four potential future research directions that follow on from the results of this thesis.

5.2.1 What generates phases of increased deposition on lobes: Increased flow magnitude or flow frequency?

Chapter 3 showed that sediment delivery to the lobe at the terminus of the submarine channel in Bute Inlet is discontinuous. The repeat surveys that were acquired between 2008 and 2018 show that deposition on the lobe occurred almost exclusively between the surveys performed in 2010 and 2014, and between 2014 and 2015. This phase of enhanced deposition between 2010 and 2015 cannot be directly linked to obvious external triggers, or increases in sediment input. However, the repeat surveys lack the temporal resolution to observe the nature of the internal processes that generated the flows that caused this phase of deposition on the lobe. Furthermore, no turbidity current monitoring equipment was moored in the system during this

period. Therefore, the magnitude and frequency of events that build lobes remains unknown. First, the deposition on the lobe could be created by a minimum of two major flow events, which are larger in magnitude than the flows reaching the lobe in 2016 and 2018. Second, an increase in the number of flows of similar magnitude as those reaching the lobe in 2016 and 2018 could have been responsible for the observed deposition on the lobe. This research question can be answered through acquiring sediment cores on the lobe that could help to identify the nature of this sediment delivery. If the deposition that occurred between 2010 and 2014 consists of one thick bed, then the observed large surge in the discharge of the feeding river is most likely responsible. However, if the lobe deposit contains a higher number of thinner beds, then the sediment delivery to the lobe is most likely controlled by internal processes, and any clear external signal has become shredded (e.g. Jerolmack and Paola, 2010; Romans et al., 2016). Previous expeditions have attempted coring of the lobe using a piston corer, but these efforts were unsuccessful, presumably due to the deposits being sand-rich, which prevents penetration of piston corers. Therefore, a next attempt should make use of a vibracorer (Finkl and Khalil, 2005). The number of individual turbidites present in these deposits would give an indication of the frequency and magnitude of the events responsible for this deposition (e.g. Jobe et al., 2018). This would provide a better understanding of the processes involved in the transporting land-derived material to lobes.

5.2.2 What is the architecture of the stratigraphy left behind in the rock record by knickpoint-dominated submarine channels?

Studying the deposits left behind by ancient submarine channel systems has been an important source of information, as they hold longer-timescale records of how these systems evolve (e.g. Hodgson et al., 2016; Pemberton et al., 2016). However, observations of present-day systems are needed to develop and verify depositional models that explain the architecture of the deposits preserved in the stratigraphic record. Such a depositional model has not yet been developed for knickpoint-dominated submarine channels, and hence, no ancient system has been interpreted as such. However, it has been noted that some ancient systems lack lateral accretion packages (i.e. the stratigraphic remains of migrating meander bends (e.g. Hubbard et al., 2014; Jobe et al., 2016). In order to develop such a depositional model and identify the diagnostic criteria needed to interpret deposits as generated by a knickpoint-dominated channel, it is important to select appropriate site(s). Results from chapter 2 suggests that the deposition downstream of knickpoints forms channel-wide, upstream-migrating bodies that are in the order of 1 m thick and in the order of 100 – 1000 m long. These bodies onlap on the erosional surface generated by the migrating knickpoint and form an apparent truncation (backlap) at their downstream end. Such

thin and long bodies are challenging to observe in outcrop and are likely to fall below the resolution of most subsurface imagery. The recent advancement of drone imagery in outcrop studies can potentially mitigate these limitations and image such bodies. Initial potential study sites should be coarse grained systems, as knickpoints have been more commonly recognised in sandy systems (e.g. Paull et al., 2011; Corella et al., 2016; Guiastrennec-Faugas et al., 2020a). Furthermore, long and well exposed sections of along-strike exposure of ancient systems are required to capture theses depositional bodies. A potential suitable study site would be the dip-oriented outcrop exposure of one of the channel system of the Tres Pasos Formation, along the Alvarez Ridge in Southern Chile (Nesbit et al., 2021).

5.2.3 What is the impact of flows triggered by catastrophic events, such as earthquakes and floods, on the evolution of submarine channels and sediment delivery to the deep-sea?

Conventional models of turbidity currents suggested that turbidity currents are episodic events that involve some sort of catastrophic triggering event, such as earthquake-generated landslides and storms (e.g. Normark and Piper, 1991; Masson et al., 2011; Jobe et al., 2018). This thesis, especially chapter 3, and other recent monitoring work has demonstrated that turbidity currents occur much more frequently than previously anticipated, and do not always need an external trigger (e.g. Knudson and Hendy, 2009; Azpiroz-Zabala et al., 2017a; Paull et al., 2018; Hage et al., 2019; Heerema et al., 2020). Yet, large flows triggered by a catastrophic event can be very impactful (e.g. Heezen and Ewing, 1952; Mountjoy et al., 2018). However, the impact of a large catastrophic event has never been compared to the effect of successive more frequent internally generated events, due to a lack of repeat seafloor surveys of active submarine channel systems. As more systems are being mapped repeatedly, the opportunities will arise for obtaining a set of surveys that capture a period which includes an externally-triggered catastrophic event occurs, as well as a period without such an event. One opportunity would be an additional repeat survey in Bute Inlet after the glacial outburst flood that occurred at Elliot Creek, which feeds into one of the main feeding rivers, on 28 November 2020, as outburst floods have been shown to be able to trigger tubidity currents (e.g. St-Onge and Lajeunesse, 2007; Duller et al., 2008, 2014; Piper and Normark, 2009; Clare et al., 2018).

5.2.4 How efficient are submarine channels systems in burying young land-derived organic carbon?

Submarine channel systems have been identified as important sites for the burial of organic carbon (Schlünz et al., 1999; Baudin et al., 2010, 2017; Stetten et al., 2015; McArthur et al., 2017;

Zheng et al., 2017; Hage et al., 2020). However, it is not understood how efficiently this carbon is buried. First, the overall budgets of sediment input into the system, and that released through erosion within the system, have not been balanced against the observed deposits. Furthermore, the preservation potential of modern deposits in submarine channel systems is often unclear, as is the extent to which seafloor deposits are sites of temporary storage, which are later re-excavated, allowing the previously buried organic carbon to be oxidised. Repeat seafloor surveys that cover a system from source to sink, such as those in Bute Inlet, should enable more robust reconstruction of sediment budgets. However, the mass balance of river input, erosion, and deposition over the entire survey period in Bute Inlet is shown in chapter 3 to miss 70 – 80 % of the river input. This may be (partly) accounted for by thin and widespread deposition in areas such as the overbanks and distal end of the lobe that falls below the vertical resolution of the difference maps. Furthermore, the surveys do not cover the upper parts (< 60 m water depth) of the prodeltas, which could potentially store sediment. Besides accuracy and coverage limitations, the 11-year timespan of the set of repeat surveys, is insufficient to observe the reworking of the recent deposits. Based on the analysis in Bute Inlet, it is expected that deposits downstream of knickpoints will ultimately be reworked when the next knickpoint downstream migrates up the channel. Longer time-scale repeat surveys will allow this reworking to be observed. Furthermore, longer time-scale observations will generate more resolvable change, and will decrease the relative impact of the vertical accuracy on the mass balance. Forward numerical models based on observed seafloor change could be used to predict the evolution of well-mapped systems and understand the likely stratigraphic architectures that would result.

5.3 Concluding remarks and broader implications

This thesis presented a series of new insights of how submarine channel systems work, and has demonstrated the complexity of the internal processes present in these systems. The following text now summarises the key findings and some wider implications.

5.3.1 Upstream-migrating knickpoints can control submarine channel evolution, but could pose geohazards to seafloor infrastructure.

This thesis demonstrated how upstream-migrating knickpoints can control how sections of channels, or entire channel systems, evolve. The erosion related to this migration can also pose a hazard to infrastructure crossing submarine channel systems, such as seafloor cables and pipelines, as the upstream migration of a knickpoint can be associated with tens of metres of incision. Infrastructure that has been placed just upstream of knickpoints might be prone to damage, due to exposure, undermining, or generation of free spans as the substrate that

supported it can be removed as knickpoints migrate upstream (Chiew, 1991; Sumer et al., 2001; Bruschi et al., 2006).

5.3.2 If flow frequency decreases with distance along the channel, does that make distal parts less prone to geohazards?

Chapter 3 showed that turbidity current frequency deceases with distance along the submarine channel of Bute Inlet. This might suggest that more distal parts of a submarine channel are less prone to geohazards posed by turbidity currents. However, the more powerful flows, that have a larger runout distance might be the most hazardous, and flows might ignite and become more powerful further downstream the system. Future geohazard assessments should therefore weigh up the anticipated design life of the structure (often 20-30 years) with the anticipated recurrence of long runout distance flows to determine the risk posed by such events (Spinewine et al., 2013; Carter et al., 2014).

5.3.3 Different internal processes rework deposits along the entire length of submarine channel system, and can re-excavate buried organic carbon and pollutants.

The difference maps presented in this thesis all show that submarine channel deposits experience reworking as a result of a range of different internal processes. This reworking can include erosion that is tens of metres deep. As a result, organic carbon and pollutants that were buried in these deposits might be re-excavated and therefore can be re-introduced into the environment. It is important to assess the preservation potential of deposits before interpreting how efficient submarine channel systems can bury organic carbon and pollutants (Hage et al., 2020; Azaroff et al., 2020; Pohl et al., 2020; Zhong and Peng, 2021).

5.3.4 Sediment delivery to the lobe can be modulated by internal processes, and overprint external signals to be recorded in the deposits.

Chapter 3 combined repeat seafloor mapping, turbidity current monitoring, and discharge measurements of the main feeding river to demonstrate how externally controlled variations in sediment supply can be obscured by internal processes. We show that surges in discharge on the main feeding river cannot be directly related to phases of deposition on the lobe. Furthermore, the repeat seafloor surveys and turbidity current measurements show how one or two beds on the lobe can represent an active system upstream that experiences many turbidity currents and tens of metres of erosion locally. This is an important consideration when using lobe deposits to reconstruct turbidity current frequency for geohazards, or past episodic events such as floods and

earthquakes (e.g. Mulder et al., 2001; St.-Onge et al., 2004; Moernaut et al., 2014). However, the impact of the largest scale flow events has not been captured by this thesis.

This thesis has made use of technological advances to better understand how submarine channels evolve and how sediment is transported through these systems. While many aspects of submarine channels remain unresolved, this thesis has provided a number of new insights into the dynamics of active systems, and it is hoped that the new models established here will be used as the basis for future studies that will further strengthen our understanding of these globally-important systems.

Bibliography

Adeogba, A.A., McHargue, T.R., and Graham, S.A., 2005, Transient fan architecture and depositional controls from near-surface 3-D seismic data, Niger Delta continental slope: AAPG Bulletin, v. 89, p. 627–643, doi: 10.1306/11200404025.

Allin, J.R., Hunt, J.E., Talling, P.J., Clare, M.A., Pope, E., and Masson, D.G., 2016, Different frequencies and triggers of canyon filling and flushing events in Nazaré Canyon, offshore Portugal: Marine Geology, v. 371, p. 89–105, doi: 10.1016/j.margeo.2015.11.005.

Armitage, D.A., Romans, B.W., Covault, J.A., and Graham, S.A., 2009, The influence of mass-transport-deposit surface topography on the evolution of turbidite architecture: The sierra contreras, tres pasos formation (Cretaceous), Southern Chile: Journal of Sedimentary Research, doi: 10.2110/jsr.2009.035.

Armitage, D.A., McHargue, T., Fildani, A., and Graham, S.A., 2012, Postavulsion channel evolution: Niger Delta continental slope: AAPG Bulletin, v. 96, p. 823–843, doi: 10.1306/09131110189.

Azaroff, A., Miossec, C., Lanceleur, L., Guyoneaud, R., and Monperrus, M., 2020, Priority and emerging micropollutants distribution from coastal to continental slope sediments: A case study of Capbreton Submarine Canyon (North Atlantic Ocean): Science of the Total Environment, v. 703, p. 135057, doi: 10.1016/j.scitotenv.2019.135057.

Azpiroz-Zabala, M., Cartigny, M.J.B., Talling, P.J., Parsons, D.R., Sumner, E.J., Clare, M.A., Simmons, S.M., Cooper, C., and Pope, E.L., 2017a, Newly recognized turbidity current structure can explain prolonged flushing of submarine canyons: Science Advances, v. 3, p. e1700200, doi: 10.1126/sciadv.1700200.

Azpiroz-Zabala, M., Cartigny, M.J.B., Sumner, E.J., Clare, M.A., Talling, P.J., Parsons, D.R., and Cooper, C., 2017b, A General Model for the Helical Structure of Geophysical Flows in Channel Bends: Geophysical Research Letters, v. 44, p. 11,932-11,941, doi: 10.1002/2017GL075721.

Babonneau, N., Savoye, B., Cremer, M., and Klein, B., 2002, Morphology and architecture of the present canyon and channel system of the Zaire deep-sea fan: Marine and Petroleum Geology, v. 19, p. 445–467, doi: 10.1016/S0264-8172(02)00009-0.

Babonneau, N., Savoye, B., Cremer, M., and Bez, M., 2004, Multiple terraces within the deep incised Zaire Valley (ZaïAngo Project): Are they confined levees? Geological Society Special

Publication, v. 222, p. 91–114, doi: 10.1144/GSL.SP.2004.222.01.06.

Bagnold, R.A., 1962, Auto-Suspension of Transported Sediment; Turbidity Currents: Proceedings of the Royal Society A: Mathematical, Physical and Engineering Sciences, v. 265, p. 315–319, doi: 10.1098/rspa.1962.0012.

Baudin, F., Disnar, J.-R., Martinez, P., and Dennielou, B., 2010, Distribution of the organic matter in the channel-levees systems of the Congo mud-rich deep-sea fan (West Africa). Implication for deep offshore petroleum source rocks and global carbon cycle: Marine and Petroleum Geology, v. 27, p. 995–1010, doi: 10.1016/J.MARPETGEO.2010.02.006.

Baudin, F., Stetten, E., Schnyder, J., Charlier, K., Martinez, P., Dennielou, B., and Droz, L., 2017, Origin and distribution of the organic matter in the distal lobe of the Congo deep-sea fan – A Rock-Eval survey: Deep-Sea Research Part II: Topical Studies in Oceanography, v. 142, p. 75–90, doi: 10.1016/j.dsr2.2017.01.008.

Beard, D.C., and Weyl, P.K., 1973, INFLUENCE OF TEXTURE ON POROSITY AND PERMEABILITY OF UNCONSOLIDATED SAND.: American Association of Petroleum Geologists Bulletin, v. 57, p. 349–369, doi: 10.1306/819a4272-16c5-11d7-8645000102c1865d.

Biscara, L., Hanquiez, V., Leynaud, D., Marieu, V., Mulder, T., Gallissaires, J.-M., Crespin, J.-P., Braccini, E., and Garlan, T., 2012, Submarine slide initiation and evolution offshore Pointe Odden, Gabon — Analysis from annual bathymetric data (2004–2009): Marine Geology, v. 299–302, p. 43–50, doi: 10.1016/J.MARGEO.2011.11.008.

Bornhold, B.D., Ren, P., and Prior, D.B., 1994, High-frequency turbidity currents in British Columbia fjords: Geo-Marine Letters, v. 14, p. 238–243, doi: 10.1007/BF01274059.

Bouma, A.H., 1962, Sedimentology of some Flysch deposits; a graphic approach to facies interpretation.: Amsterdam, Elsevier Pub. Co., https://searchworks.stanford.edu/view/1143766

Brice, S.E., Cochran, M.D., Pardo, G., and Edwards, A.D., 1982, Tectonics and Sedimentation of the South Atlantic Rift Sequence: Cabinda, Angola: Rifted Margins: Field Investigations of Margin Structure and Stratigraphy: Stud. Cont. Margin Geol., v. 34, p. 5–18, http://archives.datapages.com/data/specpubs/history2/data/a110/a110/0001/0000/0005.htm

Brucker, S., Hughes Clarke, J., Beaudoin, J., Lessels, C., Czotter, K., Loschiavo, R., Iwanowska, K., and Hill, P., 2007, Flood-related change on the Squamish Delta:,

http://www.omg.unb.ca/orig/omg/papers/Brucker_Steve_USHydro07.pdf

Bruschi, R., Bughi, S., Spinazzé, M., Torselletti, E., and Vitali, L., 2006, Impact of debris flows and turbidity currents on seafloor structures, in Norsk Geologisk Tidsskrift, v. 86, p. 317–336, https://njg.geologi.no/images/NJG_articles/60713_NGT_no_3_06_18.pdf.

Burbank, D.W., and Anderson, R.S. (Robert S., 2012, Tectonic geomorphology: J. Wiley & Sons, 454 p.

Burgess, P.M., Masiero, I., Toby, S.C., and Duller, R.A., 2019, A big fan of signals? Exploring autogenic and allogenic process and product in a numerical stratigraphic forward model of submarine-fan development: Journal of Sedimentary Research, v. 89, p. 1–12, doi: 10.2110/jsr.2019.3.

Canals, M., Puig, P., de Madron, X.D., Heussner, S., Palanques, A., and Fabres, J., 2006, Flushing submarine canyons: Nature, v. 444, p. 354–357, doi: 10.1038/nature05271.

Carlson, P.R., and Karl, H.A., 1988, Development of large submarine canyons in the Bering Sea, indicated by morphologic, seismic, and sedimentologic characteristics: Bulletin of the Geological Society of America, v. 100, p. 1594–1615, doi: 10.1130/0016-7606(1988)100<1594:DOLSCI>2.3.CO;2.

Carter, L., Carter, R.M., Nelson, C.S., Fulthorpe, C.S., and Neil, H.L., 1990, Evolution of Pliocene to Recent abyssal sediment waves on Bounty Channel levees, New Zealand: Marine Geology, v. 95, p. 97–109, doi: 10.1016/0025-3227(90)90043-J.

Carter, L., Burnett, D., Drew, S., Marle, G., Hagadorn, L., Bartlett-McNeil, D., and Irvine, N., 2009, Submarine cables and the oceans: connecting the world: v. 108, 206–209 p., doi: 10.1016/0016-0032(79)90434-4.

Carter, L., Gavey, R., Talling, P.J., and Liu, J.T., 2014, Insights into submarine geohazards from breaks in subsea telecommunication cables: Oceanography, v. 24, p. 58–67, doi: 10.5670/oceanog.2011.65.

Casalbore, D., Chiocci, F.L., Scarascia Mugnozza, G., Tommasi, P., and Sposato, A., 2011, Flash-flood hyperpycnal flows generating shallow-water landslides at Fiumara mouths in Western Messina Strait (Italy): Marine Geophysical Research, v. 32, p. 257–271, doi: 10.1007/s11001-011-9128-y.

Chiew, Y., 1991, Prediction of Maximum Scour Depth at Submarine Pipelines: Journal of Hydraulic Engineering, v. 117, p. 452–466, doi: 10.1061/(asce)0733-9429(1991)117:4(452).

Clare, M.A., Le Bas, T., Price, D.M., Hunt, J.E., Sear, D., Cartigny, M.J.B., Vellinga, A., Symons, W., Firth, C., and Cronin, S., 2018, Complex and Cascading Triggering of Submarine Landslides and Turbidity Currents at Volcanic Islands Revealed From Integration of High-Resolution Onshore and Offshore Surveys: Frontiers in Earth Science, v. 6, doi: 10.3389/feart.2018.00223.

Clare, M., Lintern, D.G., Rosenberger, K., Clarke, J.E.H., Paull, C., Gwiazda, R., Cartigny, M.J.B., Talling, P.J., Perara, D., Xu, J., Parsons, D., Jacinto, R.S., and Apprioual, R., 2020, Lessons learned from the monitoring of turbidity currents and guidance for future platform designs, in Geological Society Special Publication, doi: 10.1144/SP500-2019-173.

Clift, P., and Gaedicke, C., 2002, Accelerated mass flux to the Arabian Sea during the middle to late Miocene: Geology, v. 30, p. 207, doi: 10.1130/0091-7613(2002)030<0207:AMFTTA>2.0.CO;2.

Constantine, J.A., and Dunne, T., 2008, Meander cutoff and the controls on the production of oxbow lakes: Geology, v. 36, p. 23, doi: 10.1130/G24130A.1.

Conway, K.W., Barrie, J.V., Picard, K., and Bornhold, B.D., 2012, Submarine channel evolution: Active channels in fjords, British Columbia, Canada: Geo-Marine Letters, v. 32, p. 301–312, doi: 10.1007/s00367-012-0280-4.

Corella, J.P., Loizeau, J.L., le Dantec, N., Hilbe, M., Gerard, J., le Dantec, N., Stark, N., González-Quijano, M., and Girardclos, S., 2016, The role of mass-transport deposits and turbidites in shaping modern lacustrine deepwater channels: Marine and Petroleum Geology, v. 77, p. 515–525, doi: 10.1016/j.marpetgeo.2016.07.004.

Corney, R.K.T., Peakall, J., Parsons, D.R., Elliott, L., Amos, K.J., Best, J.L., Keevil, G.M., and Ingham, D.B., 2006, The orientation of helical flow in curved channels: Sedimentology, v. 53, p. 249–257, doi: 10.1111/j.1365-3091.2006.00771.x.

Covault, J.A., 2011, Submarine fans and canyon-channel systems: a review of processes, products, and models.: Nature Education Knowledge, v. 3, p. 4.

Covault, J.A., Kostic, S., Paull, C.K., Ryan, H.F., and Fildani, A., 2014, Submarine channel initiation, filling and maintenance from sea-floor geomorphology and morphodynamic modelling of cyclic steps: Sedimentology, v. 61, p. 1031–1054, doi: 10.1111/sed.12084.

Covault, J.A., Sylvester, Z., Hubbard, S.M., Jobe, Z.R., and Sech, R.P., 2016, The Stratigraphic Record of Submarine-Channel Evolution: The Sedimentary Record, v. 14, p. 4–11, doi:

10.2110/sedred.2016.3.4.

Covault, J.A., Kostic, S., Paull, C.K., Sylvester, Z., and Fildani, A., 2017, Cyclic steps and related supercritical bedforms: Building blocks of deep-water depositional systems, western North America: Marine Geology, v. 393, p. 4–20, doi: 10.1016/j.margeo.2016.12.009.

Covault, J.A., Sylvester, Z., Hudec, M.R., Ceyhan, C., and Dunlap, D., 2019, Submarine channels 'swept' downstream after bend cutoff in salt basins: The Depositional Record, p. dep2.75, doi: 10.1002/dep2.75.

Crosby, B.T., and Whipple, K.X., 2006, Knickpoint initiation and distribution within fluvial networks: 236 waterfalls in the Waipaoa River, North Island, New Zealand: Geomorphology, v. 82, p. 16–38, doi: 10.1016/j.geomorph.2005.08.023.

Curray, J.R., and Moore, D.G., 1971, Growth of the Bengal deep-sea fan and denudation in the Himalayas: Bulletin of the Geological Society of America, v. 82, p. 563–572, doi: 10.1130/0016-7606(1971)82[563:GOTBDF]2.0.CO;2.

Curray, J.R., Emmel, F.J., and Moore, D.G., 2002, The Bengal Fan: morphology, geometry, stratigraphy, history and processes: Marine and Petroleum Geology, v. 19, p. 1191–1223, doi: 10.1016/S0264-8172(03)00035-7.

Dalla Valle, G., and Gamberi, F., 2011, Slope channel formation, evolution and backfilling in a wide shelf, passive continental margin (Northeastern Sardinia slope, Central Tyrrhenian Sea): Marine Geology, v. 286, p. 95–105, doi: 10.1016/J.MARGEO.2011.06.005.

Daly, R.A., 1936, Origin of submarine canyons: American Journal of Science, v. s5-31, p. 401–420, doi: 10.2475/ajs.s5-31.186.401.

Damuth, J.E., 1983, Distributary channel meandering and bifurcation patterns on the Amazon deep-sea fan as revealed by long-range side-scan sonar (GLORIA).: Geology, v. 11, p. 94–98, doi: 10.1130/0091-7613(1983)11<94:DCMABP>2.0.CO;2.

Damuth, J.E., Flood, R.D., Kowsmann, R.O., Belderson, R.H., and Gorini, M.A., 1988, Anatomy and growth pattern of Amazon deep-sea fan as revealed by long-range side-scan sonar (GLORIA) and high-resolution seismic studies: AAPG Bull.; (United States), v. 72:8, https://www.osti.gov/biblio/5924498-anatomy-growth-pattern-amazon-deep-sea-fan-revealed-long-range-side-scan-sonar-gloria-high-resolution-seismic-studies.

Damuth, J.E., and Kumar, N., 1975, Amazon Cone: Morphology, Sediments, Age, and Growth Pattern: Bulletin of the Geological Society of America, v. 86, p. 863–878, doi: 10.1130/0016-

7606(1975)86<863:ACMSAA>2.0.CO;2.

Dennielou, B., Droz, L., Babonneau, N., Jacq, C., Bonnel, C., Picot, M., Le Saout, M., Saout, Y., Bez, M., Savoye, B., Olu, K., and Rabouille, C., 2017, Morphology, structure, composition and build-up processes of the active channel-mouth lobe complex of the Congo deep-sea fan with inputs from remotely operated underwater vehicle (ROV) multibeam and video surveys: Deep-Sea Research Part II: Topical Studies in Oceanography, v. 142, p. 25–49, doi: 10.1016/j.dsr2.2017.03.010.

Deptuck, M.E., Steffens, G.S., Barton, M., and Pirmez, C., 2003, Architecture and evolution of upper fan channel-belts on the Niger Delta slope and in the Arabian Sea: Marine and Petroleum Geology, v. 20, p. 649–676, doi: 10.1016/J.MARPETGEO.2003.01.004.

Deptuck, M.E., and Sylvester, Z., 2018, Submarine Fans and Their Channels, Levees, and Lobes, in Springer Geology, Springer, p. 273–299, doi: 10.1007/978-3-319-57852-1_15.

Dietrich, W.E., Smith, J.D., and Dunne, T., 1979, Flow and Sediment Transport in a Sand Bedded Meander: The Journal of Geology, v. 87, p. 305–315, doi: 10.1086/628419.

Droz, L., Rigaut, F., Cochonat, P., and Tofani, R., 1996, Morphology and recent evolution of the Zaire turbidite system (Gulf of Guinea): Bulletin of the Geological Society of America, v. 108, p. 253–269, doi: 10.1130/0016-7606(1996)108<0253:MAREOT>2.3.CO;2.

Droz, L., Marsset, T., Ondréas, H., Lopez, M., Savoye, B., and Spy-Anderson, F.L., 2003, Architecture of an active mud-rich turbidite system: The Zaire Fan (Congo-Angola margin southeast Atlantic): Results from ZaïAngo 1 and 2 cruises: American Association of Petroleum Geologists Bulletin, v. 87, p. 1145–1168, doi: 10.1306/03070300013.

Duller, R.A., Mountney, N.P., Russell, A.J., and Cassidy, N.C., 2008, Architectural analysis of a volcaniclastic jökulhlaup deposit, southern Iceland: Sedimentary evidence for supercritical flow: Sedimentology, v. 55, p. 939–964, doi: 10.1111/j.1365-3091.2007.00931.x.

Duller, R.A., Warner, N.H., McGonigle, C., De Angelis, S., Russell, A.J., and Mountney, N.P., 2014, Landscape reaction, response, and recovery following the catastrophic 1918 Katla jökulhlaup, southern Iceland: Geophysical Research Letters, v. 41, p. 4214–4221, doi: 10.1002/2014GL060090.

Estrada, F., Ercilla, G., and Alonso, B., 2005, Quantitative study of a Magdalena submarine channel (Caribbean Sea): implications for sedimentary dynamics: Marine and Petroleum Geology, v. 22, p. 623–635, doi: 10.1016/J.MARPETGEO.2005.01.004.

Farre, J.A., McGregor, B.A., Ryan, W.B.F., and Robb, J.M., 1983, Breaching the Shelfbreak: Passage from Youthful to Mature Phase in Submarine Canyon Evolution:

Ferguson, R.A., Kane, I.A., Eggenhuisen, J.T., Pohl, F., Tilston, M., Spychala, Y.T., and Brunt, R.L., 2020, Entangled external and internal controls on submarine fan evolution: an experimental perspective: The Depositional Record, doi: 10.1002/dep2.109.

Fernandez, R.L., Cantelli, A., Pirmez, C., Sequeiros, O., and Parker, G., 2014, Growth patterns of subaqueous depositional channel lobe systems developed over a basement with a downdip break in slope: Laboratory experiments: Journal of Sedimentary Research, v. 84, p. 168–182, doi: 10.2110/jsr.2014.10.

Fildani, A., Hubbard, S.M., Covault, J.A., Maier, K.L., Romans, B.W., Traer, M., and Rowland, J.C., 2013, Erosion at inception of deep-sea channels: Marine and Petroleum Geology, v. 41, p. 48–61, doi: 10.1016/J.MARPETGEO.2012.03.006.

Fildani, A., Normark, W.R., Kostic, S., and Parker, G., 2006, Channel formation by flow stripping: Large-scale scour features along the Monterey East Channel and their relation to sediment waves: Sedimentology, v. 53, p. 1265–1287, doi: 10.1111/j.1365-3091.2006.00812.x.

Fildani, A., Kostic, S., Covault, J.A., Maier, K.L., Caress, D.W., and Paull, C.K., 2020, Exploring a new breadth of cyclic steps on distal submarine fans: Sedimentology, p. sed.12803, doi: 10.1111/sed.12803.

Finkl, C.W., and Khalil, S.M., 2005, Vibracore, in Schwartz, M.L. ed., The Encyclopedia of Coastal Science, Kluwer Academic, Dordrecht, The Netherlands, p. 1272–12848.

Flood, R.D., Manley, P.L., Kowsmann, R.O., Appi, C.J., and Pirmez, C., 1991, Seismic Facies and Late Quaternary Growth of Amazon Submarine Fan, in Springer, New York, NY, p. 415–433, doi: 10.1007/978-1-4684-8276-8_23.

Foreman, B.Z., and Straub, K.M., 2017, Autogenic geomorphic processes determine the resolution and fidelity of terrestrial paleoclimate records: Science Advances, v. 3, p. e1700683, doi: 10.1126/sciadv.1700683.

France-Lanord, C., Derry, L., and Michard, A., 1993, Evolution of the Himalaya since Miocene time: Isotopic and sedimentological evidence from the Bengal Fan: Geological Society Special Publication, v. 74, p. 603–621, doi: 10.1144/GSL.SP.1993.074.01.40.

Gales, J.A., Talling, P.J., Cartigny, M.J.B., Hughes Clarke, J., Lintern, G., Stacey, C., and Clare, M.A., 2019, What controls submarine channel development and the morphology of deltas

entering deep-water fjords? Earth Surface Processes and Landforms, v. 44, p. 535–551, doi: 10.1002/esp.4515.

Galy, V., France-Lanord, C., Beyssac, O., Faure, P., Kudrass, H., and Palhol, F., 2007, Efficient organic carbon burial in the Bengal fan sustained by the Himalayan erosional system: Nature, v. 450, p. 407–410, doi: 10.1038/nature06273.

Gardner, T.W., 1983, Experimental study of knickpoint and longitudinal profile evolution in cohesive, homogeneous material.: Geological Society of America Bulletin, v. 94, p. 664–572, doi: 10.1130/0016-7606(1983)94<664:ESOKAL>2.0.CO;2.

Gardner, J., Bohannon, R., Field, M., and Masson, D., 2010, The Morphology, Processes, and Evolution of Monterey Fan: A Revisit, in Geology of the United States' Seafloor, p. 193–220, doi: 10.1017/cbo9780511529481.017.

Gee, M.J.R., and Gawthorpe, R.L., 2006, Submarine channels controlled by salt tectonics: Examples from 3D seismic data offshore Angola: Marine and Petroleum Geology, v. 23, p. 443–458, doi: 10.1016/J.MARPETGEO.2006.01.002.

Gnibidenko, H.S., and Svarichevskaya, L. V., 1984, The submarine canyons of Kamchatka: Marine Geology, v. 54, p. 277–307, doi: 10.1016/0025-3227(84)90043-4.

Greene, H.G., Maher, N.M., and Paull, C.K., 2002, Physiography of the Monterey Bay National Marine Sanctuary and implications about continental margin development: Marine Geology, v. 181, p. 55–82, doi: 10.1016/S0025-3227(01)00261-4.

Gregory, J.W., 1931, A Submarine Trough off the Coast of Cyprus: The Geographical Journal, v. 78, p. 357, doi: 10.2307/1784754.

Guiastrennec-Faugas, L., Gillet, H., Silva Jacinto, R., Dennielou, B., Hanquiez, V., Schmidt, S., Simplet, L., and Rousset, A., 2020a, Upstream migrating knickpoints and related sedimentary processes in a submarine canyon from a rare 20-year morphobathymetric time-lapse (Capbreton submarine canyon, Bay of Biscay, France): Marine Geology, v. 423, p. 106143, doi: 10.1016/j.margeo.2020.106143.

Guiastrennec-Faugas, L., Gillet, H., Peakall, J., Dennielou, B., Gaillot, A., and Silva Jacinto, R., 2020b, Initiation and evolution of knickpoints and their role in cut-and-fill processes in active submarine channels: Geology, v. 1, doi: 10.1130/g48369.1.

de Haas, T., Van Den Berg, W., Braat, L., and Kleinhans, M.G., 2016, Autogenic avulsion, channelization and backfilling dynamics of debris-flow fans: Sedimentology, v. 63, p. 1596–

1619, doi: 10.1111/sed.12275.

Hage, S., Cartigny, M.J.B., Clare, M.A., Sumner, E.J., Vendettuoli, D., Hughes Clarke, J.E., Hubbard, S.M., Talling, P.J., Lintern, D.G., Stacey, C.D., Englert, R.G., Vardy, M.E., Hunt, J.E., Yokokawa, M., et al., 2018, How to recognize crescentic bedforms formed by supercritical turbidity currents in the geologic record: Insights from active submarine channels: Geology, v. 46, p. 563–566, doi: 10.1130/G40095.1.

Hage, S., Cartigny, M.J.B., Sumner, E.J., Clare, M.A., Hughes Clarke, J.E., Talling, P.J., Lintern, D.G., Simmons, S.M., Silva Jacinto, R., Vellinga, A.J., Allin, J.R., Azpiroz-Zabala, M., Gales, J.A., Hizzett, J.L., et al., 2019, Direct Monitoring Reveals Initiation of Turbidity Currents From Extremely Dilute River Plumes: Geophysical Research Letters, v. 46, p. 11310–11320, doi: 10.1029/2019GL084526.

Hage, S., Galy, V.V., Cartigny, M.J.B., Acikalin, S., Clare, M.A., Gröcke, D.R., Hilton, R.G., Hunt, J.E., Lintern, D.G., McGhee, C.A., Parsons, D.R., Stacey, C.D., Sumner, E.J., and Talling, P.J., 2020, Efficient preservation of young terrestrial organic carbon in sandy turbidity-current deposits: Geology, doi: 10.1130/g47320.1.

Hagen, R.A., Vergara, H., and Naar, D.F., 1996, Morphology of San Antonio submarine canyon on the central Chile forearc: Marine Geology, v. 129, p. 197–205, doi: 10.1016/0025-3227(96)83345-7.

Hansen, L., Janocko, M., Kane, I., and Kneller, B., 2017, Submarine channel evolution, terrace development, and preservation of intra-channel thin-bedded turbidites: Mahin and Avon channels, offshore Nigeria: Marine Geology, v. 383, p. 146–167, doi: 10.1016/j.margeo.2016.11.011.

Harris, P.T., and Whiteway, T., 2011, Global distribution of large submarine canyons: Geomorphic differences between active and passive continental margins: Marine Geology, v. 285, p. 69–86, doi: 10.1016/j.margeo.2011.05.008.

Hay, A.E., Burling, R.W., and Murray, J.W., 1982, Remote acoustic detection of a turbidity current surge: Science, doi: 10.1126/science.217.4562.833.

Hayakawa, Y., and Matsukura, Y., 2003, Recession rates of waterfalls in Boso Peninsula, Japan, and a predictive equation: Earth Surface Processes and Landforms, v. 28, p. 675–684, doi: 10.1002/esp.519.

He, Y., Zhong, G., Wang, L., and Kuang, Z., 2014, Characteristics and occurrence of submarine

canyon-associated landslides in the middle of the northern continental slope, South China Sea: Marine and Petroleum Geology, v. 57, p. 546–560, doi: 10.1016/j.marpetgeo.2014.07.003.

Heerema, C.J., Talling, P.J., Cartigny, M.J., Paull, C.K., Bailey, L., Simmons, S.M., Parsons, D.R., Clare, M.A., Gwiazda, R., Lundsten, E., Anderson, K., Maier, K.L., Xu, J.P., Sumner, E.J., et al., 2020, What determines the downstream evolution of turbidity currents? Earth and Planetary Science Letters, v. 532, p. 116023, doi: 10.1016/j.epsl.2019.116023.

Heezen, B.C., and Ewing, M., 1952, Turbidity currents and submarine slumps, and the 1929 Grand Banks Earthquake: American Journal of Science, v. 250, p. 849–873, doi: 10.2475/ajs.250.12.849.

Heezen, B.C., Ewing, M., and Menzies, R.J., 1955, The Influence of Submarine Turbidity Currents on Abyssal Productivity: Oikos, v. 6, p. 170, doi: 10.2307/3564853.

Heezen, B.C., Menzies, R.J., Schneider, E.D., Ewing, W.M., and Graneli, N.C.L., 1964, Congo Submarine Canyon: AAPG Bulletin, v. 48, p. 1126–1149, http://archives.datapages.com/data/bulletns/1961-64/data/pg/0048/0007/1100/1126.htm?doi=10.1306%2FBC743D7F-16BE-11D7-8645000102C1865D#purchaseoptions.

Heijnen, M.S., Clare, M.A., Cartigny, M.J.B., Talling, P.J., Hage, S., Lintern, D.G., Stacey, C., Parsons, D.R., Simmons, S.M., Chen, Y., Sumner, E.J., Dix, J.K., and Hughes Clarke, J.E., 2020, Rapidly-migrating and internally-generated knickpoints can control submarine channel evolution: Nature Communications, v. 11, doi: 10.1038/s41467-020-16861-x.

van Heijst, M.W.I.M., and Postma, G., 2001, Fluvial response to sea-level changes: a quantitative analogue, experimental approach: Basin Research, v. 13, p. 269–292, doi: 10.1046/j.1365-2117.2001.00149.x.

Heiniö, P., and Davies, R.J., 2007, Knickpoint migration in submarine channels in response to fold growth, western Niger Delta: Marine and Petroleum Geology, v. 24, p. 434–449, doi: 10.1016/j.marpetgeo.2006.09.002.

Heiniö, P., and Davies, R.J., 2009, Trails of depressions and sediment waves along submarine channels on the continental margin of Espirito Santo Basin, Brazil: Bulletin of the Geological Society of America, v. 121, p. 698–711, doi: 10.1130/B26190.1.

Henry W. Menard, J. (2), 1955, Deep-Sea Channels, Topography, and Sedimentation: AAPG

Bulletin, v. 39, p. 236–255, doi: 10.1306/5ceae136-16bb-11d7-8645000102c1865d.

Hickin, E.J., 1974, The development of meanders in natural river-channels: American Journal of Science, v. 274, p. 414–442, doi: 10.2475/ajs.274.4.414.

Hill, P.R., 2013, Changes in Submarine Channel Morphology and Slope Sedimentation Patterns from Repeat Multibeam Surveys in the Fraser River Delta, Western Canada, in Sediments, Morphology and Sedimentary Processes on Continental Shelves, Chichester, West Sussex, UK, John Wiley & Sons, Ltd, p. 47–69, doi: 10.1002/9781118311172.ch3.

Hizzett, J.L., Hughes Clarke, J.E., Sumner, E.J., Cartigny, M.J.B., Talling, P.J., and Clare, M.A., 2018, Which Triggers Produce the Most Erosive, Frequent, and Longest Runout Turbidity Currents on Deltas? Geophysical Research Letters, v. 45, p. 855–863, doi: 10.1002/2017GL075751.

Hodgson, D.M., Kane, I.A., Flint, S.S., Brunt, R.L., and Ortiz-Karpf, A., 2016, Time-Transgressive Confinement On the Slope and the Progradation of Basin-Floor Fans: Implications For the Sequence Stratigraphy of Deep-Water Deposits: Journal of Sedimentary Research, v. 86, p. 73–86, doi: 10.2110/jsr.2016.3.

Holland, W.N., and Pickup, G., 1976, Flume study of knickpoint development in stratified sediment: Bulletin of the Geological Society of America, v. 87, p. 76–82, doi: 10.1130/0016-7606(1976)87<76:FSOKDI>2.0.CO;2.

Houston, J., Butcher, A., Ehren, P., Evans, K., and Godfrey, L., 2011, The evaluation of brine prospects and the requirement for modifications to filing standards: Economic Geology, v. 106, p. 1125–1239, doi: 10.2113/econgeo.106.7.1225.

Howard, A.D., Dietrich, W.E., and Seidl, M.A., 1994, Modeling fluvial erosion on regional to continental scales: Journal of Geophysical Research: Solid Earth, v. 99, p. 13971–13986, doi: 10.1029/94JB00744.

Hubbard, S.M., Covault, J.A., Fildani, A., and Romans, B.W., 2014, Sediment transfer and deposition in slope channels: Deciphering the record of enigmatic deep-sea processes from outcrop: Geological Society of America Bulletin, v. 126, p. 857–871, doi: 10.1130/B30996.1.

Hubbard, S.M., Jobe, Z.R., Romans, B.W., Covault, J.A., Sylvester, Z., and Fildani, A., 2020, The stratigraphic evolution of a submarine channel: Linking seafloor dynamics to depositional products: Journal of Sedimentary Research, v. 90, p. 673–686, doi: 10.2110/jsr.2020.36.

Hübscher, C., Spieß, V., Breitzke, M., and Weber, M.E., 1997, The youngest channel-levee system of the Bengal Fan: Results from digital sediment echosounder data: Marine Geology, v. 141,

p. 125–145, doi: 10.1016/S0025-3227(97)00066-2.

Hughes Clarke, J.E., Brucker, S., Hill, P., and Conway, K., 2009, Monitoring morphological evolution of fjord deltas in temperate and Arctic regions, in Rendiconti Online Societa Geologica Italiana, v. 7, p. 147–150.

Hughes Clarke, J.E., Brucker, S., Muggah, J., Hamilton, T., Cartwright, D., Church, I., and Kuus, P., 2012, Temporal progression and spatial extent of mass wasting events on the Squamish prodelta slope, in Landslides and Engineered Slopes: Protecting Society through Improved Understanding - Proceedings of the 11th International and 2nd North American Symposium on Landslides and Engineered Slopes, 2012, p. 1091–1096, http://citeseerx.ist.psu.edu/viewdoc/download?doi=10.1.1.459.4289&rep=rep1&type=pdf.

Hughes Clarke, J.E., Vidiera Marques, C.R., and Pratomo, D., 2014, Imaging active mass-wasting and sediment flows on a Fjord Delta, Squamish, British Columbia, in Submarine Mass Movements and Their Consequences, 6th International Symposium, Kluwer Academic Publishers, p. 249–260, doi: 10.1007/978-3-319-00972-8_22.

Hughes-Clarke, J.E., Muggah, J., Renoud, W., Bell, T., Forbes, D.L., Cowan, B., and Kennedy, J., 2015, Reconnaissance seabed mapping around Hall and Cumberland peninsulas , Nunavut : opening up southeastern Baffin Island to nearshore geological investigations: Summary of Activities 2014, p. 133–144, https://scholars.unh.edu/ccom/1375/

Hughes Clarke, J.E., Vidiera Marques, C.R., and Pratomo, D., 2016, Imaging active mass-wasting and sediment flows on a Fjord Delta, Squamish, British Columbia, in Submarine Mass Movements and Their Consequences, 6th International Symposium, Springer, Cham, p. 249–260, doi: 10.1007/978-3-319-00972-8_22.

Hughes Clarke, J.E., 2016, First wide-angle view of channelized turbidity currents links migrating cyclic steps to flow characteristics: Nature Communications, v. 7, p. 1–13, doi: 10.1038/ncomms11896.

Hughes Clarke, J.E., 2018a, Multibeam Echosounders, in Springer Geology, Springer, p. 25–41, doi: 10.1007/978-3-319-57852-1_3.

Hughes Clarke, J.E., 2018b, The impact of acoustic imaging geometry on the fidelity of seabed bathymetric models: Geosciences (Switzerland), doi: 10.3390/geosciences8040109.

Huvenne, V.A.I., Robert, K., Marsh, L., Lo Iacono, C., Le Bas, T., and Wynn, R.B., 2018, ROVs and AUVs, in Springer Geology, doi: 10.1007/978-3-319-57852-1_7.

Huyghe, P., Foata, M., Deville, E., Mascle, G., and Group, C.W., 2004, Channel profiles through the active thrust front of the southern Barbados prism: Geology, v. 32, p. 429–432, doi: 10.1130/g20000.1.

Imran, J., Parker, G., and Katopodes, N., 1998, A numerical model of channel inception on submarine fans: Journal of Geophysical Research: Oceans, v. 103, p. 1219–1238, doi: 10.1029/97jc01721.

Imran, J., Islam, M.A., Huang, H., Kassem, A., Dickerson, J., Pirmez, C., and Parker, G., 2007, Helical flow couplets in submarine gravity underflows: Geology, v. 35, p. 659–662, doi: 10.1130/G23780A.1.

Inman, D.L., Nordstrom, C.E., and Flick, R.E., 1976, Currents in Submarine Canyons: An Air-Sea-Land Interaction: Annual Review of Fluid Mechanics, v. 8, p. 275–310, doi: 10.1146/annurev.fl.08.010176.001423.

Iverson, R.M., Reid, M.E., Logan, M., LaHusen, R.G., Godt, J.W., and Griswold, J.P., 2011, Positive feedback and momentum growth during debris-flow entrainment of wet bed sediment: Nature Geoscience, v. 4, p. 116–121, doi: 10.1038/ngeo1040.

Jerolmack, D.J., and Paola, C., 2010, Shredding of environmental signals by sediment transport: Geophysical Research Letters, v. 37, doi: 10.1029/2010GL044638.

Jobe, Z.R., Howes, N.C., and Auchter, N.C., 2016, Comparing submarine and fluvial channel kinematics: Implications for stratigraphic architecture: Geology, v. 44, p. 931–934, doi: 10.1130/G38158.1.

Jobe, Z.R., Howes, N., Romans, B.W., and Covault, J.A., 2018, Volume and recurrence of submarine-fan-building turbidity currents: The Depositional Record, v. 4, p. 160–176, doi: 10.1002/dep2.42.

Kane, I.A., and Hodgson, D.M., 2011, Sedimentological criteria to differentiate submarine channel levee subenvironments: Exhumed examples from the Rosario Fm. (Upper Cretaceous) of Baja California, Mexico, and the Fort Brown Fm. (Permian), Karoo Basin, S. Africa: Marine and Petroleum Geology, v. 28, p. 807–823, doi: 10.1016/j.marpetgeo.2010.05.009.

Kane, I.A., and Clare, M.A., 2019, Dispersion, Accumulation, and the Ultimate Fate of Microplastics in Deep-Marine Environments: A Review and Future Directions: Frontiers in Earth Science, v. 7, p. 80, doi: 10.3389/feart.2019.00080.

Kane, I.A., Clare, M.A., Miramontes, E., Wogelius, R., Rothwell, J.J., Garreau, P., and Pohl, F., 2020,

Seafloor microplastic hotspots controlled by deep-sea circulation: Science, v. 368, p. 1140–1145, doi: 10.1126/science.aba5899.

Kelner, M., Migeon, S., Tric, E., Couboulex, F., Dano, A., Lebourg, T., and Taboada, A., 2016, Frequency and triggering of small-scale submarine landslides on decadal timescales: Analysis of 4D bathymetric data from the continental slope offshore Nice (France): Marine Geology, v. 379, p. 281–297, doi: 10.1016/J.MARGEO.2016.06.009.

Khripounoff, A., Vangriesheim, A., Babonneau, N., Crassous, P., Dennielou, B., and Savoye, B., 2003, Direct observation of intense turbidity current activity in the Zaire submarine valley at 4000 m water depth: Marine Geology, v. 194, p. 151–158, doi: 10.1016/S0025-3227(02)00677-1.

Khripounoff, A., Vangriesheim, A., Crassous, P., and Etoubleau, J., 2009, High frequency of sediment gravity flow events in the Var submarine canyon (Mediterranean Sea): Marine Geology, v. 263, p. 1–6, doi: 10.1016/J.MARGEO.2009.03.014.

Knudson, K.P., and Hendy, I.L., 2009, Climatic influences on sediment deposition and turbidite frequency in the Nitinat Fan, British Columbia: Marine Geology, v. 262, p. 29–38, doi: 10.1016/j.margeo.2009.03.002.

Kodagali, V.N., and Jauhari, P., 1999, The meandering Indus channels: Study in a small area by the multibeam swath bathymetry system - Hydrosweep: Current Science, v. 76, p. 240–243, https://www.jstor.org/stable/24101246.

Kolla, V., and Coumes, F., 1987, Morphology, internal structure, seismic stratigraphy, and sedimentation of Indus Fan: American Association of Petroleum Geologists Bulletin, v. 71, p. 650–677, doi: 10.1306/94887889-1704-11d7-8645000102c1865d.

Kolla, V., Bandyopadhyay, A., Gupta, P., Mukherjee, B., and V.Ramana, D., 2012, Morphology and Internal Structure of a Recent Upper Bengal Fan-Valley Complex, in Application of the Principles of Seismic Geomorphology to Continental-Slope and Base-of-Slope Systems: Case Studies from Seafloor and Near-Seafloor Analogues, p. 347–369, doi: 10.2110/pec.12.99.0347.

Komar, P.D., 1971, Hydraulic jumps in turbidity currents: Bulletin of the Geological Society of America, v. 82, p. 1477–1488, doi: 10.1130/0016-7606(1971)82[1477:HJITC]2.0.CO;2.

Kuenen, P.H., 1937, Experiments in connection with Daly's hypothesis on the formation of submarine canyons: Leidsche Geol. Meded., v. 8, p. 327–351,

https://ci.nii.ac.jp/naid/10018293062/.

Kuenen, P.H., and Migliorini, C.I., 1950, Turbidity Currents as a Cause of Graded Bedding: The Journal of Geology, v. 58, p. 91–127, doi: 10.1086/625710.

Lamb, M.P., Parsons, J.D., Mullenbach, B.L., Finlayson, D.P., Orange, D.L., and Nittrouer, C.A., 2008, Evidence for superelevation, channel incision, and formation of cyclic steps by turbidity currents in Eel Canyon, California: Bulletin of the Geological Society of America, v. 120, p. 463–475, doi: 10.1130/B26184.1.

de Leeuw, J., Eggenhuisen, J.T., and Cartigny, M.J.B., 2016, Morphodynamics of submarine channel inception revealed by new experimental approach: Nature Communications, v. 7, p. 10886, doi: 10.1038/ncomms10886.

De Leo, F.C., Smith, C.R., Rowden, A.A., Bowden, D.A., and Clark, M.R., 2010, Submarine canyons: hotspots of benthic biomass and productivity in the deep sea: royalsocietypublishing.org, v. 277, p. 2783–2792, doi: 10.1098/rspb.2010.0462.

Levoy, F., Anthony, E.J., Monfort, O., Robin, N., and Bretel, P., 2013, Formation and migration of transverse bars along a tidal sandy coast deduced from multi-temporal Lidar datasets: Marine Geology, v. 342, p. 39–52, doi: 10.1016/j.margeo.2013.06.007.

Lewis, G.W., and Lewin, J., 2009, Alluvial Cutoffs in Wales and the Borderlands, in Modern and Ancient Fluvial Systems, Oxford, UK, Blackwell Publishing Ltd., p. 145–154, doi: 10.1002/9781444303773.ch11.

Locat, J., and Sanfaçon, R., 2000, Multibeam surveys: a major tool for geosciences Seafloor Geomorphology Using Multibeam Techniques, in Proceedings of the Canadian Hydraugraphics Conference, p. 1–11.

Lonergan, L., Jamin, N.H., Jackson, C.A.L., and Johnson, H.D., 2013, U-shaped slope gully systems and sediment waves on the passive margin of gabon (west africa): Marine Geology, v. 337, p. 80–97, doi: 10.1016/j.margeo.2013.02.001.

Maier, K.L., Fildani, A., McHargue, T.R., Paull, C.K., Graham, S.A., and Caress, D.W., 2012, Punctuated Deep-Water Channel Migration: High-Resolution Subsurface Data from the Lucia Chica Channel System, Offshore California, U.S.A: Journal of Sedimentary Research, v. 82, p. 1–8, doi: 10.2110/jsr.2012.10.

Maier, K.L., Fildani, A., Paull, C.K., McHargue, T.R., Graham, S.A., and Caress, D.W., 2013, Deep-sea channel evolution and stratigraphic architecture from inception to abandonment from high-

resolution Autonomous Underwater Vehicle surveys offshore central California (P. Talling, Ed.): Sedimentology, v. 60, p. 935–960, doi: 10.1111/j.1365-3091.2012.01371.x.

Maier, K.L., Paull, C.K., Caress, D.W., Anderson, K., Nieminski, N.M., Lundsten, E., Erwin, B.E., Gwiazda, R., and Fildani, A., 2020, Submarine-fan development revealed by integrated high-resolution datasets from La Jolla fan, offshore California, U.S.A.: Journal of Sedimentary Research, v. 90, p. 468–479, doi: 10.2110/jsr.2020.22.

Marín, L., Forman, S.L., Valdez, A., and Bunch, F., 2005, Twentieth century dune migration at the Great Sand Dunes National Park and Preserve, Colorado, relation to drought variability: Geomorphology, v. 70, p. 163–183, doi: 10.1016/j.geomorph.2005.04.014.

Marton, G.L., Taril, G.C., and Lehmann, C.T., 2000, Evolution of the angolan passive margin, West Africa, with emphasis on post-salt structural styles, in Geophysical Monograph Series, v. 115, p. 129–149, doi: 10.1029/GM115p0129.

Masson, D.G., Huvenne, V.A.I., de Stigter, H.C., Wolff, G.A., Kiriakoulakis, K., Arzola, R.G., and Blackbird, S., 2010, Efficient burial of carbon in a submarine canyon: Geology, v. 38, p. 831–834, doi: 10.1130/G30895.1.

Masson, D.G., Arzola, R.G., Wynn, R.B., Hunt, J.E., and Weaver, P.P.E., 2011, Seismic triggering of landslides and turbidity currents offshore Portugal: Geochemistry, Geophysics, Geosystems, v. 12, p. n/a-n/a, doi: 10.1029/2011GC003839.

Mastbergen, D., van den Ham, G., Cartigny, M., Koelewijn, A., de Kleine, M., Clare, M., Hizzett, J., Azpiroz, M., and Vellinga, A., 2016, Multiple flow slide experiment in the Westerschelde estuary, The Netherlands, in Advances in Natural and Technological Hazards Research, Springer, Cham, v. 41, p. 241–249, doi: 10.1007/978-3-319-20979-1_24.

Mayall, M., Jones, E., and Casey, M., 2006, Turbidite channel reservoirs—Key elements in facies prediction and effective development: Marine and Petroleum Geology, v. 23, p. 821–841, doi: 10.1016/J.MARPETGEO.2006.08.001.

Mazières, A., Gillet, H., Castelle, B., Mulder, T., Guyot, C., Garlan, T., and Mallet, C., 2014, High-resolution morphobathymetric analysis and evolution of Capbreton submarine canyon head (Southeast Bay of Biscay-French Atlantic Coast) over the last decade using descriptive and numerical modeling: Marine Geology, v. 351, p. 1–12, doi: 10.1016/j.margeo.2014.03.001.

McArthur, A.D., Gamberi, F., Kneller, B.C., Wakefield, M.I., Souza, P.A., and Kuchle, J., 2017, Palynofacies classification of submarine fan depositional environments: Outcrop examples

from the Marnoso-Arenacea Formation, Italy: Marine and Petroleum Geology, v. 88, p. 181–199, doi: 10.1016/j.marpetgeo.2017.08.018.

McHargue, T., Pyrcz, M.J., Sullivan, M.D., Clark, J.D., Fildani, A., Romans, B.W., Covault, J.A., Levy, M., Posamentier, H.W., and Drinkwater, N.J., 2011, Architecture of turbidite channel systems on the continental slope: Patterns and predictions: Marine and Petroleum Geology, v. 28, p. 728–743, doi: 10.1016/j.marpetgeo.2010.07.008.

Micallef, A., Ribó, M., Canals, M., Puig, P., Lastras, G., and Tubau, X., 2014, Space-for-time substitution and the evolution of a submarine canyon-channel system in a passive progradational margin: Geomorphology, v. 221, p. 34–50, doi: 10.1016/j.geomorph.2014.06.008.

Migeon, S., Savoye, B., and Faugeres, J.C., 2000, Quaternary development of migrating sediment waves in the Var deep-sea fan: Distribution, growth pattern, and implication for levee evolution: Sedimentary Geology, v. 133, p. 265–293, doi: 10.1016/S0037-0738(00)00043-9.

Milliman, J.D., and Farnsworth, K.L., 2011, Runoff, erosion, and delivery to the coastal ocean, in River Discharge to the Coastal Ocean, doi: 10.1017/cbo9780511781247.003.

Mitchell, N.C., 2004, Form of submarine erosion from confluences in Atlantic USA continental slope Canyons: American Journal of Science, v. 304, p. 590–611, doi: 10.2475/ajs.304.7.590.

Mitchell, N.C., 2006, Morphologies of knickpoints in submarine canyons: Bulletin of the Geological Society of America, v. 118, p. 589–605, doi: 10.1130/B25772.1.

Moernaut, J., Van Daele, M., Heirman, K., Fontijn, K., Strasser, M., Pino, M., Urrutia, R., and De Batist, M., 2014, Lacustrine turbidites as a tool for quantitative earthquake reconstruction: New evidence for a variable rupture mode in south central Chile: Journal of Geophysical Research: Solid Earth, v. 119, p. 1607–1633, doi: 10.1002/2013JB010738.

Mountjoy, J.J., Howarth, J.D., Orpin, A.R., Barnes, P.M., Bowden, D.A., Rowden, A.A., Schimel, A.C.G., Holden, C., Horgan, H.J., Nodder, S.D., Patton, J.R., Lamarche, G., Gerstenberger, M., Micallef, A., et al., 2018, Earthquakes drive large-scale submarine canyon development and sediment supply to deep-ocean basins: Science Advances, v. 4, p. eaar3748, doi: 10.1126/sciadv.aar3748.

Mulder, T., Migeon, S., Savoye, B., and Faugères, J., 2001, Inversely graded turbidite sequences in the deep Mediterranean: A record of deposits from flood-generated turbidity currents? Geo-Marine Letters, v. 21, p. 86–93, doi: 10.1007/s003670100071.

Mutti, E., and Normark, W.R., 1987, Comparing Examples of Modern and Ancient Turbidite Systems: Problems and Concepts, in Marine Clastic Sedimentology, Springer Netherlands, p. 1–38, doi: 10.1007/978-94-009-3241-8_1.

Nakajima, R., Yoshida, T., Azman, B.A.R., Zaleha, K., Othman, B.H.R., and Toda, T., 2009, In situ release of coral mucus by Acropora and its influence on the heterotrophic bacteria: Aquatic Ecology, v. 43, p. 815–823, doi: 10.1007/s10452-008-9210-y.

Nesbit, P.R., Hubbard, S.M., Daniels, B.G., Bell, D., Englert, R.G., and Hugenholtz, C.H., 2021, Digital re-evaluation of down-dip channel-fill architecture in deep-water slope deposits: multi-scale perspectives from UAV-SfM: The Depositional Record, p. dep2.137, doi: 10.1002/dep2.137.

Normandeau, A., Lajeunesse, P., St-Onge, G., Bourgault, D., Drouin, S.S.-O., Senneville, S., and Bélanger, S., 2014, Morphodynamics in sediment-starved inner-shelf submarine canyons (Lower St. Lawrence Estuary, Eastern Canada): Marine Geology, v. 357, p. 243–255, doi: 10.1016/J.MARGEO.2014.08.012.

Normandeau, A., Dietrich, P., Hughes Clarke, J., Van Wychen, W., Lajeunesse, P., Burgess, D., and Ghienne, J. -F., 2019, Retreat Pattern of Glaciers Controls the Occurrence of Turbidity Currents on High-Latitude Fjord Deltas (Eastern Baffin Island): Journal of Geophysical Research: Earth Surface, v. 124, p. 1559–1571, doi: 10.1029/2018JF004970.

Normandeau, A., Bourgault, D., Neumeier, U., Lajeunesse, P., St-Onge, G., Gostiaux, L., and Chavanne, C., 2020, Storm-induced turbidity currents on a sediment-starved shelf: Insight from direct monitoring and repeat seabed mapping of upslope migrating bedforms (F. Felletti, Ed.): Sedimentology, v. 67, p. 1045–1068, doi: 10.1111/sed.12673.

Normark, W.R., 1970, Growth Patterns of Deep-Sea Fans: AAPG Bulletin, v. 54, p. 2170–2195, http://archives.datapages.com/data/bulletns/1968-70/data/pg/0054/0011/2150/2170.htm

Normark, W.R., 1978, Fan Valleys, Channels, and Depositional Lobes on Modern Submarine Fans: Characters for Recognition of Sandy Turbidite Environments: AAPG Bulletin, v. 62, p. 912–931, doi: 10.1306/c1ea4f72-16c9-11d7-8645000102c1865d.

Normark, W.R., and Piper, D.J.W., 1991, Initiation processes and flow evolution of turbidity currents: implications for the depositional record: From shoreline to abyss: contributions in marine geology in honor of Francis Parker Shepard, p. 207–230, http://archives.datapages.com/data/sepm_sp/SP46/Initiation_Processes_and_Flow.htm

Normark, W.R., and Carlson, P.R., 2003, Giant submarine canyons: Is size any clue to their importance in the rock record? Special Paper of the Geological Society of America, v. 370, p. 175–190, doi: 10.1130/0-8137-2370-1.175.

Nyberg, B., Helland-Hansen, W., Gawthorpe, R.L., Sandbakken, P., Eide, C.H., Sømme, T., Hadler-Jacobsen, F., and Leiknes, S., 2018, Revisiting morphological relationships of modern source-to-sink segments as a first-order approach to scale ancient sedimentary systems: Sedimentary Geology, v. 373, p. 111–133, doi: 10.1016/J.SEDGEO.2018.06.007.

Pantin, H.M., 1979, Interaction between velocity and effective density in turbidity flow: Phase-plane analysis, with criteria for autosuspension: Marine Geology, v. 31, p. 59–99, doi: 10.1016/0025-3227(79)90057-4.

Paola, C., 2016, A mind of their own: Recent advances in autogenic dynamics in rivers and deltas: SEPM Special Publications, v. 106, p. 5–17, doi: 10.2110/sepmsp.106.04.

Parker, G., 1982, Conditions for the ignition of catastrophically erosive turbidity currents: Marine Geology, v. 46, p. 307–327, doi: 10.1016/0025-3227(82)90086-X.

Parker, G., Diplas, P., and Akiyama, J., 1983, Meander Bends of High Amplitude: Journal of Hydraulic Engineering, v. 109, p. 1323–1337, doi: 10.1061/(ASCE)0733-9429(1983)109:10(1323).

Parker, G., and Andrews, E., 1986, On the time developmentof meander bends: Journal of Fluid Mechanics, v. 162, p. 139–156, doi: 10.1017/S0022112086001970.

Parker, G., Pantin, H.M., and Fukushima, Y., 1986, Self-accelerating turbidity currents.: cambridge.org, https://www.cambridge.org/core/journals/journal-of-fluid-mechanics/article/selfaccelerating-turbidity-currents/09FFC00AF020A435682EEB28AE49AB04

Paull, C.K., Mitts, P., Ussler, W., Keaten, R., and Greene, H.G., 2005, Trail of sand in upper Monterey Canyon: Offshore California: Bulletin of the Geological Society of America, v. 117, p. 1134–1145, doi: 10.1130/B25390.1.

Paull, C.K., Ussler, W., Caress, D.W., Lundsten, E., Covault, J.A., Maier, K.L., Xu, J., and Augenstein, S., 2010, Origins of large crescent-shaped bedforms within the axial channel of Monterey Canyon, Offshore California: Geosphere, v. 6, p. 755–774, doi: 10.1130/GES00527.1.

Paull, C.K., Caress, D.W., Ussler, W., Lundsten, E., and Meiner-Johnson, M., 2011, High-resolution bathymetry of the axial channels within Monterey and Soquel submarine canyons, offshore

central California: Geosphere, v. 7, p. 1077–1101, doi: 10.1130/GES00636.1.

Paull, C.K., Caress, D.W., Lundsten, E., Gwiazda, R., Anderson, K., McGann, M., Conrad, J., Edwards, B., and Sumner, E.J., 2013, Anatomy of the La Jolla Submarine Canyon system; offshore southern California: Marine Geology, v. 335, p. 16–34, doi: 10.1016/J.MARGEO.2012.10.003.

Paull, C.K., Talling, P.J., Maier, K.L., Parsons, D., Xu, J., Caress, D.W., Gwiazda, R., Lundsten, E.M., Anderson, K., Barry, J.P., Chaffey, M., O'Reilly, T., Rosenberger, K.J., Gales, J.A., et al., 2018, Powerful turbidity currents driven by dense basal layers: Nature Communications, v. 9, p. 4114, doi: 10.1038/s41467-018-06254-6.

Peakall, J., McCaffrey, B., and Kneller, B., 2000, A Process Model for the Evolution, Morphology, and Architecture of Sinuous Submarine Channels: Journal of Sedimentary Research, v. 70, p. 434–448, doi: 10.1306/2DC4091C-0E47-11D7-8643000102C1865D.

Peakall, J., Amos, K.J., Keevil, G.M., William Bradbury, P., and Gupta, S., 2007, Flow processes and sedimentation in submarine channel bends: Marine and Petroleum Geology, v. 24, p. 470–486, https://www.sciencedirect.com/science/article/pii/S0264817207000360.

Peakall, J., and Sumner, E.J., 2015, Submarine channel flow processes and deposits: A process-product perspective: Geomorphology, v. 244, p. 95–120, doi: 10.1016/j.geomorph.2015.03.005.

Pemberton, E.A.L., Hubbard, S.M., Fildani, A., Romans, B., and Stright, L., 2016, The stratigraphic expression of decreasing confinement along a deep-water sediment routing system: Outcrop example from southern Chile: Geosphere, v. 12, p. 114–134, doi: 10.1130/GES01233.1.

Picot, M., Droz, L., Marsset, T., Dennielou, B., and Bez, M., 2016, Controls on turbidite sedimentation: Insights from a quantitative approach of submarine channel and lobe architecture (Late Quaternary Congo Fan): Marine and Petroleum Geology, v. 72, p. 423–446, doi: 10.1016/j.marpetgeo.2016.02.004.

Picot, M., Marsset, T., Droz, L., Dennielou, B., Baudin, F., Hermoso, M., de Rafelis, M., Sionneau, T., Cremer, M., Laurent, D., and Bez, M., 2019, Monsoon control on channel avulsions in the Late Quaternary Congo Fan: Quaternary Science Reviews, doi: 10.1016/j.quascirev.2018.11.033.

Pierdomenico, M., Casalbore, D., and Chiocci, F.L., 2019, Massive benthic litter funnelled to deep sea by flash-flood generated hyperpycnal flows: Scientific Reports, v. 9, doi:

10.1038/s41598-019-41816-8.

Pierdomenico, M., Casalbore, D., and Chiocci, F.L., 2020, The key role of canyons in funnelling litter to the deep sea: A study of the Gioia Canyon (Southern Tyrrhenian Sea): Anthropocene, v. 30, p. 100237, doi: 10.1016/j.ancene.2020.100237.

Piper, D.J.W., and Normark, W.R., 2009, Processes That Initiate Turbidity Currents and Their Influence on Turbidites: A Marine Geology Perspective: Journal of Sedimentary Research, v. 79, p. 347–362, doi: 10.2110/jsr.2009.046.

Pirmez, C., Beaubouef, R.T., Friedmann, S.J., and Mohrig, D.C., 2000, Equilibrium Profile and Baselevel in Submarine Channels: Examples from Late Pleistocene Systems and Implications for the Architecture of Deepwater Reservoirs, in Deep-Water Reservoirs of the World: 20th Annual, SOCIETY OF ECONOMIC PALEONTOLOGISTS AND MINERALOGISTS, p. 782–805, doi: 10.5724/gcs.00.15.0782.

Pohl, F., Eggenhuisen, J.T., Kane, I.A., and Clare, M.A., 2020, Transport and Burial of Microplastics in Deep-Marine Sediments by Turbidity Currents: Environmental Science and Technology, v. 54, p. 4180–4189, doi: 10.1021/acs.est.9b07527.

Pope, E.L., Talling, P.J., and Carter, L., 2017a, Which earthquakes trigger damaging submarine mass movements: Insights from a global record of submarine cable breaks? Marine Geology, v. 384, p. 131–146, doi: 10.1016/j.margeo.2016.01.009.

Pope, E.L., Talling, P.J., Carter, L., Clare, M.A., and Hunt, J.E., 2017b, Damaging sediment density flows triggered by tropical cyclones: Earth and Planetary Science Letters, v. 458, p. 161–169, doi: 10.1016/j.epsl.2016.10.046.

Pope, E.L., Heijnen, M.S., Talling, P.J., Silva Jacinto, R., Baker, M.L., Hage, S., Hasenhündl, M., Heerema, C.J., McGhee, C., Ruffell, S., Simmons, S.M., Cartigny, M.J.B., Clare, M.A., Dennielou, B., Gaillot, A., Parsons, D.R., Peirce, C., Urlaub, M., In Review, Landslide-dams profoundly affect sediment and carbon fluxes in deep-sea submarine canyons.

Popescu, I., Lericolais, G., Panin, N., Normand, A., Dinu, C., and Le Drezen, E., 2004, The Danube submarine canyon (Black Sea): morphology and sedimentary processes: Marine Geology, v. 206, p. 249–265, doi: 10.1016/J.MARGEO.2004.03.003.

Postma, G., and Cartigny, M.J.B., 2014, Supercritical and subcritical turbidity currents and their deposits--A synthesis: Geology, v. 42, p. 987–990, doi: 10.1130/G35957.1.

Pratson, L.F., Ryan, W.B.F., Mountain, G.S., and Twichell, D.C., 1994, Submarine canyon initiation

by downslope-eroding sediment flows: evidence in late Cenozoic strata on the New Jersey continental slope.: Geological Society of America Bulletin, v. 106, p. 395–412, doi: 10.1130/0016-7606(1994)106<0395:SCIBDE>2.3.CO;2.

Prins, M.A., and Postma, G., 2000, Effects of climate, sea level, and tectonics unraveled for last deglaciation turbidite records of the Arabian Sea: Geology, v. 28, p. 375, doi: 10.1130/0091-7613(2000)28<375:EOCSLA>2.0.CO;2.

Prior, D.B., Bornhold, B.D., and Johns, M.W., 1986, Active sand transport along a fjord-bottom channel, Bute Inlet, British Columbia.: Geology, v. 14, p. 581–584, doi: 10.1130/0091-7613(1986)14<581:ASTAAF>2.0.CO;2.

Prior, D.B., Bornhold, B.D., Wiseman, W.J., and Lowe, D.R., 1987, Turbidity current activity in a British Columbia Fjord: Science, v. 237, p. 1330–1333, doi: 10.1126/science.237.4820.1330.

Puig, P., Palanques, A., and Martín, J., 2014, Contemporary sediment-transport processes in submarine canyons: Annual Review of Marine Science, v. 6, p. 53–77, doi: 10.1146/annurev-marine-010213-135037.

Quadfasel, D., Kudrass, H., and Frische, A., 1990, Deep-water renewal by turbidity currents in the Sulu Sea: Nature, v. 348, p. 320–322, doi: 10.1038/348320a0.

Reece, R.S., Gulick, S.P.S., Horton, B.K., Christeson, G.L., and Worthington, L.L., 2011, Tectonic and climatic influence on the evolution of the Surveyor Fan and channel system, Gulf of Alaska: Geosphere, v. 7, p. 830–844, doi: 10.1130/GES00654.1.

Reimchen, A.P., Hubbard, S.M., Stright, L., and Romans, B.W., 2016, Using sea-floor morphometrics to constrain stratigraphic models of sinuous submarine channel systems: Marine and Petroleum Geology, v. 77, p. 92–115, doi: 10.1016/j.marpetgeo.2016.06.003.

Romans, B.W., Castelltort, S., Covault, J.A., Fildani, A., and Walsh, J.P., 2016, Environmental signal propagation in sedimentary systems across timescales: Earth-Science Reviews, v. 153, p. 7–29, doi: 10.1016/j.earscirev.2015.07.012.

Rowland, J.C., Hilley, G.E., and Fildani, A., 2010, A Test of Initiation of Submarine Leveed Channels by Deposition Alone: Journal of Sedimentary Research, v. 80, p. 710–727, doi: 10.2110/jsr.2010.067.

Sadler, P.M., 1981, Sediment accumulation rates and the completeness of stratigraphic sections.: Journal of Geology, v. 89, p. 569–584, doi: 10.1086/628623.

Seabeam (2000), Multibeam Sonar Theory of Operation: L-3 Communications SeaBeam Instruments, http://www3.mbari.org/data/mbsystem/sonarfunction/SeaBeamMultibeamTheoryOperation.pdf

Schlünz, B., Schneider, R.R., Müller, P.J., Showers, W.J., and Wefer, G., 1999, Terrestrial organic carbon accumulation on the Amazon deep sea fan during the last glacial sea level low stand: Chemical Geology, v. 159, p. 263–281, doi: 10.1016/S0009-2541(99)00041-8.

Scholl, D.W., Buffington, E.C., Hopkins, D.M., and Alpha, T.R., 1970, The structure and origin of the large submarine canyons of the Bering Sea: Marine Geology, v. 8, p. 187–210, doi: 10.1016/0025-3227(70)90043-5.

Sequeiros, O.E., Naruse, H., Endo, N., Garcia, M.H., and Parker, G., 2009, Experimental study on self-accelerating turbidity currents: Journal of Geophysical Research: Oceans, v. 114, doi: 10.1029/2008JC005149.

Sequeiros, O.E., Bolla Pittaluga, M., Frascati, A., Pirmez, C., Masson, D.G., Weaver, P., Crosby, A.R., Lazzaro, G., Botter, G., and Rimmer, J.G., 2019, How typhoons trigger turbidity currents in submarine canyons: Scientific Reports, v. 9, doi: 10.1038/s41598-019-45615-z.

Shepard, F.P., 1933, Submarine Valleys: Geographical Review, v. 23, p. 77, doi: 10.2307/209555.

Shepard, F.P., 1981, Submarine canyons: multiple causes and long-time persistence.: American Association of Petroleum Geologists Bulletin, v. 65, p. 1062–1077, doi: 10.1306/03B59459-16D1-11D7-8645000102C1865D.

Smith, D.P., Ruiz, G., Kvitek, R., and Iampietro, P.J., 2005, Semiannual patterns of erosion and deposition in upper Monterey Canyon from serial multibeam bathymetry: Geological Society of America Bulletin, v. 117, p. 1123, doi: 10.1130/B25510.1.

Smith, D.P., Kvitek, R., Iampietro, P.J., and Wong, K., 2007, Twenty-nine months of geomorphic change in upper Monterey Canyon (2002-2005): Marine Geology, v. 236, p. 79–94, doi: 10.1016/j.margeo.2006.09.024.

Soh, W., and Tokuyama, H., 2002, Rejuvenation of submarine canyon associated with ridge subduction, Tenryu Canyon, off Tokai, central Japan: Marine Geology, v. 187, p. 203–220, doi: 10.1016/S0025-3227(02)00267-0.

Spencer, J.W., 1903, Submarine valleys off the American coast and in the north Atlantic: Geological Society of America Bulletin, v. 14, p. 207–226, doi: 10.1130/GSAB-14-207.

Spinewine, B., Rensonnet, D., Clare, M., Capart, H., De Thier, T., and Dan-unterseh, G., 2013, Numerical Modelling of Runout and Velocity for Slide-Induced Submarine Density Flows: A Building Block of an Integrated Geohazards Assessment for Deepwater Developments, in onepetro.org, doi: 10.4043/24180-ms.

St.-Onge, G., Mulder, T., Piper, D.J.W., Hillaire-Marcel, C., and Stoner, J.S., 2004, Earthquake and flood-induced turbidites in the Saguenay Fjord (Québec): A Holocene paleoseismicity record: Quaternary Science Reviews, v. 23, p. 283–294, doi: 10.1016/j.quascirev.2003.03.001.

St-Onge, G., and Lajeunesse, P., 2007, Flood-induced turbidites from northern Hudson bay and western Hudson Strait: A two-pulse record of Lake Agassiz final outburst flood?, in Submarine Mass Movements and Their Consequences, 3rd International Symposium, doi: 10.1007/978-1-4020-6512-5_14.

Stetten, E., Baudin, F., Reyss, J.L., Martinez, P., Charlier, K., Schnyder, J., Rabouille, C., Dennielou, B., Coston-Guarini, J., and Pruski, A., 2015, Organic matter characterization and distribution in sediments of the terminal lobes of the Congo deep-sea fan: Evidence for the direct influence of the Congo River: Marine Geology, v. 369, p. 182–195, doi: 10.1016/j.margeo.2015.08.020.

Stevenson, C.J., Talling, P.J., Wynn, R.B., Masson, D.G., Hunt, J.E., Frenz, M., Akhmetzhanhov, A., and Cronin, B.T., 2013, The flows that left no trace: Very large-volume turbidity currents that bypassed sediment through submarine channels without eroding the sea floor: Marine and Petroleum Geology, v. 41, p. 186–205, doi: 10.1016/J.MARPETGEO.2012.02.008.

Stevenson, C.J., Jackson, C.A.-L., Hodgson, D.M., Hubbard, S.M., and Eggenhuisen, J.T., 2015, Deep-Water Sediment Bypass: Journal of Sedimentary Research, v. 85, p. 1058–1081, doi: 10.2110/jsr.2015.63.

Straub, K.M., and Pyles, D.R., 2012, Quantifying the hierarchical organization of compensation in submarine fans using surface statistics: Journal of Sedimentary Research, v. 82, p. 889–898, doi: 10.2110/jsr.2012.73.

Straub, K.M., and Esposito, C.R., 2013, Influence of water and sediment supply on the stratigraphic record of alluvial fans and deltas: Process controls on stratigraphic completeness: Journal of Geophysical Research: Earth Surface, v. 118, p. 625–637, doi: 10.1002/jgrf.20061.

Strauss, D., and Sadler, P.M., 1989, Stochastic models for the completeness of stratigraphic sections: Mathematical Geology, v. 21, p. 37–59, doi: 10.1007/BF00897239.

Sullivan, M.D., Foreman, J.L., Jennette, D.C., Stern, D., Jensen, G.N., and Goulding, F.J., 2004, An integrated approach to characterization and modeling of deep-water reservoirs, Diana field, western Gulf of Mexico: AAPG Memoir, p. 215–234, doi: 10.1306/m80924c11.

Sumer, B.M., Truelsen, C., Sichmann, T., and Fredsøe, J., 2001, Onset of scour below pipelines and self-burial: Coastal Engineering, v. 42, p. 313–335, doi: 10.1016/S0378-3839(00)00066-1.

Sumner, E.J., and Paull, C.K., 2014, Swept away by a turbidity current in Mendocino submarine canyon, California: Geophysical Research Letters, v. 41, p. 7611–7618, doi: 10.1002/2014GL061863.

Syahnur, Y., 2018, Geomatics Best Practices in Saka Indonesia Pangkah Limited (Case Study: Ujung Pangkah Pipeline Integrity), in Indonesian Petroleum Association, doi: 10.29118/ipa.0.15.e.143.

Sylvester, Z., Pirmez, C., and Cantelli, A., 2011, A model of submarine channel-levee evolution based on channel trajectories: Implications for stratigraphic architecture: Marine and Petroleum Geology, v. 28, p. 716–727, doi: 10.1016/j.marpetgeo.2010.05.012.

Sylvester, Z., and Covault, J.A., 2016, Development of cutoff-related knickpoints during early evolution of submarine channels: Geology, v. 44, p. 835–838, doi: 10.1130/G38397.1.

Sylvester, Z., Durkin, P., and Covault, J.A., 2019, High curvatures drive river meandering: Geology, v. 47, p. 263–266, doi: 10.1130/G45608.1.

Symons, W.O., Sumner, E.J., Talling, P.J., Cartigny, M.J.B., and Clare, M.A., 2016, Large-scale sediment waves and scours on the modern seafloor and their implications for the prevalence of supercritical flows: Marine Geology, v. 371, p. 130–148, doi: 10.1016/j.margeo.2015.11.009.

Syvitski, J.P.M., and Farrow, G.E., 1983, Structures and processes in bayhead deltas: Knight and bute inlet, British Columbia: Sedimentary Geology, v. 36, p. 217–244, doi: 10.1016/0037-0738(83)90010-6.

Syvitski, J.P.M., Burrell, D.C., and Skei, J.M., 1987, Fjords: Springer New York, doi: 10.1007/978-1-4612-4632-9.

Syvitski, J.P.M., Smith, J.N., Calabrese, E.A., and Boudreau, B.P., 1988, Basin sedimentation and the growth of prograding deltas: Journal of Geophysical Research, v. 93, p. 6895–6908, doi: 10.1029/JC093iC06p06895.

Talling, P.J., 2014, On the triggers, resulting flow types and frequencies of subaqueous sediment density flows in different settings: Marine Geology, v. 352, p. 155–182, doi: 10.1016/j.margeo.2014.02.006.

Talling, P.J., Allin, J., Armitage, D. a, Arnott, R.W., Cartigny, M.J., Clare, M. a, Felletti, F., Covault, J. a, Girardclos, S., Hansen, E., Hill, P.R., Hiscott, R.N., Hogg, A.J., Hughes Clarke, J., et al., 2015, Key Future Directions for Research on Turbidity Currents and Their Deposits: Journal of Sedimentary Research, v. 85, p. 153–169, doi: 10.2110/jsr.2015.03.

Taylor, B., and Smoot, N.C., 1984, Morphology of Bonin fore-arc submarine canyons.: Geology, v. 12, p. 724–727, doi: 10.1130/0091-7613(1984)12<724:MOBFSC>2.0.CO;2.

Toebes, G.H., and Sooky, A.A., 1967, Hydraulics of meandering rivers with flood plains: Journal of the Waterways and Harbors Division, A.S.C.E., v. 88, p. 213–236.

Toniolo, H., and Cantelli, A., 2007, Experiments on Upstream-Migrating Submarine Knickpoints: Journal of Sedimentary Research, v. 77, p. 772–783, doi: 10.2110/jsr.2007.067.

Traganos, D., Poursanidis, D., Aggarwal, B., Chrysoulakis, N., and Reinartz, P., 2018, Estimating satellite-derived bathymetry (SDB) with the Google Earth Engine and sentinel-2: Remote Sensing, v. 10, doi: 10.3390/rs10060859.

Tubau, X., Paull, C.K., Lastras, G., Caress, D.W., Canals, M., Lundsten, E., Anderson, K., Gwiazda, R., and Amblas, D., 2015, Submarine canyons of Santa Monica Bay, Southern California: Variability in morphology and sedimentary processes: Marine Geology, v. 365, p. 61–79, doi: 10.1016/J.MARGEO.2015.04.004.

Turmel, D., Locat, J., Cauchon-Voyer, G., Lavoie, C., Simpkin, P., Parker, G., and Lauziere, P., 2010, Morphodynamic and Slope Instability Observations at Wabush Lake, Labrador: Submarine Mass Movements and Their Consequences, v. 28, p. 435–446, doi: 10.1007/978-90-481-3071-9_36.

Turmel, D., Locat, J., and Parker, G., 2015, Morphological evolution of a well-constrained, subaerial-subaqueous source to sink system: Wabush Lake: Sedimentology, v. 62, p. 1636–1664, doi: 10.1111/sed.12197.

Turmel, D., Locat, J., and Parker, G., 2012, Upstream migration of knickpoints: Geotechnical considerations, in Submarine Mass Movements and Their Consequences - 5th International Symposium, Dordrecht, Springer Netherlands, p. 123–132, doi: 10.1007/978-94-007-2162-3_11.

Vangriesheim, A., Pierre, C., Aminot, A., Metzl, N., Baurand, F., and Caprais, J.-C., 2009, The influence of Congo River discharges in the surface and deep layers of the Gulf of Guinea: Deep Sea Research Part II: Topical Studies in Oceanography, v. 56, p. 2183–2196, doi: 10.1016/J.DSR2.2009.04.002.

Vendettuoli, D., Clare, M.A., Clarke, J.E.H., Vellinga, A., Hizzett, J., Hage, S., Cartigny, M.J.B., Talling, P.J., Waltham, D., Hubbard, S.M., Stacey, C., and Lintern, D.G., 2019, Daily bathymetric surveys document how stratigraphy is built and its extreme incompleteness in submarine channels: Earth and Planetary Science Letters, v. 515, p. 231–247, doi: 10.1016/J.EPSL.2019.03.033.

Wells, M., and Cossu, R., 2013, The possible role of Coriolis forces in structuring large-scale sinuous patterns of submarine channel-levee systems: Philosophical Transactions of the Royal Society A: Mathematical, Physical and Engineering Sciences, v. 371, doi: 10.1098/rsta.2012.0366.

Wynn, R.B., Cronin, B.T., and Peakall, J., 2007, Sinuous deep-water channels: Genesis, geometry and architecture: Marine and Petroleum Geology, v. 24, p. 341–387, doi: 10.1016/j.marpetgeo.2007.06.001.

Xu, J.P., Noble, M.A., and Rosenfeld, L.K., 2004, In-situ measurements of velocity structure within turbidity currents: Geophysical Research Letters, v. 31, p. n/a-n/a, doi: 10.1029/2004GL019718.

Yin, S., Lin, L., Pope, E.L., Li, J., Ding, W., Wu, Z., Ding, W., Gao, J., and Zhao, D., 2019, Continental slope-confined canyons in the Pearl River Mouth Basin in the South China Sea dominated by erosion, 2004–2018: Geomorphology, v. 344, p. 60–74, doi: 10.1016/j.geomorph.2019.07.016.

Yu, B., Cantelli, A., Marr, J., Pirmez, C., O'Byrne, C., and Parker, G., 2006, Experiments on Self-Channelized Subaqueous Fans Emplaced by Turbidity Currents and Dilute Mudflows: Journal of Sedimentary Research, v. 76, p. 889–902, doi: 10.2110/jsr.2006.069.

Yu, H.S., Chiang, C.S., and Shen, S.M., 2009, Tectonically active sediment dispersal system in SW Taiwan margin with emphasis on the Gaoping (Kaoping) Submarine Canyon: Journal of Marine Systems, v. 76, p. 369–382, doi: 10.1016/j.jmarsys.2007.07.010.

Zeng, J., Lowe, D.R., Prior, D.B., Wiseman, W.J., and Bornhold, B.D., 1991, Flow properties of turbidity currents in Bute Inlet, British Columbia: Sedimentology, v. 38, p. 975–996, doi: 10.1111/j.1365-3091.1991.tb00367.x.

Zheng, L.W., Ding, X., Liu, J.T., Li, D., Lee, T.Y., Zheng, X., Zheng, Z., Xu, M.N., Dai, M., and Kao, S.J., 2017, Isotopic evidence for the influence of typhoons and submarine canyons on the sourcing and transport behavior of biospheric organic carbon to the deep sea: Earth and Planetary Science Letters, v. 465, p. 103–111, doi: 10.1016/j.epsl.2017.02.037.

Zhong, G., Cartigny, M.J.B., Kuang, Z., and Wang, L., 2015, Cyclic steps along the South Taiwan Shoal and West Penghu submarine canyons on the northeastern continental slope of the South China Sea: Geological Society of America Bulletin, v. 127, p. 804–824, doi: 10.1130/B31003.1.

Zhong, G., and Peng, X., 2021, Transport and accumulation of plastic litter in submarine canyons-The role of gravity flows: Geological Society of America | GEOLOGY, v. 1, doi: 10.1130/G48536.1.